Sigmatropic and Haptotropic Shifts in Complexes of Cyclopenta[*l*]phenanthrene

By

Suzie S. Rigby, M.Sc.

A Thesis

Submitted to the School of Graduate Studies

In Partial Fulfillment of the Requirements

for the Degree

Doctor of Philosophy

McMaster University

January 1997

Complexes of Cyclopenta[*l*]phenanthrene

DOCTOR OF PHILOSOPHY (1997) McMaster University

(Chemistry) Hamilton, Ontario

Title: Sigmatropic and Haptotropic Shifts in Complexes of Cyclopenta[*l*]phenanthrene

Author: Suzie S. Rigby

SUPERVISORS: Dr. M.J. McGlinchey and Dr. A.D. Bain

NUMBER OF PAGES: xii

154

Abstract

In a calculational study at the unrestricted Hartree-Fock (UHF) level of theory, it has been predicted that strategically incorporating an aromatic ring onto indenyltrimethylsilane would lower the barrier for [1,5]-sigmatropic shifts of silicon around the five-membered ring through retention of aromatic character in the transition state and in the intermediate *iso*-indene. In this thesis, the synthesis and dynamic behavior of the tricyclic system angular trimethylsilylbenzindene, **50**, and also the tetracycle trimethylsilylcyclopenta[*l*]phenanthrene, **53**, are reported. Incorporation of one aromatic ring onto the indenyl ligand does lower the barrier for [1,5]-silatropic shifts to 21.9 ± 0.5 kcal/mol, compared to 24 kcal/mol for the indenyl system. Addition of a second aromatic ring further lowers the barrier to 17.6 ± 0.2 kcal/mol, in good agreement with calculations. The intermediate *iso*-indenes for both systems have been trapped as their Diels-Alder adducts with tetracyanoethylene.

In an attempt to study the migration of transition metals over the surface of cyclopenta[*l*]phenanthrene, **55**, a series of complexes have been synthesized in which the metals are bonded to the 5-membered ring in án η^5-fashion. It seemed reasonable that the ligand might behave as a "super-indenyl" in that a transition state in a ligand substitution reaction would be stabilized by two aromatic rings compared to the single aromatic ring in the indenyl system. The experimental data revealed that haptotropic shifts, in which a metal migrates from a five-membered ring to a six-membered ring have a high barrier and are not observed. Moreover, it was not possible to substitute ligands such as phosphines for carbonyls or ethylene. One can conclude that the ligand is behaving as a cyclopentadienyl ligand rather than an indenyl unit.

We hypothesized that we might be able to induce haptotropic shifts in complexes in which the transition-metal is bound to a six-membered ring of cyclopenta[*l*]phenanthrene, by deprotonating such complexes. However, attempts to bond transition-metals to a six-membered

ring of the ligand were unsuccessful. When the ligand was not carefully dried, the result was to hydrogenate the double bond of the five-membered ring and yield a complex with $Cr(CO)_3$ attached to a terminal six-membered ring. This molecule, (cyclopenta[*l*]dihydrophenanthrene)$Cr(CO)_3$, **88**, was characterized by X-ray crystallography.

In an attempt to bond $Cr(CO)_3$ to a six-membered ring by using carefully dried ligand, we isolated the Diels-Alder dimer, **94**, of the ligand cyclopenta[*l*]phenanthrene. It was also possible to synthesize this molecule by heating it under reflux in *n*-butyl ether, and we obtained an X-ray crystal structure of the molecule. Of course, it is well-known that cyclopentadiene dimerizes at relatively low temperature; in contrast, indene itself does not dimerize, but instead yields a styrene-type polymer. Theoretical studies on indene and cyclopenta[*l*]phenanthrene revealed that both have a high barrier (≈ 43 kcal/mol for cyclopenta[*l*]phenanthrene and 46 kcal/mol for indene) to hydrogen migration, but that the *iso*-indene type intermediate structure for cyclopenta[*l*]phenanthrene is only 4.3 kcal/mol above the ground state, while the intermediate for indene is 9.0 kcal/mol above the ground state.

Acknowledgements

To my co-supervisors, Dr. Michael J. McGlinchey and Dr. Alex D. Bain, I sincerely thank you for the opportunity to learn both a little NMR and a little organometallic synthesis. Thank you both for your guidance, support and many helpful discussions over the years.

I would also like to thank the other member of my supervisory committee, Dr. Michael A. Brook, for his assistance and many invaluable suggestions. I am indebted to Dr. Nick H. Werstiuk for teaching me to calculate transition states, and for the interesting discussions about canoeing.

I am especially grateful to all of the technical staff and to the office staff in the Chemistry department. To Dr. Jim Britten, thank you for the crystal structures, but more importantly, thank you for listening to me sound off. Thank you Brian Sayer and Dr. Don Hughes for your always patient assistance in the NMR room. I would like to thank Dr. Richard Smith and Fadjar A. Ramalan for obtaining mass spectra for me. Faj, visiting the mass spec room was always something to look forward to. To Carol, Josie, Marilyn, Nancy and Paula - thank you for handling all the details and for bringing a dose of reality to my time here.

I would like to thank all of the people who have worked in MJM's lab and ADB's group during my stay at McMaster. Andreas, thank you for introducing me to organometallic synthesis. Luc, thanks for proof-reading documents and being a friend. Mark Stradiotto, your enthusiasm is infectious; thank you for always taking the time to listen to my chemistry problems and making many valuable suggestions. Pippa, thank you for being my voice of reason. Stacey, thanks for the company on the trip to Kingston. Ralph, thanks for your help with power point, etc. Jamie, I never thought I would say this, but thanks for making me laugh in the lab. Paul and Dan, thanks for putting up with my abuse on the way to Quebec City (also during the conference and on the way home).

I am especially fortunate to have enjoyed the friendship of Theresa Fauconnier, Dave Pole (who also served as my personal post doc, even before he got his Ph.D.), Carol Kingsmill and Al Postigo during my years at McMaster.

Most importantly, I would like to thank my family.

Table of Contents

List of Figures

List of Tables

CHAPTER ONE

Introduction

1.1 Silicon Migrations : Overview

The migration of organosilyl groups over molecular surfaces is a subject of considerable interest.[1] In particular, molecules of the type L_2ZrX_2, where L = cyclopentadienyl, indenyl or fluorenyl, are important because of their relevance to stereospecific polymerizations of alkenes.[2] Moreover, when the metallocene rings are linked via alkyl or silyl bridges, the resulting complexes can be chiral catalysts. Thus, any process which might bring about loss of stereochemical integrity in the catalytic species needs to be understood at a rather fundamental level.

1.1.1 [1,5]-Silicon Migrations

For over a decade it has been known that the migration of an R_3E group (E = Si, Ge, Sn) around a cyclopentadienyl ring proceeds via successive [1,5]-metallotropic shifts with retention of configuration at the migrating Group 14 centre.[3,4] The barriers for these migrations have been reported as 15 kcal/mol for Me_3Si, 13 kcal/mol for Me_3Ge and 7 kcal/mol for Me_3Sn.[5-11] Incorporation of a six-membered ring into these molecules gives the corresponding indenyl systems, **1**, in which the barriers towards Me_3E migration increase to 24 kcal/mol for Si, 22 kcal/mol for Ge and 15 kcal/mol for Sn.[12-14] These increased barriers, relative to the values measured in their cyclopentadienyl analogues, have been attributed to a decrease in aromaticity during the migration process. The intermediacy of the *iso*-indene, **2**, has been unequivocally demonstrated [15,16] by trapping it as the Diels-Alder adduct, **3**, which has since been characterized by X-ray crystallography.[17] The barrier for hydrogen migration in these systems is considerably higher than for silatropic migrations; products such as **4**, that result from prototropic shifts in R_3E(indenyl), are evident only above 150°C.

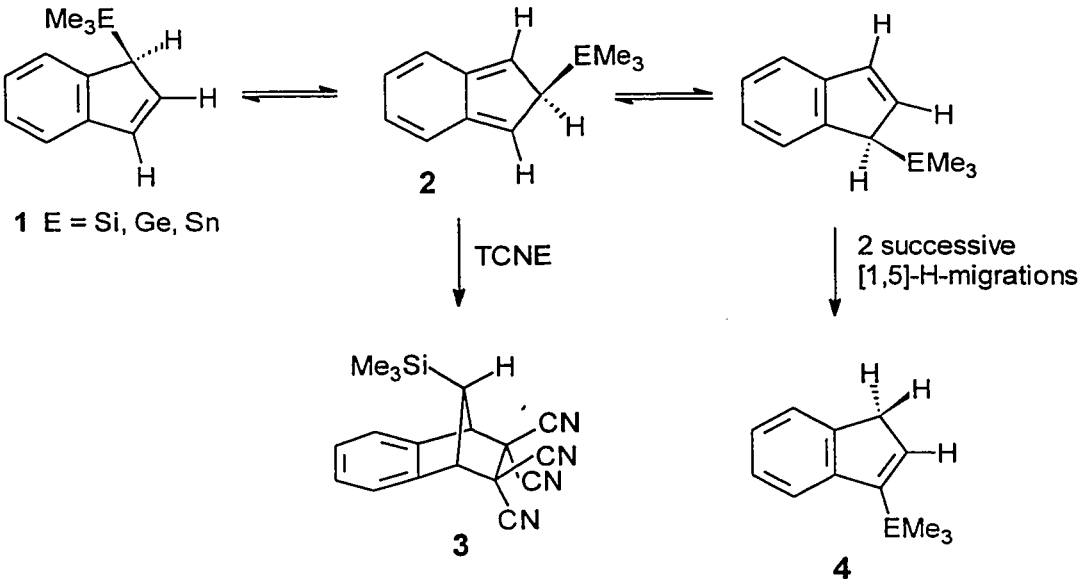

Despite these reports, it was recently proposed[1] that in bis(indenyl)$SiMe_2$, **5**, rearrangement proceeds through [1,3]-silatropic shifts. This hypothesis has since been disproven,[18] and the [1,5]-shift mechanism has been established by trapping the intermediate *iso*-indene **6**, as the double Diels-Alder adduct, **7**, as shown in Scheme 1.1. Furthermore, the sterically encumbered molecule tris(indenyl)methylsilane, **8**, has been synthesized and interconversion of the *RRR*, *RRS*, *RSS*, and *SSS* stereoisomers has been found to proceed through successive [1,5]-silatropic shifts, as in Scheme 1.2.[17]

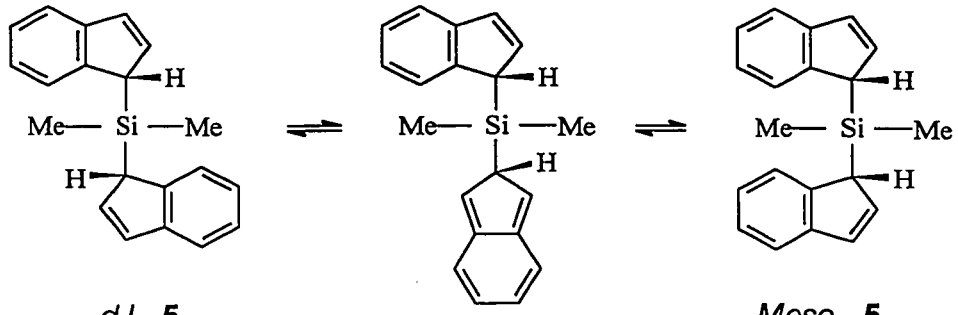

d,l - **5** **6** *Meso* - **5**

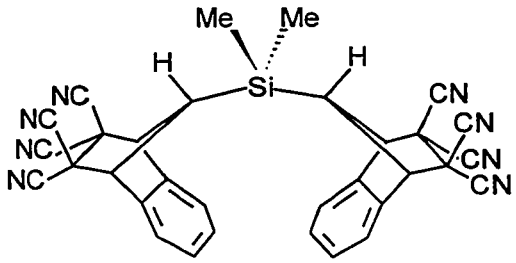

7

Scheme 1.1

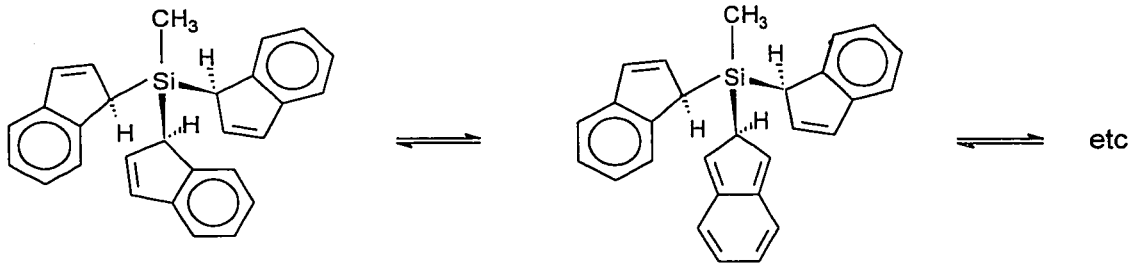

***R,R,R* 8** **9**

Scheme 1.2

Silatropic shifts in both **5** and **8** occur with activation energies of 24 kcal/mol —a $\Delta G^{\ddagger}$ value too high to be determined by using conventional NMR line-broadening methods. Rather, they have been measured by using single selective inversion relaxation techniques, in which magnetization transfer between exchanging sites is monitored over a range of temperatures.[18-25] The relative ease with which the iso-indenes **2**, **6** and **9** are trapped suggests that the organosilyl group plays a significant role in stabilizing these non-aromatic intermediates. The mechanism of stabilization involves the overlap of π-orbitals with a silicon orbital. The role of silicon 3*d* orbitals has long been a controversial issue,[26] but the majority of recent commentators have rejected the use of the 3*d* orbitals, at least in rationalizing the bonding in Si-O-Si systems.[27-30] Thus the question of how the silicon provides stabilization needs to be resolved.

1.1.2 Migrations of Other Functional Groups?

The migration of several other functional groups in the dimethylindene system **10** has been studied by Jones *et al.*[31] They found that the formyl group migrates 10^3 times more rapidly than does the acetyl group, which in turn migrates 10^4 times more rapidly than does the carbomethoxy group. Jones rationalized these results in terms of the electron-accepting ability of the migrating group (in a resonance sense, rather than purely inductively). In contrast, Epiotis and Shaik interpreted the data in a different manner.[32] They suggested that these sigmatropic shifts were controlled by the donor and acceptor character of the migrating group, and of the cyclic framework over which the rearrangment occurred. Thus, they viewed the cyclopentadienyl moiety in $C_5H_5SiMe_3$, **11**, as being "an instrinsic acceptor" because of the aromatic nature of $C_5H_5^-$; in contrast, the cycloheptatrienyl fragment in $C_7H_7SiMe_3$, **12**, behaves like "an intrinsic donor" owing to the aromatic nature of $C_7H_7^+$. As shown in Scheme 1.3, the trimethylsilyl substituent undergoes facile rearrangement over the five-membered ring, while the prototropic shift has a very high barrier. In the seven-membered ring, it is the hydrogen which undergoes the [1,5]-

suprafacial shift, while the $SiMe_3$ group is much more reluctant to migrate.[33] However, we note that in $C_7H_7SnMe_3$, the trimethyltin moiety is apparently fluxional.[34]

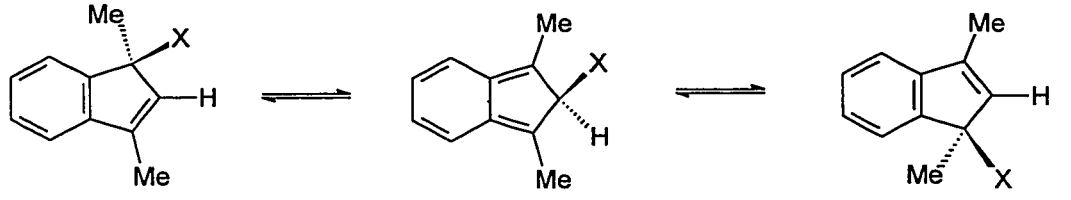

10

X = $-\overset{O}{\overset{\|}{C}}-H$; $-\overset{O}{\overset{\|}{C}}-Me$; $-\overset{O}{\overset{\|}{C}}-OMe$

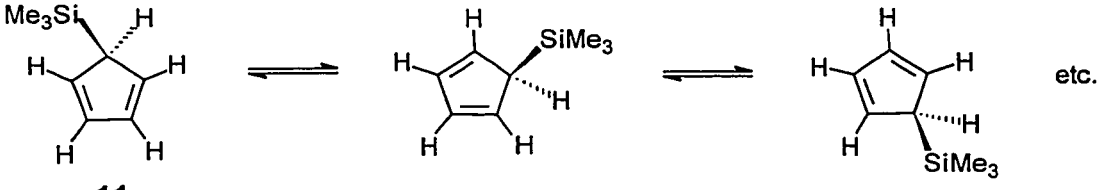

11

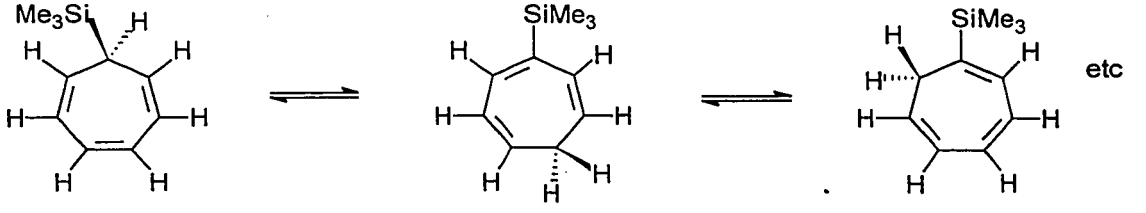

12

Scheme 1.3

1.2 Metal Complexes of Multifused Ring Systems

The discovery of the first transition metal sandwich complex, ferrocene **13** changed the course of organometallic chemistry.[35,36]

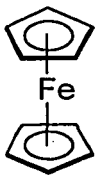

13

Shortly thereafter, it was discovered that one cyclopentadienyl ring could be replaced by an arene ligand. Treatment of ferrocene with $AlCl_3$, Al and the arene, followed by anion metathesis yielded cations such as **14**.

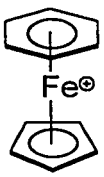

14

Fischer and Hafner synthesized $(C_6H_6)_2Cr$ in 1955.[37] Reaction of $CrCl_3$ with benzene, $AlCl_3$ and Al, followed by reduction with sodium dithionite gave the sandwich complex. Various sandwich complexes may be prepared by vaporization of metals in a high vacuum system, followed by co-condensation of the metal vapours with ligands at -196°C.[38]

The "half-sandwich" complexes $(\eta^6\text{-}C_6H_6)Cr(CO)_3$ and $(\eta^6\text{-}C_6H_3Me_3)Mn(CO)_3^+$ were first reported in 1957.[39,40]

In some synthetic approaches to benzene complexes, the C_6H_6 ring can be replaced by a multi-fused ring system containing one or more six-membered rings. Thus polycyclic aromatic complexes of $Cr(CO)_3$, $Mn(CO)_3^+$ and $Fe(\eta^5\text{-}C_5H_5)^+$ have been prepared for a variety of

ligands. In each of these systems the metal was found to bind to a terminal six-membered ring, as shown in Figure 1.1.

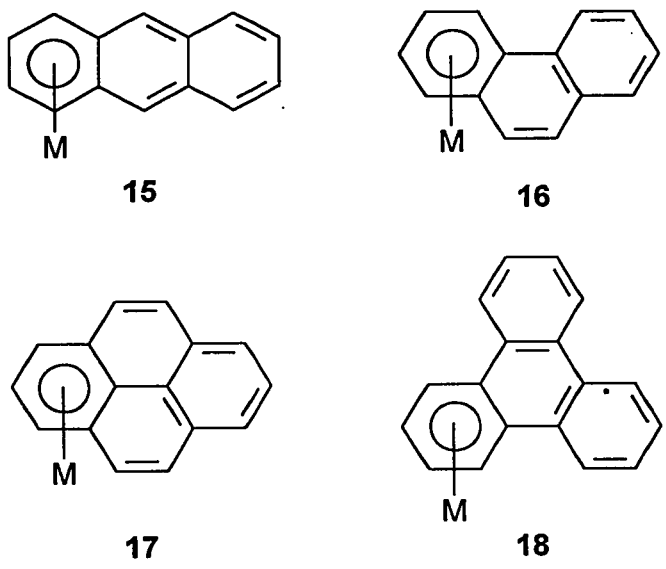

15 16 17 18

Figure 1.1 Metal coordination in multifused ring systems.

This behaviour has been explained by attributing greater aromatic character to a terminal ring[41] or by noting that in each case the observed isomer leaves conjugated the maximum number of non-complexed rings.[42]

1.3 Haptotropic Shifts

The term haptotropic rearrangement has been coined to cover those cases where an ML_n unit changes its connectivity (hapto number) to some ligand with multicoordinate site possibilities.[43] Therefore a haptotropic rearrangement in a polyene-ML_n complex is one where the ML_n unit migrates from one coordination site to another over the surface of the polyene. Ring slippage reactions cover those instances where the metal remains bonded to the same ring,

whereas in inter-ring metal migrations, the metal changes coordination between adjacent rings in a multi-fused ring system.

1.3.1 Ring Slippage Reactions

As stated above, ring slippage is a type of metal migration in which the metal fragment changes its coordination number to the ligand while remaining bonded to the same ring. This can occur in systems where the ligand consists of a single ring or is polycyclic.

Kundig and Timms proposed that in the very efficient hydrogenation catalyst, naphthalene $Cr(CO)_3$, **19**, the naphthalene ligand underwent such a ring slippage.[44]

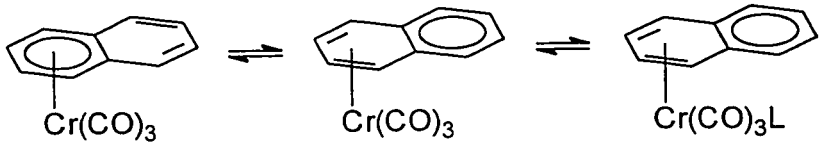

19

Scheme 1.4

The intermediate formed on attack by the ligand L, possesses an aromatic uncomplexed benzene ring (scheme 1.4), which lowers the activation energy for the process.

Ring slippage has been invoked to explain the facile replacement of carbonyl ligands by phosphines in indenyl complexes of rhodium.[45] In the well known "indenyl effect", it is proposed that an η^5- complex, **20**, can "slip" to an η^3 position, generating an aromatic ring in the 18 electron intermediate, **21**, as shown in Scheme 1.5.

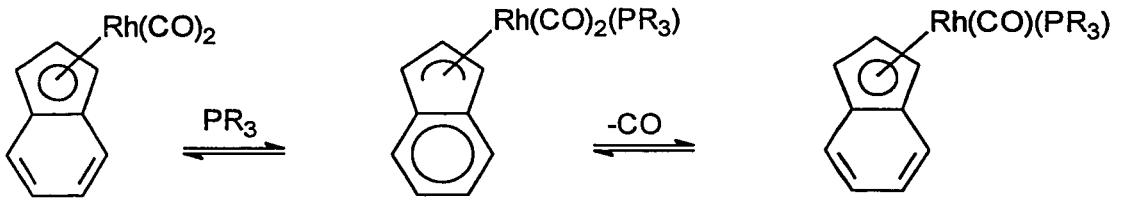

20 **21**

Scheme 1.5

The rate of phosphine substitution is 10^8 times faster than in the analogous cyclopentadienyl system.[45] The reaction is a bimolecular associative process, which is first order in both the initial complex and the incoming ligand.

In the analogous cyclopentadienyl complex, **22**, ring slippage does not appear to play a role in ligand substitution reactions. The kinetics for such reactions have been shown to be first order and involve dissociation of a carbonyl ligand to generate a 16-electron species, **23**, as shown in Scheme 1.6. A fast second step yields the product.

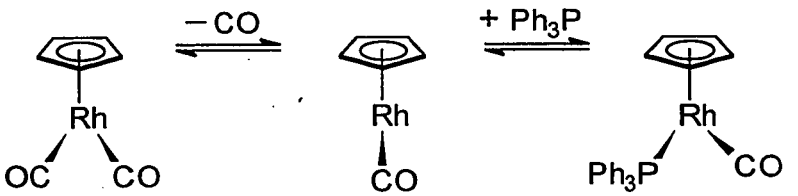

22 **23**

Scheme 1.6

If this process were to proceed through an associative process to generate $(C_5H_5)Rh(CO)_2L$, the metal would have a 20-electron configuration, typically an energetically unfavorable situation. Phosphine substitution has not been observed in the related system (η^5-cyclopentadienyl)$Mn(CO)_3$, even after three days at 140°C.

While the cyclopentadienyl complexes noted above do not appear to undergo ring slippage reactions, there is some evidence of ring slippage in cyclopentadienyl systems. Reaction

of $(\eta^5\text{-}C_5H_5)_2W(CO)$ with excess CO yielded $(\eta^3\text{-}C_5H_5)(\eta^5\text{-}C_5H_5)W(CO)_2$, **24**, in which one of the C_5H_5 rings was found to be significantly bent.[46,47] Similarly, $(\eta^5\text{-}C_5H_5)_2Cr$ was converted to $(\eta^1\text{-}C_5H_5)(\eta^5\text{-}C_5H_5)Cr(NO)_2$, **25**.

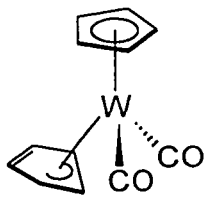

24

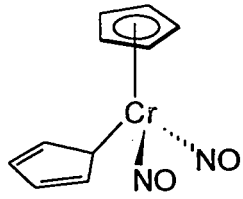

25

1.3.2 Inter-ring Metal Migrations

The first experimental example of a haptotropic inter-ring rearrangement was presented by Müller *et al.* in 1969.[48] Irradiation of (bis-benzo[*ae*]cyclooctatetraene)$Cr(CO)_4$, **26**, resulted in the irreversible migration of chromium from the eight- to the six-membered ring.

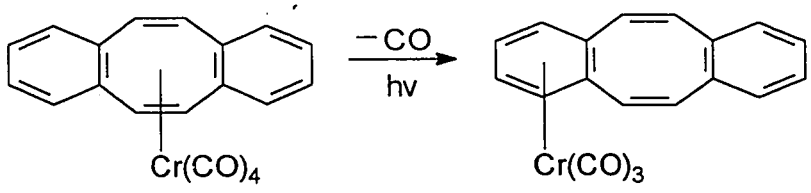

26

Scheme 1.7

Since this discovery, rearrangements in organometallic complexes of naphthalene, anthracene, indene and fluorene have been intensively studied.

Complexes of naphthalene have been reported for Ni,[49,50] Co,[51] Cr,[52-54] Rh[55] and Ir.[55,56]

It has been proposed that in the nickel complex of anthracene, **27**, the metal exchanges between η^6 and η^4 complexes, but the evidence is not conclusive.[49,57]

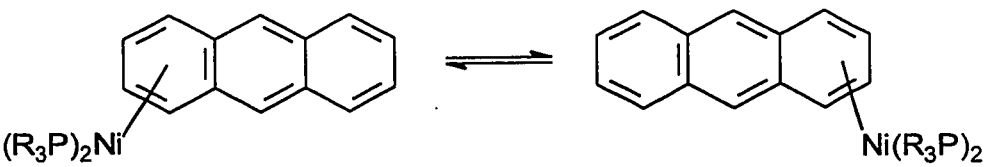

27

Scheme 1.8

Metal migrations between rings of different sizes have also been studied. The simplest cases are those of indene or indenyl complexes, such as Fe,[58] Re,[59] Ir,[55,56] Cr,[60] Mo,[60,61] and W.[60,61]

Rearrangements of the type $\eta^6 \rightarrow \eta^5$ in which η^6 complexes of indene, **28**, are treated with base to yield the η^5 isomers, **29**, have been studied (Scheme 1.9).

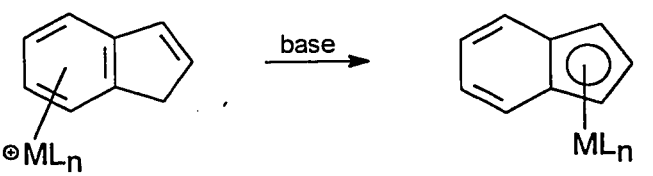

28 **29**

Scheme 1.9

The reverse rearrangement was observed upon protonation of bis(η^5-indenyl)iron, **30**.[58] Protonation was believed to occur at the metal, with subsequent proton migration to the ligand, followed by migration of iron to the six-membered ring of one of the ligands.

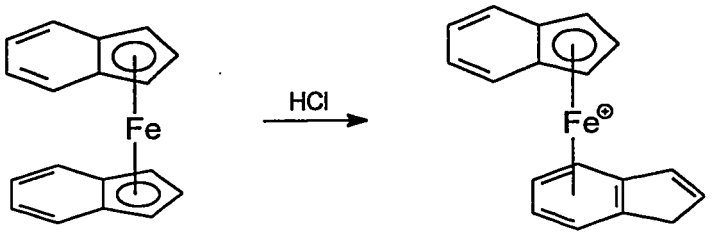

30

Scheme 1.10

When (η^5-indenyl)Rh(1,5-cyclooctadiene) and (η^5-indenyl)Rh(norbornadiene) were protonated with HBF_4, it was found that protonation occurred on the indenyl ring, and that the metal migrated to the six-membered ring.[62]

McGlinchey *et al.* protonated (η^5-indenyl)Rh(C_2H_4)$_2$, **31**, and found that protonation occurred at the 1-position of the indenyl ring,[63] and the metal had shifted to the six-membered ring, as in **32**. Resonances associated with free indene were also found.

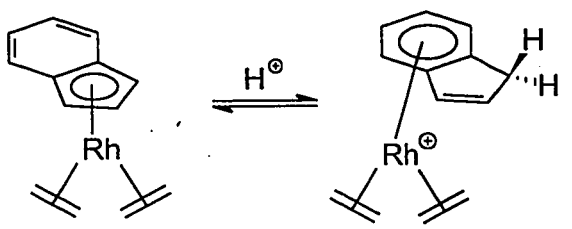

31 **32**

Scheme 1.11

When the indenyl ligand was methylated at the 1-position, the barrier to rotation about the metal-ligand bond was measured.

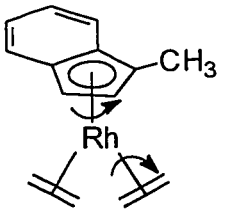

33

There has also been a great deal of work dealing with the protonation of cyclopentadienyl rhodium complexes. Protonation of (η^5-C_5H_5)Rh(cyclooctatetraene), **34**, with trifluoroacetic acid was found to occur on the COT ligand.[64] A bicyclic cation, **35**, was initially produced, which subsequently isomerized to the preferred monocyclic form, **36**.

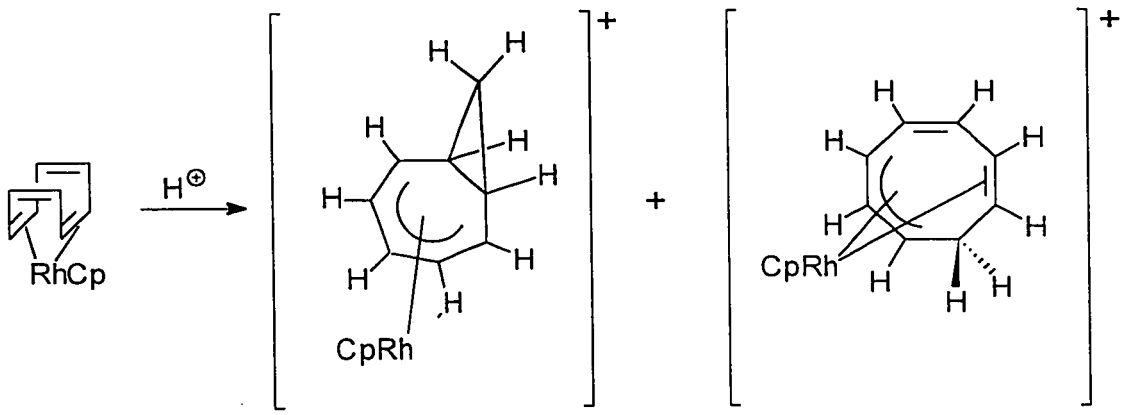

34 **35** **36**

Scheme 1.13

While many transition metal complexes of fluorene have been characterized, studies on haptotropic rearrangements deal largely with complexes of Cr,[60,65] Mn,[66] and Fe.[67]

Nicholas and coworkers deprotonated $(C_{13}H_{10})Cr(CO)_3$, which yielded $(C_{13}H_9)Cr(CO)_3^-$, **37**.[66]

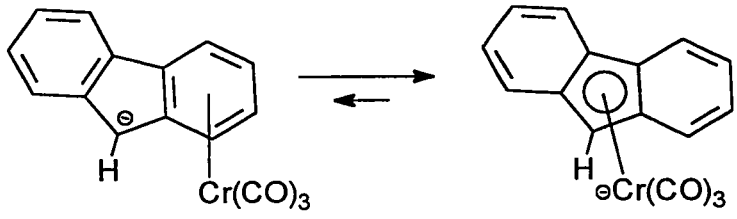

37

Scheme 1.14

The compounds were difficult to study as they were sensitive towards heat, moisture and air and could only be studied in solution.

Treichel and coworkers found a more convenient method for studying haptotropic shifts in fluorene complexes.[67] They started with cationic complexes of manganese and iron, **38**, which yielded neutral molecules, **39**, upon deprotonation.

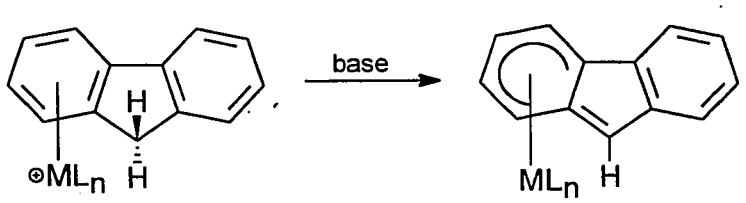

38 **39**

$ML_n = Mn(CO)_3, Fe(C_5H_5$

Scheme 1.15

X-ray crystal structures were obtained for both neutral molecules and revealed that in each case the metals were significantly displaced away from one of the ring junction carbons. Also in both cases, the plane containing the five-membered ring and the uncomplexed six-membered ring is folded away from the plane of the five metal-bonded carbons by approximately 10°. [68-70]

Neither of the fluorenyl complexes rearranged at room temperature. Upon heating (η^6-$C_{13}H_9$)$Mn(CO)_3$, **40**, under reflux, in hexane for one hour, (η^5-$C_{13}H_9$)$Mn(CO)_3$, **41**, was obtained.[69]

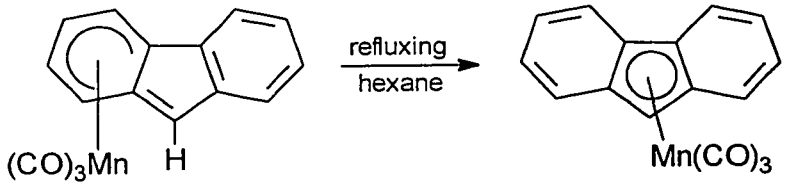

40 **41**

Scheme 1.16

Using fairly high concentrations of organic acids, the rearrangement can be reversed. [71]

Several groups have tried to prepare (η^5-$C_{13}H_9$)$Fe(C_5H_5)$ from (η^6-$C_{13}H_9$)$Fe(C_5H_5)$ by thermal rearrangement. Treichel *et al.* reported the decomposition of the iron compound upon heating.[68] On the other hand, Ustynyuk reported the rearrangement to the ferrocene analogue in 1986. The issue remains unresolved.

Metal complexes of the ligand cyclopenta[*def*]phenanthrene mirror the behaviour of the above mentioned fluorene complexes.[73] When (η^6-cppH)$Cr(CO)_3$, **42**, where cppH = cyclopenta[*def*]phenanthrene, is deprotonated at room temperature, NMR data indicate that the $Cr(CO)_3$ moiety has migrated to the five-membered ring. If the deprotonation is performed at low temperature, the complex **43**, is identified spectroscopically. Upon warming, **43** rearranges to the η^5- complex, **44**.

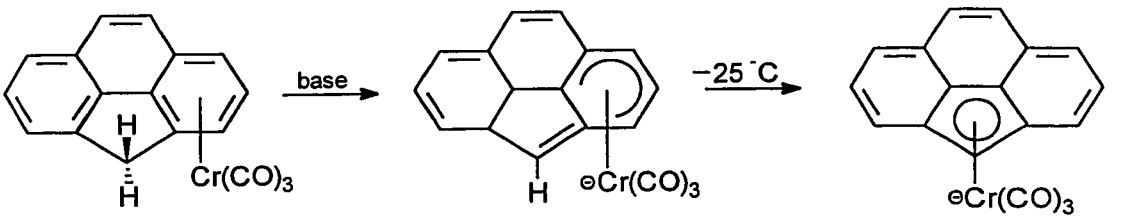

42 **43** **44**

Scheme 1.17

Deprotonation of the cation **45** at -40°C yields the intermediate **46**, which rearranges to **47** upon warming above 15°C.[73]

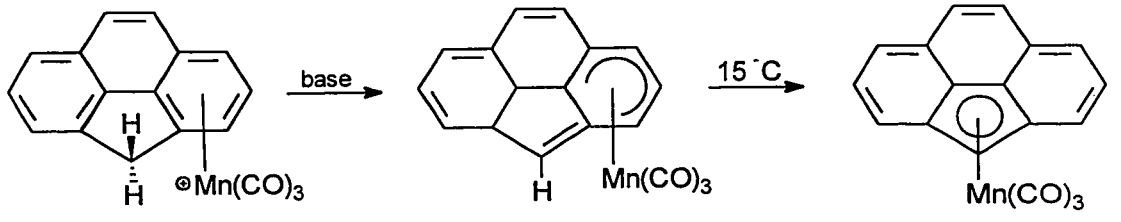

45 **46** **47**

Scheme 1.18

Deprotonation of the salt $(\eta^6$-cppH)Fe$(C_5H_5)^+PF_6^-$ yields the unstable complex $(\eta^6$-cppH)Fe(C_5H_5).[73] Attempts to thermally induce migration of iron into the five-membered ring were unsuccessful.

Most of the well characterized examples of haptotropic shifts above and in the literature involve systems in which the metal migrates between two rings which are adjacent to each other. That is, the ligands may be thought of as substituted bicyclic systems. Albright and Hoffmann presented an EHMO study of haptotropic rearrangements of polyene-ML_n complexes, in which the polyenes are bicyclic.[43]

In the tetracyclic ligand *1H*-cyclopenta[*l*]phenanthrene shown below, the potential exists for studying haptotropic shifts of organometallic complexes in which the metal centre may migrate from one ring, through a second ring and into a third.

1.4 *1H*-cyclopenta[*l*]phenanthrene

The molecule *1H*-cyclopenta[*l*]phenanthrene contains the carbon skeletons of indene, angular benzindene, phenanthrene and cyclopentadiene.

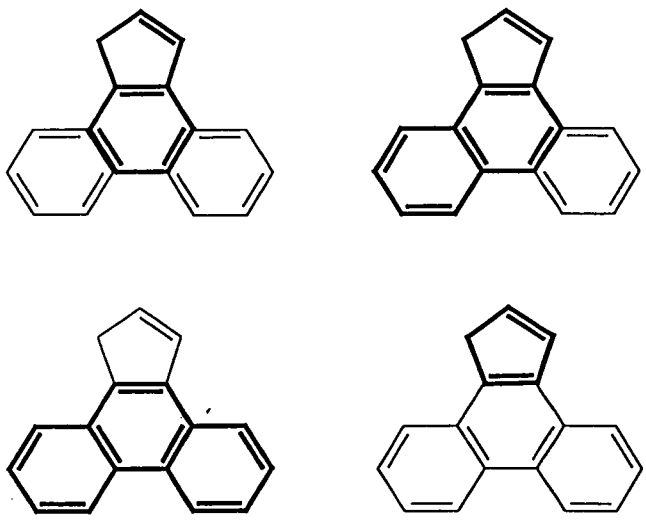

Figure 1.2

Few transition-metal complexes have been published for the angular benzindene.[47,74] Transition-metal complexes of indene, phenanthrene and cyclopentadiene display quite different chemical behaviour. Would complexes of *1H*-cyclopenta[*l*]phenanthrene behave like any of these other ligands, or something intermediate between them?

1H-cyclopenta[*l*]phenanthrene offers multiple sites for the attachment of organometallic moieties, which could bind in an η^6-, η^5-, η^4-, η^3-, η^2-, or η^1- fashion. No transition metal

complexes of *1H*-cyclopenta[*l*]phenanthrene have been reported in the literature. Aside from gas chromatographic analyses of cigarette smoke, very little is known of the organic chemistry of this ligand.

1.5 Objectives of this Thesis

We have a general interest in the preparation and characterization of transition metal complexes. In addition to the , we reasoned that intriguing metal rearrangements of the type noted above might occur. Therefore, we decided to examine the chemistry of this compound.

Although the synthesis of cyclopenta[*l*]phenanthrene is known,[75,76] it is not trivial. The molecule has now been prepared in quantities such that transition-metal complexes and silanes can be prepared.

The silyl derivative was of interest for use in the study of [1,5]-silicon migrations. We had previously looked at silicon migrations in indenyl silanes,[17,18] and wanted to look at the effect of adding one or two aromatic rings to the trimethylsilylindene system. Specifically, we wished to ascertain whether the addition of aromatic rings would lower the barrier to silicon migration around the five-membered ring.

The transition-metal complexes were of interest for studies of haptotropic shifts of organometallic moieties over polycyclic ring systems. Would metals bond to the central or a terminal six-membered ring? Moreover, upon deprotonation, would they migrate into the five-membered ring? Alternatively, would a metal bonded to the five-membered ring migrate into one of the six-membered rings upon protonation?

One might also conjecture that the two terminal six-membered aromatic rings might stabilize an intermediate η^3-structure, **48**, during ligand substitution reactions of organometallic complexes of cyclopenta[*l*]phenanthrene.

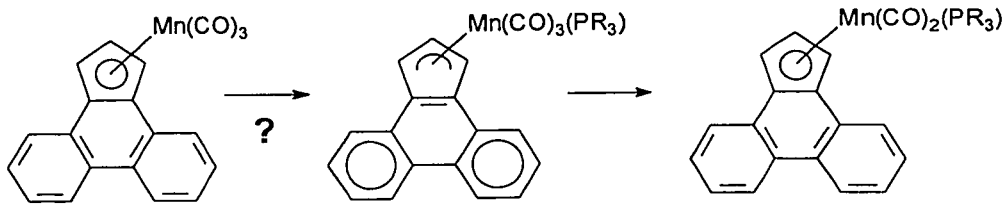

48

Scheme 1.19

For example, the above tricarbonyl monophosphine intermediate may gain the stabilization of phenanthrene, in a "super indenyl-effect", just as the analogous indenyl system gains the stability of one six-membered aromatic ring in its intermediate.[45]

Chapters Two and Three of this thesis will focus on the preparation of trimethylsilyl-benzindene and -cyclopenta[*l*]phenanthrene. The fluxional behaviour of both systems will be discussed, as will the effects of successive aromatic ring addition to trimethylsilylindene.

Chapter Four delves into the preparation and chemistry of transition-metal complexes of cyclopenta[*l*]phenanthrene in which the metal is bonded in an η^5- fashion to the ligand.

A discussion of attempts to bond transition-metals to six-membered rings of the ligand is presented in Chapter Five, along with a novel dimer of the ligand.

In Chapter Six, the preparation and fluxional behaviour of a metal-stabilized cyclopentenyl cation are presented.

Chapter Seven contains conclusions.

Finally, future work and the experimental details are contained in Chapters Eight and Nine, respectively.

CHAPTER TWO

Do Aromatic Transition States Lower Barriers to Silatropic Shifts? Calculational Results.

2.1 Introduction

One objective of the thesis was to explore the possibility of disturbing the equilibrium between organosilylindenes and their corresponding silyl-*iso*-indenes by incorporating another six-membered ring so as to maintain some aromatic character, even in the *iso*-indene isomer. For such purposes, one would expect the angular molecules **50a** and **50b** to be more effective than the linear systems **51a** and **51b**; in the *iso*-benzindene **51b** one cannot draw a conventional aromatic structure. One could envision that the stabilization provided by the aromatic group in **50** would result in a lower barrier for the [1,5]-silatropic shifts (**50a** - **50c**) than for compound **51**.

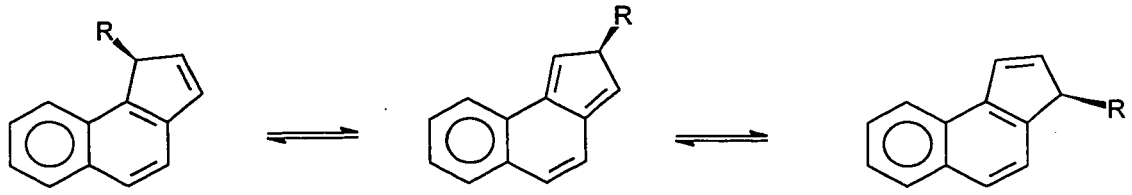

49a: R = H
50a: R = $SiMe_3$

49b: R = H
50b: R = $SiMe_3$

49c: R = H
50c: R = $SiMe_3$

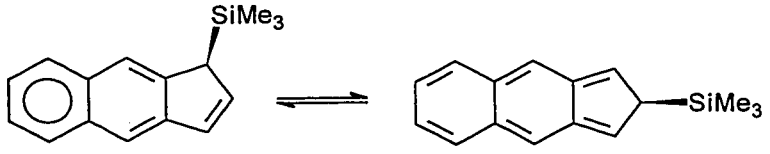

51a **51b**

Addition of a second six-membered ring, as in **53a**, would be expected to lower the barrier to silatropic migration even further, again through stabilization of the silyl-*iso*-indene intermediate **53b**, which retains aromaticity in two of the six-membered rings.

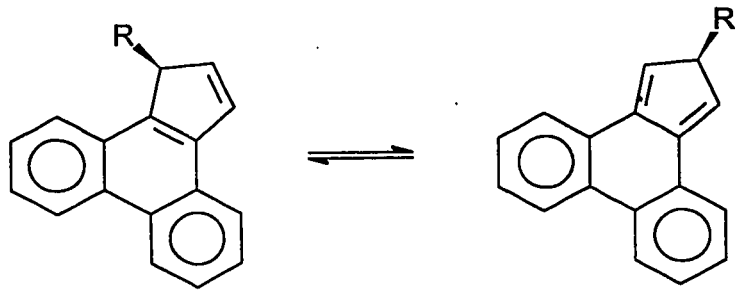

52a: R = H
53a: R = $SiMe_3$

52b: R = H
53b: R = $SiMe_3$

2.2 Results and Discussion

2.2.1 [1,5]-Silicon Shifts in Trimethylsilylindene and Trimethylsilylbenzindenes

2.2.1.1 Trimethylsilylindene

The well-characterized system trimethylsilylindene **1**, the intermediate *iso*-indene **2**, and the transition state which connects the two, were used to test the viability of a combined calculatory and experimental approach.

The energy-minimized structures were computed at the unrestricted Hartree-Fock (UHF) level using the programs AMPAC[77] and MOPAC[78], and the calculated geometries are shown in Figure 2.1. The transition state lies 26.0 kcal/mol above the energy of the starting configuration, *i.e.* trimethylsilylindene **1**, while the *iso*-indene intermediate **2** lies in a potential well 7.9 kcal/mol above the ground state. These theoretical results agree well with the experimentally determined activation energy barrier of 24 kcal/mol.[12,14] These data also suggest that the intermediate *iso*-indene should be sufficiently long-lived for Diels-Alder trapping reactions to be competitive with a

second [1,5]-silatropic shift which regenerates trimethylsilylindene. This is in accord with the experimentally observed formation of the Diels-Alder adduct, **3**, derived from trimethylsilyl-*iso*-indene and tetracyanoethylene; this adduct has been characterized not only spectroscopically[4,9,10] but also by X-ray crystallography.[16]

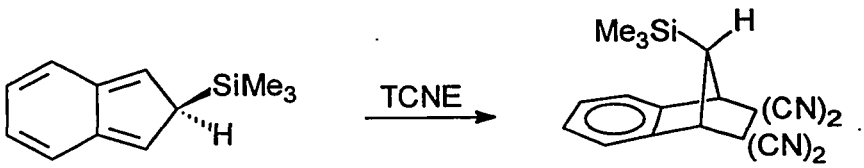

3

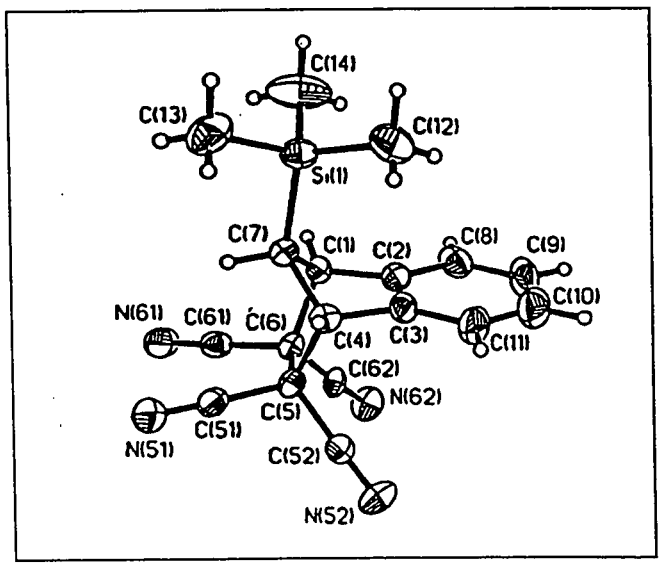

X-ray Crystal Structure of Trimethylsilylindene-Tetracyanoethylene Adduct 3

2.2.1.2 Angular Trimethylsilylbenzindene

Encouraged by the correlation between experimental and theoretical results, AMPAC calculations were then carried out on the angular and linear trimethylsilylindenes, **50** and **51**,

respectively, and also for trimethylsilylcyclopenta[*l*]phenanthrene **53**. In the linear trimethylsilylbenzindene, **51**, the activation enthalpy for silatropic shifts is calculated to be 26.8 kcal/mol. This resembles both the experimental and theoretical results for the trimethylsilylindene system. Note that, in both of these systems, one cannot draw a structure in which aromatic character is retained in either the *iso*-indene intermediates, **2** and **51b**, or the transition states. In contrast, in the angular benzindene system, one six-membered ring may retain its aromatic character in the *iso*-indene, **50b**, and in the transition state; one might envisage that this situation could result in a lowering of the barrier to silatropic migration. The computational results indicate that the two different transition states for the trimethylsilyl-benzindene system, **50**, lie 22.9 and 23.9 kcal/mol above the two isomeric ground state configurations, as shown in Figure 2.2.

2.2.1.3 Trimethylsilylcyclopenta[*l*]phenanthrene

Incorporation of a second additional benzene ring to the trimethylsilylindene skeleton gives the molecule trimethylsilylcyclopenta[*l*]phenanthrene **53a**. In this system, one would expect the silatropic shift to occur with retention of considerable aromatic character in two six-membered rings; this should result in a further lowering of the barrier to silatropic migrations around the 5-membered ring. Indeed, the calculated $\Delta H^{\ddagger}$ was found to be 21.6 kcal/mol, and the intermediate *iso*-indene lies in a potential well only 2.2 kcal/mol above the ground state, as shown in Figure 2.3.

2.2.2 [1,5]-Hydrogen Shifts in Indene and Cyclopenta[*l*]phenanthrene

Semi-empirical calculations were also carried out on the hydrocarbons indene and cyclopenta[*l*]phenanthrene. In indene, **54a**, the activation enthalpy for [1,5]-hydrogen migrations is calculated to be 46.5 kcal/mol, as shown in Figure 2.4. This is in accord with experimental results, in which products arising from [1,5]-hydrogen shifts are evident only upon heating above 150°C. Again, one cannot draw a structure in which aromatic character is retained in either the *iso*-indene

intermediate **54b**, or the transition state. The *iso*-indene intermediate is calculated to lie in a potential well 9.0 kcal/mol above the ground state.

Incorporation of two benzene rings to the indene skeleton gives the molecule cyclopenta[*l*]phenanthrene, **55a**. One might expect a [1,5]-hydrogen migration in this system to proceed with retention of significant aromatic character in the two terminal six-membered rings, which should result in a lower barrier for hydrogen shifts around the 5-membered ring. The calculated $\Delta H^{\ddagger}$ is 43.3 kcal/mol, but more noteworthy is the fact that the *iso*-indene type intermediate, **55b**, sits in a potential well only 4.3 kcal/mol above the ground state, as shown in Figure 2.5. Thus, the intermediate for a hydrogen-shift in cyclopenta[*l*]phenanthrene appears to be considerably more stable than for the analogous indene system.

In conclusion, the theoretical results obtained suggest that successive incorporation of one or two extra six-membered rings to trimethylsilylindene lowers the barrier to *iso*-indene formation, thereby enhancing the rate of silicon migration over the polycyclic ligands. In addition, the *iso*-indene type intermediate resulting from a [1,5]-hydrogen migration in the hydrocarbon cyclopenta[*l*]phenanthrene is predicted to be more stable relative to the ground state molecule than for the analogous indene system.

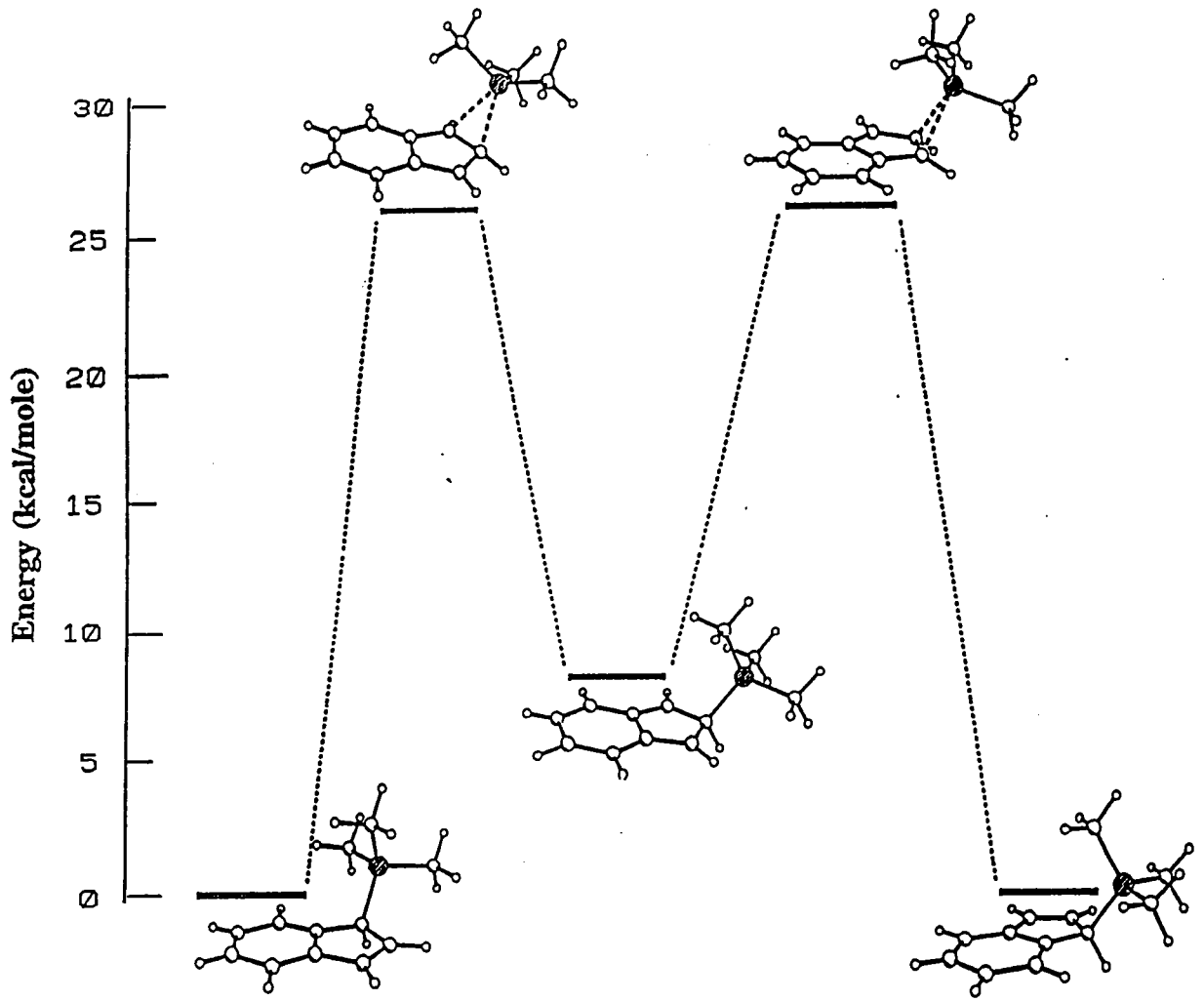

Figure 2.1 Energy profile for the [1,5]-$SiMe_3$ shifts in trimethylsilylindene

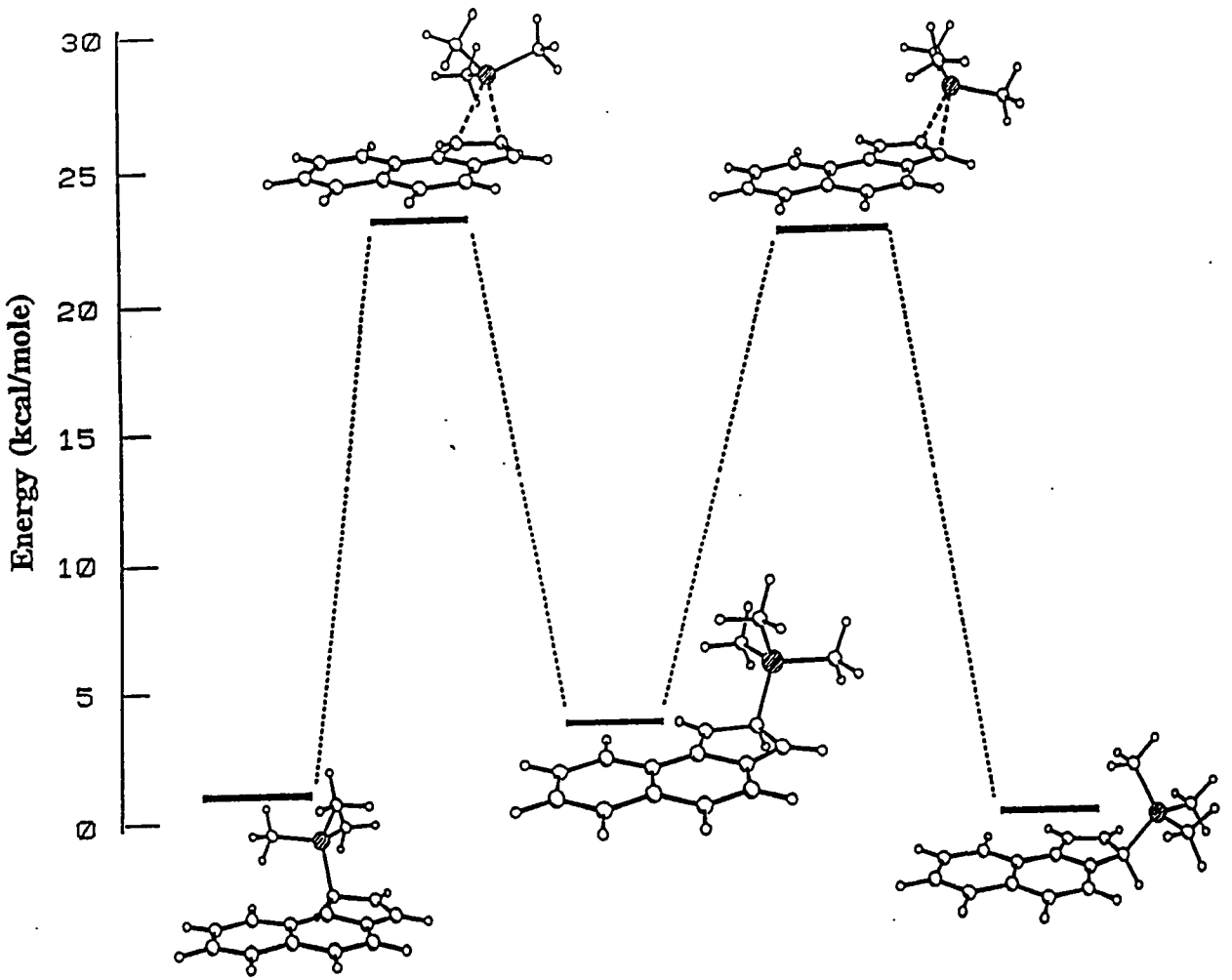

Figure 2.2 Energy profile for the [1,5]-$SiMe_3$ shifts in the angular trimethylsilylindene

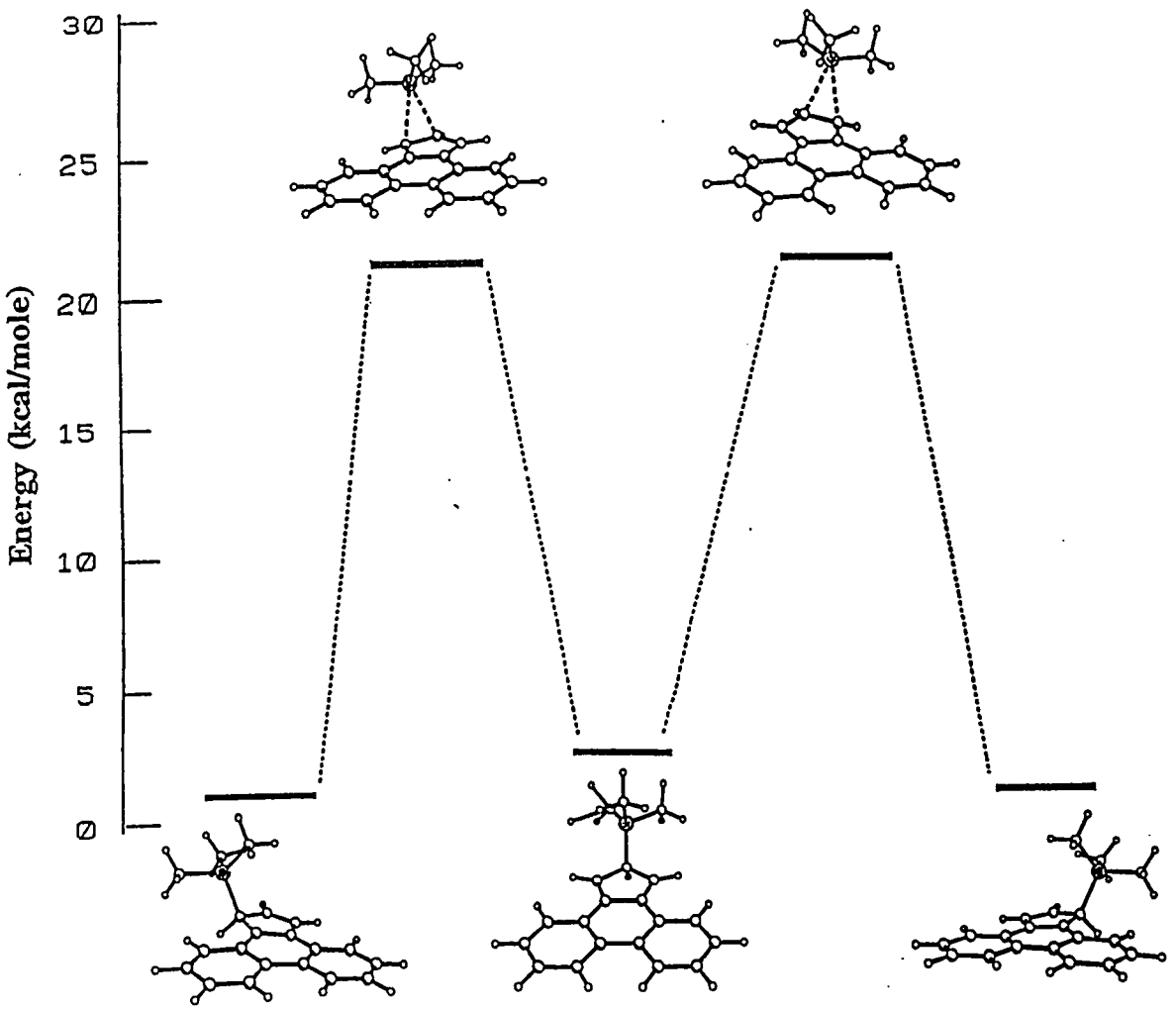

Figure 2.3 Energy profile for the [1,5]-$SiMe_3$ shifts in trimethylsilylcyclopenta[*l*]phenanthrene

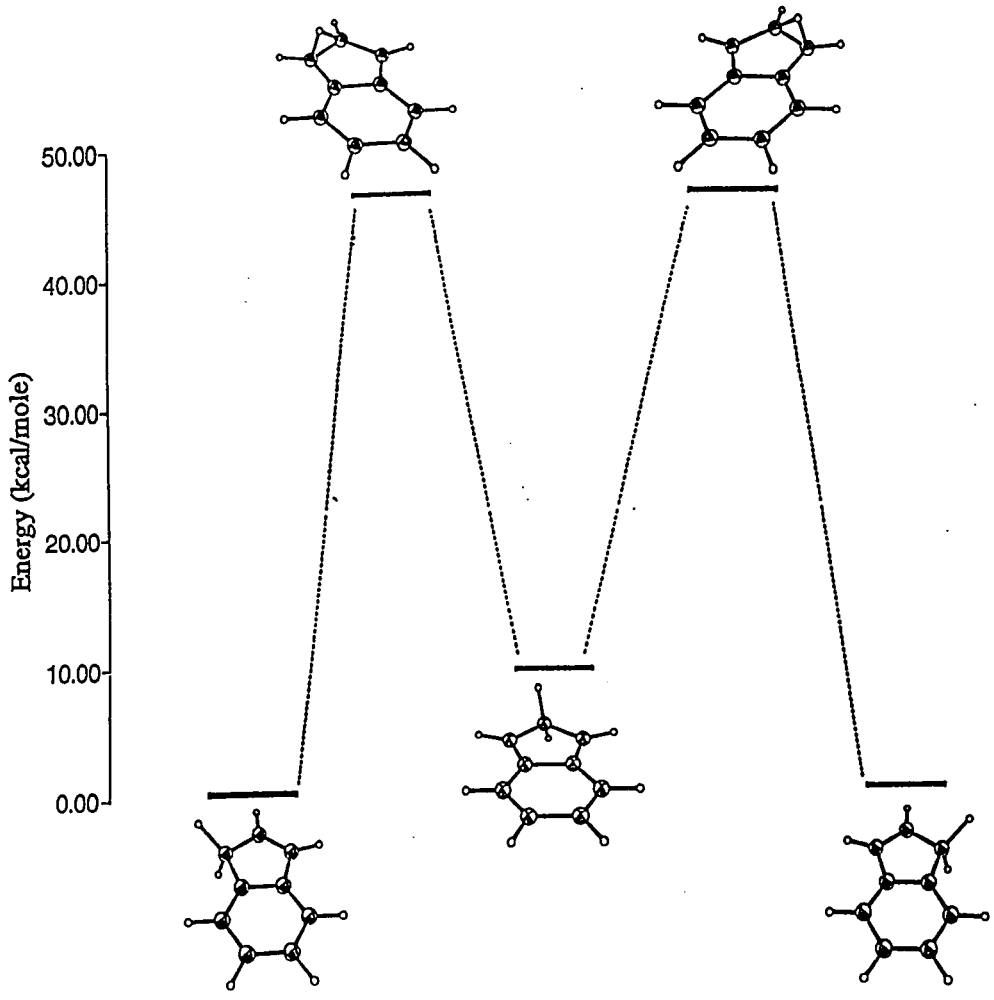

Figure 2.4 Energy profile for the [1,5]-H shifts in indene

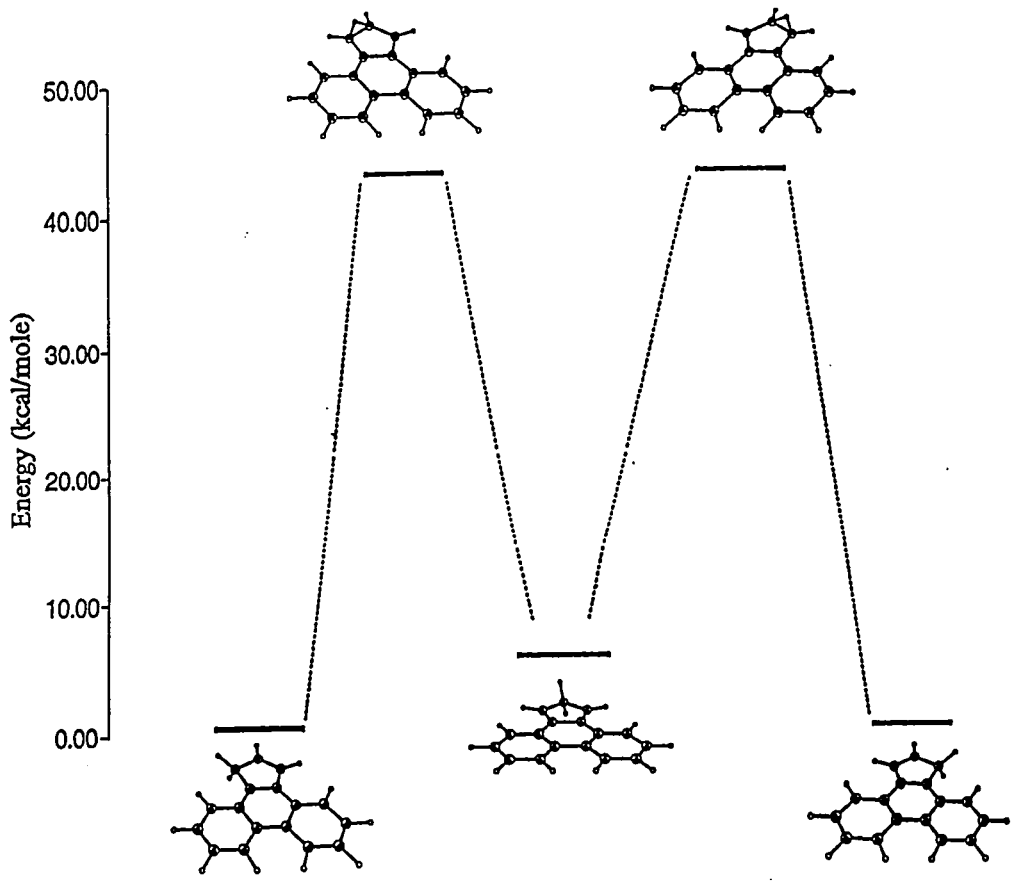

Figure 2.5 Energy profile for the [1,5]-H shifts in cyclopenta[*l*]phenanthrene

CHAPTER THREE

Preparation of Trimethylsilylbenzindenes and Elucidation of Their Molecular Dynamics

3.1 Introduction

In order to test the hypothesis that the barrier to migration of a trimethylsilyl group around the five-membered ring of trimethylsilylindene could be lowered by strategic incorporation of additional aromatic rings to the system, we decided to synthesize the angular trimethylsilylbenzindenes, **50a**, **50c**, and trimethylsilylcyclopenta[*l*]phenanthrene, **53a**.

3.2 Results and Discussion

3.2.1 Angular Trimethylsilylbenzindenes

As shown in Figure 3.1, Friedel-Crafts acylation of naphthalene, using maleic anhydride followed by cyclization, decarboxylation, ketone reduction, and elimination of water, yielded the angular benzindenes **49a** and **49c**. Since trimethylsilylation of these alkenes would result in their interconversion, the two isomers of **49** were not separated. Lithiation, followed by addition of trimethylsilyl chloride gave the angular trimethylsilylbenzindenes **50a** and **50c**. The molecules were characterized by mass spectrometry, and also by their one- and two-dimensional NMR spectra. The numbering schemes for the molecules are presented below, and the NMR data are collected in Table 3.1.

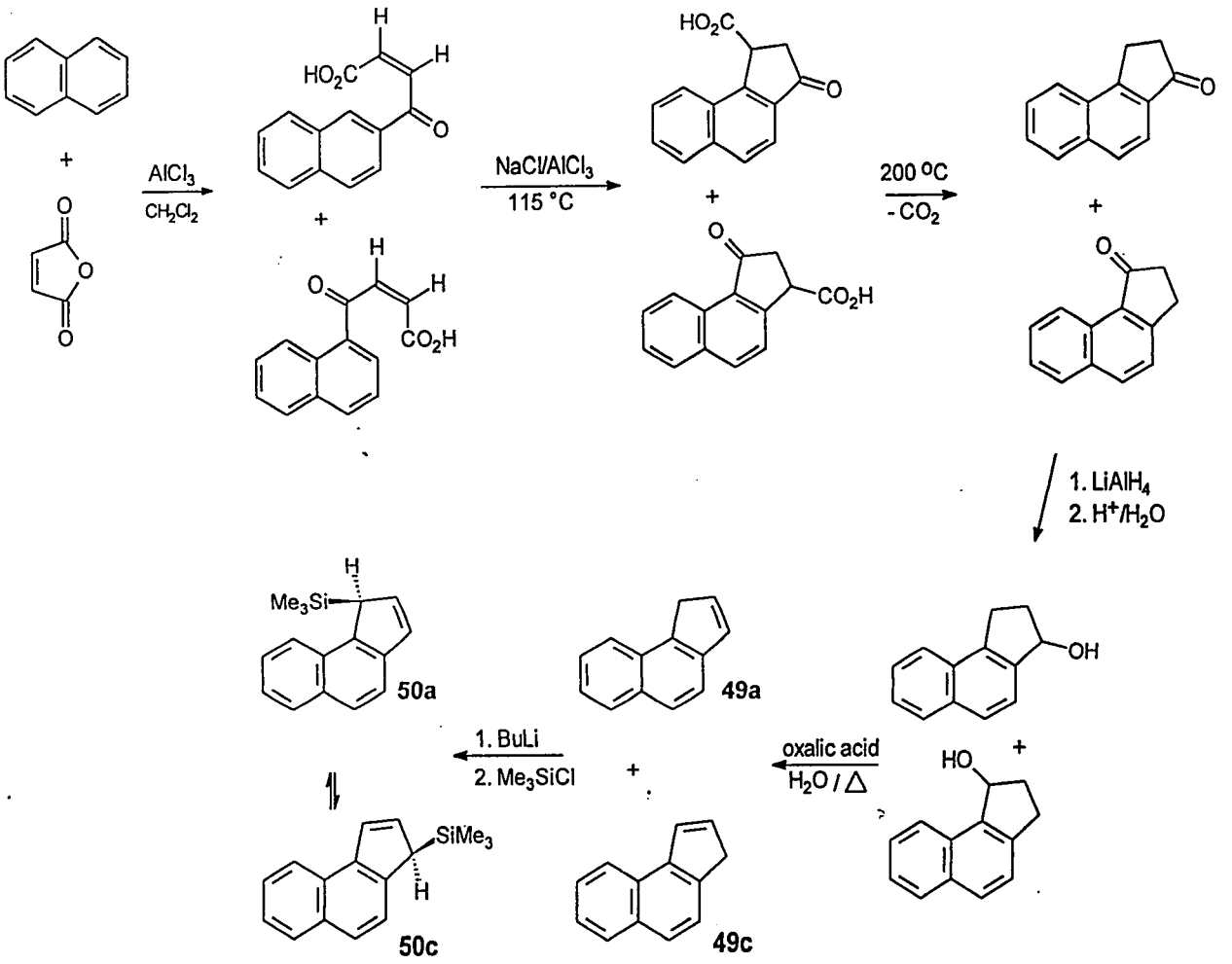

Figure 3.1 Synthesis of Angular Trimethylsilylbenzindenes 50a and 50c.

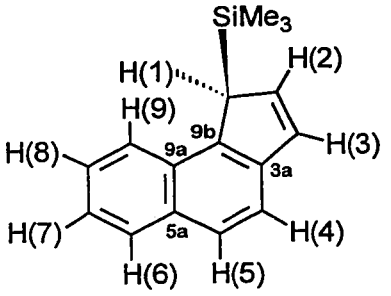

50a

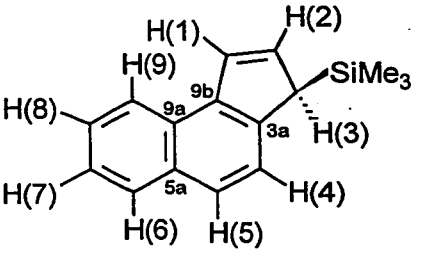

50c

Table 3.1 ^{1}H, ^{13}C and ^{29}Si NMR Data (ppm) for the Angular Trimethylsilylbenzindenes 50a and 50c.

		50a	**50c**
$SiMe_3$	^{1}H	-0.20 (s)	-0.15 (s)
	^{13}C	-0.7	-2.4
	^{29}Si	3.2	3.6
1	^{1}H	3.81 (tr, 1.6 Hz)	7.44 (d, 5.1 Hz of d, 1.3 Hz)
	^{13}C	48.7	129.6
2	^{1}H	6.58 (d, 5.2 Hz of d, 1.8 Hz)	6.63 (d, 5.1 Hz of d, 1.7 Hz)
	^{13}C	135.7	135.5
3	^{1}H	6.93 (d, 5.2 Hz of d, 1.3 Hz)	3.48 (tr, 1.5 Hz)
	^{13}C	129.3	48.7
3a	^{13}C	141.0	143.1
4	^{1}H	6.69 (d, 5.0 Hz)	7.49 (d, 8.4 Hz)
	^{13}C	137.9	122.1
5	^{1}H	7.59 (d, 5.0 Hz)	7.56 (d, 8.4 Hz)
	^{13}C	126.4	124.5
5a	^{13}C	132.1	132.6
6	^{1}H	7.82 (d, 8.2 Hz)	7.77 (d, 7.5 Hz)
	^{13}C	125.4	128.8
7	^{1}H	7.33 - 7.29 (m)	7.33 - 7.29 (m)
	^{13}C	124.8	124.8
8	^{1}H	7.36 - 7.33 (m)	7.36 - 7.33 (m)
	^{13}C	125.7	125.7
9	^{1}H	8.14 (d, 8.2 Hz)	8.08 (d, 7.6 Hz)
	^{13}C	124.3	124.2
9a	^{13}C	—	137.3

9b	^{13}C	145.2	140.5

3.2.2 Bis(trimethylsilyl)benzindene

When the benzindenes **49** were treated with two moles of butyllithium followed by trimethylsilylchloride, bis(trimethylsilyl)benzindene **58**, (Scheme 3.1) was obtained. The molecule was characterized by mass spectrometry and one- and two-dimensional NMR spectroscopy. The numbering scheme for the molecule is presented below, and the NMR data are collected in Table 3.2.

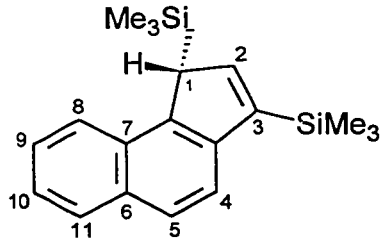

58

Table 3.2 ^{1}H NMR Data (ppm) for Angular bis(Trimethylsilyl)benzindene **58**.

	Chemical Shift (ppm)
$SiMe_3$ (C1)	-0.03 (s)
$SiMe_3$ (C3)	0.10 (s)
H-1	1.85 (d)
H-2	3.86 (d)
H-5	6.90 (d)
H-10	7.49 (d)
H-4	7.69 (d)
H-8	8.02 (d)
H-9	8.23 (d)

Presumably, the initially formed molecule **56**, with its two geminal $SiMe_3$ groups, is sterically crowded and so undergoes silicon migrations *via* the *iso*-benzindenes **57**. This gives the

favoured 1,3-bis(trimethylsilyl) isomer **58**, in which the interaction between the Me_3Si substituent at C(3) with the in-plane hydrogens is minimized.

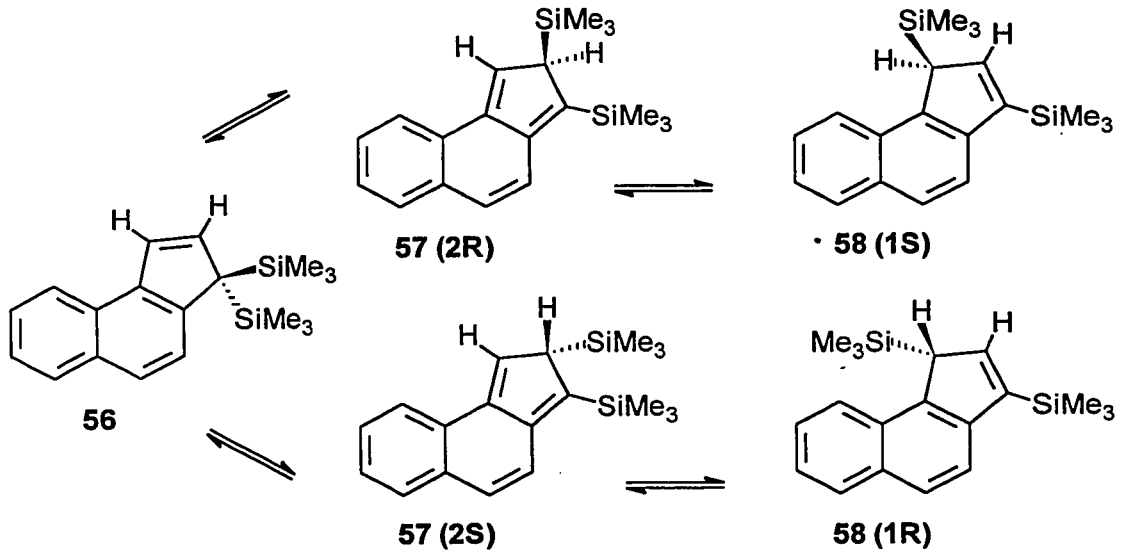

Scheme 3.1

The alternative geminal isomer **59** would yield **60**, which has been shown by molecular modelling to lead to severe steric hindrance with an aromatic hydrogen in the terminal six-membered ring. Space-filling models of the bis(trimethylsilyl)benzindenes **58** and **60** are shown in Figure 3.2.

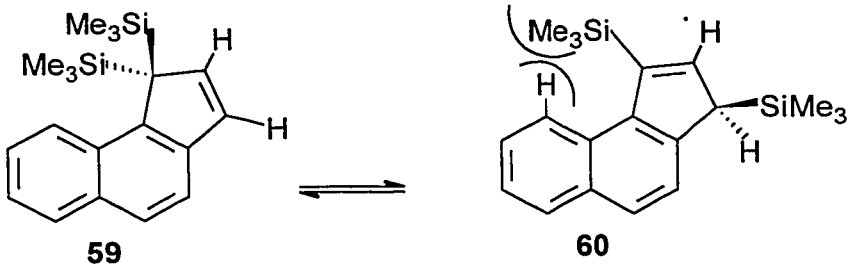

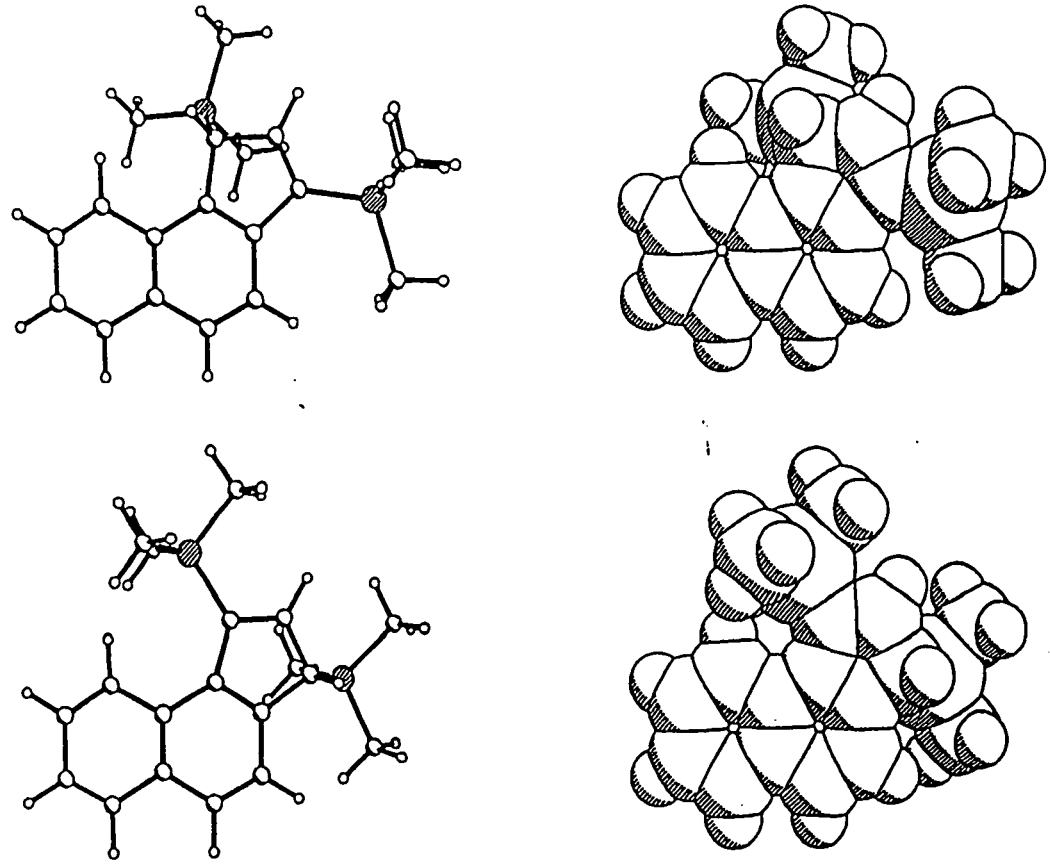

Figure 3.2 Space-filling models of the bis(trimethylsilyl)benzindenes 58 and 60.

Complex **58** exhibits ^1H NMR resonances at δ -0.03 and δ 0.10 for the two Me_3Si moieties and, even at 140°C, these peaks retain their sharp character; since the coalescence temperature must be higher than 413 K, the Gutowsky-Holm approximation[79] yields a minimum activation energy of 21 kcal/mol for the equilibration of the trimethylsilyl environments. In an attempt to evaluate the barrier, we carried out a series of single selective inversion experiments in which one of the Me_3Si signals was inverted and the return of that peak to equilibrium, and also that of the other Me_3Si peak was monitored. However, at the temperatures accessible to the instrument, it was not possible to detect exchange between the Me_3Si sites; thus we are unable to give a reliable barrier for the interconversion of the two trimethylsilyl environments which can only occur via the formation of the sterically crowded geminal bis-Me_3Si complex **56**. We note an earlier report that the attempted synthesis of 1,1-bis(trimethylsilyl)indene, **61a**, actually yields an appreciable amount of the 1,3 isomer, **61b**. However, these molecules showed no evidence of interconversion even at 206°C.[12-14] In the same vein, the Me_3Si groups in 1,2-bis(trimethylsilyl)indene, **62**, only show evidence of fluxional behavior at ≈ 140°C, and the reported barrier is ≈ 26 kcal/mol.[12-14]

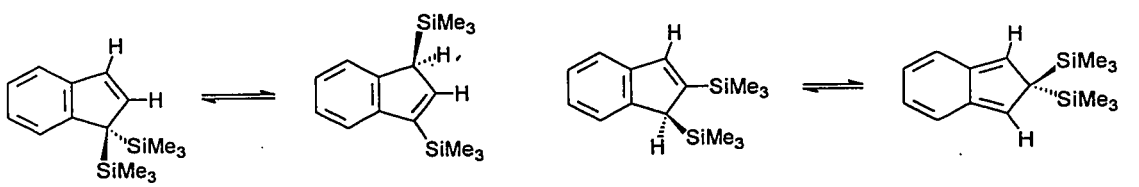

61a **61b** **62**

Even though we are unable to provide a reliable estimate of the barrier to the interconversion of the enantiomers of **58**, these experimental results do provide some insight into the chemical behavior of this system. The very ready incorporation of a second Me_3Si substituent to form the bis(trimethylsilyl)benzindene, **56**, is in accord with previous observations that carbanionic centers adjacent to Me_3Si substituents are particularly favored.[80] The facile migration of a trimethylsilyl group, as in **56** via **57** to **58**, even at room temperature, is indicative of a lowered barrier for silatropic shifts. The fact that **58** is observed, and that the alternative structure **60** is apparently

not formed, again lends credence to the idea of a relatively rapid interconversion of the mono-silylated benzindenes **50a** and **50c**.

3.2.3 Trimethylsilylcyclopenta[*l*]phenanthrene

We repeated the original synthesis[75] of cyclopenta[*l*]phenanthrene; however, it did not yield a pure product, but instead a mixture of the desired alkene, **55**, along with alkane and ketone. However, the modified procedure of Eliasson and coworkers[76] allows the isolation of pure cyclopenta[*l*]phenanthrene. As depicted in Figure 3.3, condensation of phenanthrenequinone with ethyl acetoacetate, subsequent reduction with HI, condensation with tosyl hydrazine to give the tosylhydrazone and, finally, elimination of N_2 and the tosylate anion yielded the alkene, **55**. Again, lithiation, followed by addition of trimethylsilyl chloride gave the silane **53a**. The product is sensitive to the presence of water which leads to rapid loss of the silyl moiety, presumably via protonation of the double bond of the allyl silane followed by nucleophilic attack by H_2O at silicon to liberate trimethylsilanol. The silylated molecule, **53a**, was characterized by mass spectrometry, and by its one- and two-dimensional NMR spectra. The numbering scheme for the molecule is shown below. NMR data are collected in Table 3.2.

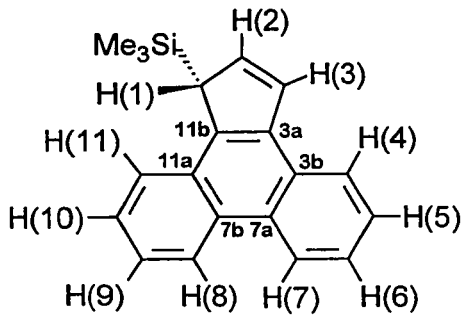

53a

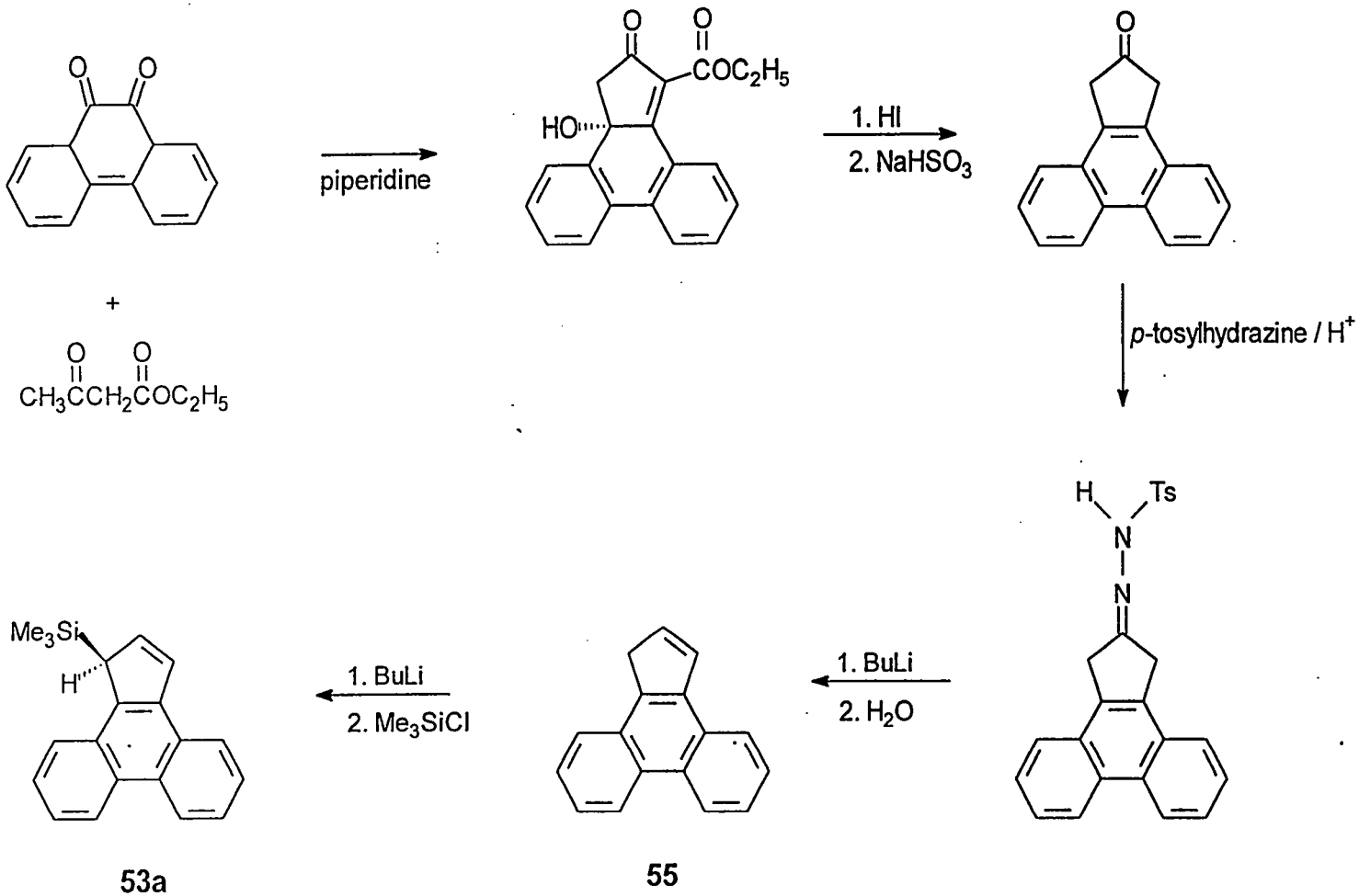

Figure 3.3 Synthesis of Trimethylsilylcyclopenta[1]phenanthrene 53a.

Table 3.2 ^{1}H, ^{13}C and ^{29}Si NMR Data (ppm) for Trimethylsilylcyclopenta[*l*]phenanthrene 53

		Chemical Shift (ppm)
$SiMe_3$	^{1}H	-0.05 (s)
	^{13}C	-1.6
	^{29}Si	5.1
1	^{1}H	4.40 (tr, 1.3 Hz)
	^{13}C	49.2
2	^{1}H	6.92 (d, 5.2 Hz of d, 1.7 Hz)
	^{13}C	136.3
3	^{1}H	7.56 (d, 5.2 Hz of d, 1.0 Hz)
	^{13}C	126.6
3a	^{13}C	138.4
3b	^{13}C	129.8
4	^{1}H	8.26 (d, 8.3 Hz of d, 1.5 Hz of d, 0.5 Hz)
	^{13}C	124.7
5	^{1}H	7.66 (d, 8.3 Hz of d, 6.8 Hz of d, 1.5 Hz)
	^{13}C	125.8
6	^{1}H	7.63 (d, 8.3 Hz of d, 6.8 Hz of d, 1.5 Hz)
	^{13}C	126.8
7	^{1}H	8.76 (d, 8.3 Hz of d, 1.5 Hz of d, 0.5 Hz)
	^{13}C	123.6
7a	^{13}C	128.6
7b	^{13}C	129.6
8	^{1}H	8.73 (d, 8.3 Hz of d, 1.8 Hz of d, 0.6 Hz)
	^{13}C	123.8
9	^{1}H	7.57 (d, 8.3 Hz of d, 6.7 Hz of d, 1.8 Hz)
	^{13}C	126.3
10	^{1}H	7.60 (d, 8.3 Hz of d, 6.7 Hz of d, 1.8 Hz)
	^{13}C	125.2
11	^{1}H	8.03 (d, 8.3 Hz of d, 1.8 Hz of d, 0.6 Hz)
	^{13}C	126.0
11a	^{13}C	129.0
11b	^{13}C	140.7

3.3 Measurement of the barriers for silatropic shifts

The molecular dynamics of the two new mono-trimethylsilylated systems were monitored by means of a variety of NMR techniques. In both systems, the exchange pathways in the slow exchange regime were determined by recording their 2-D ^{1}H EXSY spectra.[81] The exchange rates in the slow exchange regime were then measured by single selective inversion relaxation experiments at several temperatures. For the tetracyclic system, **53**, the barrier was sufficiently low that the intermediate exchange regime was also accessible. Consequently, rates obtained from lineshape analysis were combined with the rates obtained by selective inversion experiments to determine a barrier to silatropic migration for **53**.

For the angular trimethylsilylbenzindene, **50**, the 2-D ^{1}H EXSY spectrum was recorded at 102°C, at which temperature the isomers **50a** and **50c** were starting to exchange on the ^{1}H NMR timescale. The spectrum reveals cross-peaks between the sp^3-bonded H at C(3) in **50c** and the sp^2-bonded H at C(3) in **50a**. In addition, the sp^2-bonded H at C(1) in **50c** exchanges with the sp^3-bonded H at C(1) in **50a**. The methyl signals from the two isomers also exchange with each other. Subsequently, the ^{1}H methyl signal of **50c** was selectively inverted and the return of that peak to equilibrium, and also of the exchanging methyl signal of **50a**, were monitored. The time dependence of the z-magnetization of these two signals was fitted using a nonlinear least-squares program, and rate constants were extracted for several temperatures. Even though rate constants were obtainable only over a relatively narrow range of temperatures, an estimate of the barrier to silatropic migration around the five-membered ring of the angular benzindene may be obtained from a plot of *ln k/T* versus *1/T*. The value of $\Delta H^{\ddagger}$ so obtained was 21.5 ± 0.5 kcal/mol, and $\Delta S^{\ddagger}$ was -1.4 ± 1.4 cal mol^{-1}K^{-1}; these results are in excellent agreement with the barrier given by our semi-empirical calculations.

In the case of the trimethylsilyldibenzindene, **53**, the barrier to silicon migration was substantially lower than for the angular benzindene, **50**, (or for indene itself) and so it was

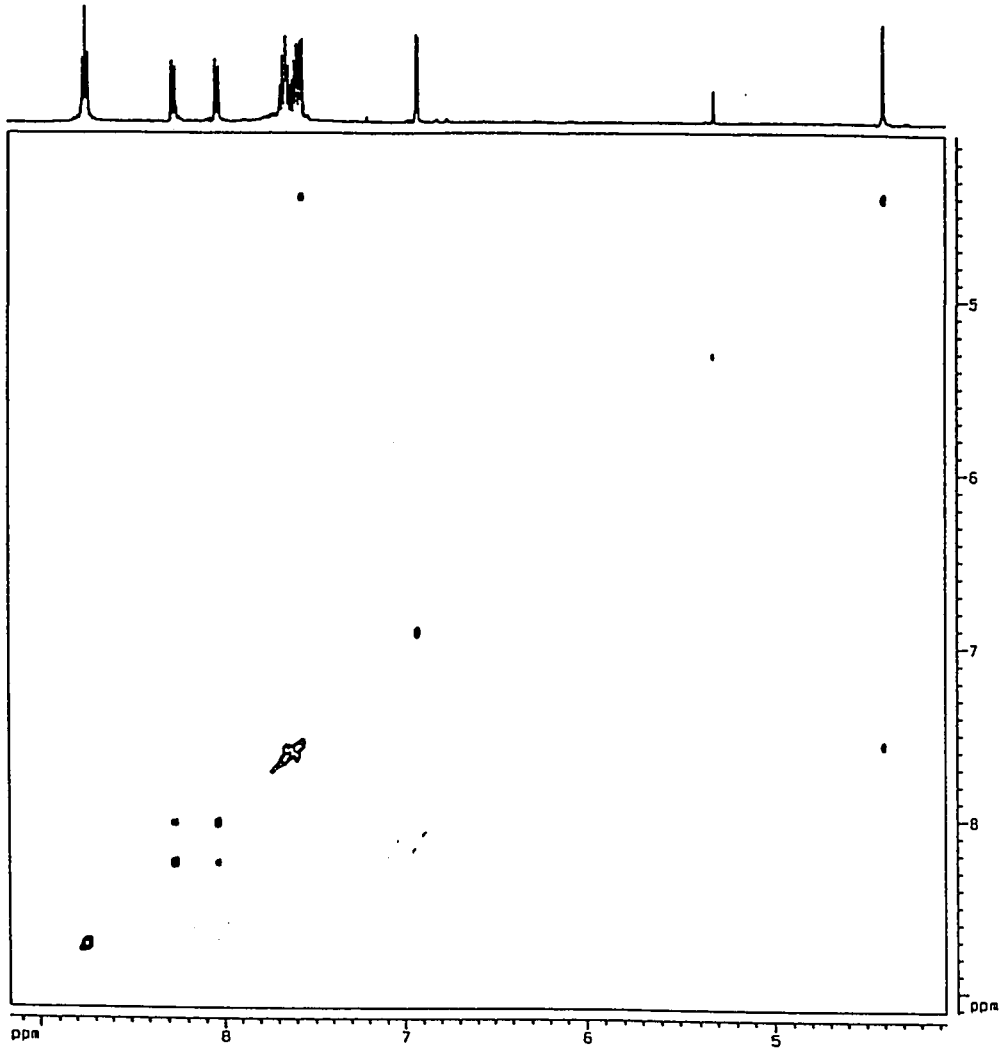

Figure 3.4 ^{1}H - ^{1}H EXSY Spectrum at 300K for trimethylsilylcyclopenta[*l*]phenanthrene, 53, with mixing time 0.7 s.

possible to acquire a 2-D ^{1}H EXSY spectrum at ambient temperature. The spectrum (Figure 3.4) reveals cross-peaks between the following pairs of hydrogens: H(1) and H(3), H(4) and H(11), H(5) and H(10), H(6) and H(9), H(7) and H(8), indicating that there is a time-averaged mirror plane through the molecule. The ^{13}C EXSY spectrum shows exchange between the carbon atoms that the above hydrogens are bonded to, and also between the following pairs of quaternary carbons: C(3b) and C(11a), C(3a) and C(11b) and between C(7a) and C(7b). In order to obtain rate constants, the H(4) signal was inverted and the return of that peak to equilibrium, and also of the exchanging H(11) signal, were monitored. The data were processed as described above for the angular benzindene system.

In the previously described indene and benzindene systems, the silicon migration barriers were sufficiently large that conventional NMR line-broadening techniques were ineffective since the peaks did not coalesce at accessible temperatures. However, for **53**, the variable-temperature ^{1}H (Figure 3.5) and ^{13}C NMR spectra exhibited normal coalescence behavior over the temperature range 30°C to 90°C. With the exchange mechanism in hand from the 2-D ^{1}H and ^{13}C EXSY spectra, the ^{1}H and ^{13}C 1-D NMR spectra of **53** were simulated by adjusting the rate constants until a good fit between the calculated and experimental spectrum at each temperature was obtained. A plot of *ln k/T* versus *1/T* yielded values of 15.2 ± 0.2 kcal mol^{-1} and -8.2 ± 0.6 cal $mol^{-1}K^{-1}$, for $\Delta H^{\ddagger}$ and $\Delta S^{\ddagger}$, respectively. As predicted by the unrestricted Hartree-Fock (UHF) calculations, the barrier towards silatropic shifts in the tetracyclic system, **53**, is lower than is found for the angular benzindene, **50**, in which only one six-membered ring retains its aromaticity.

The results of these calculations, together with the experimental data, indicate that the successive incorporation of one, or even better, two extra six-membered rings to the indenyl system lowers the barrier to *iso*-indene formation, with a consequent enhancement of the rate of silatropic shifts over the polycyclic ring systems. These results are summarized in Figure 3.6. Furthermore, in each case the [1,5]-silatropic shift mechanism was confirmed by Diels-Alder

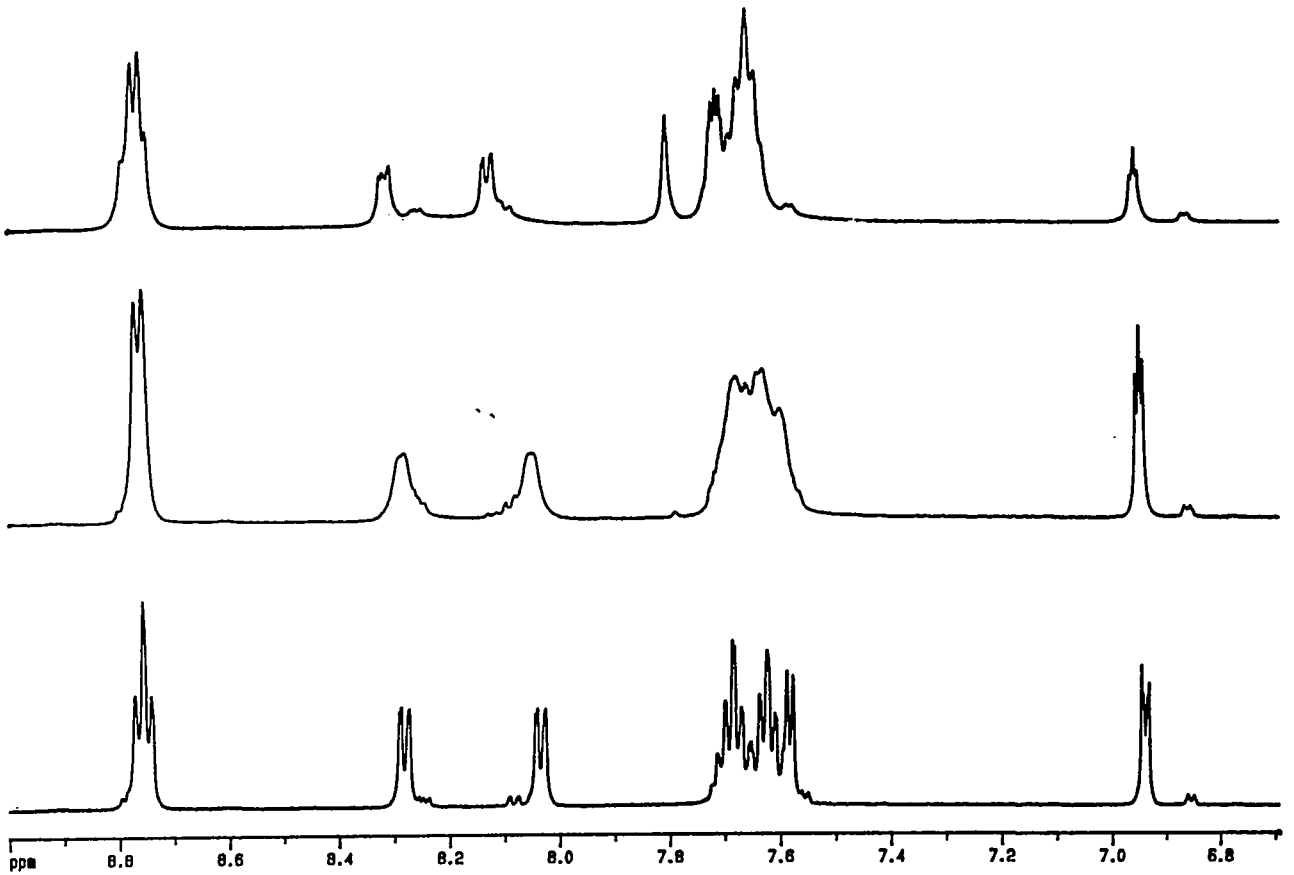

Figure 3.5 Variable Temperature ^{1}H Spectra for Trimethylsilylcyclopenta[*l*]phenanthrene

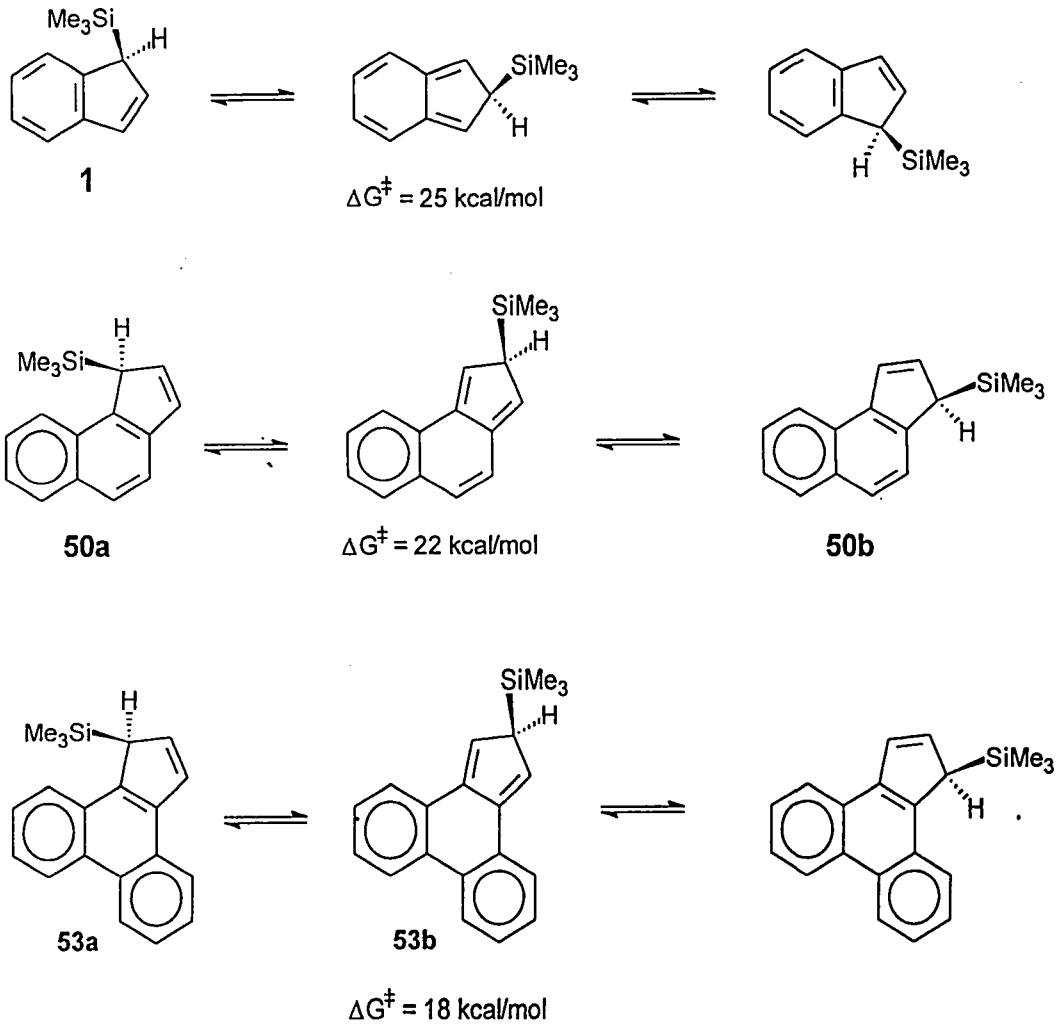

Figure 3.6 Barriers to Trimethylsilyl Migrations in Trimethylsilylindene and Derivatives

trapping of the corresponding tetracyanoethylene adducts, **63** and **64**. NMR data for these two adducts are presented in Table 3.3.

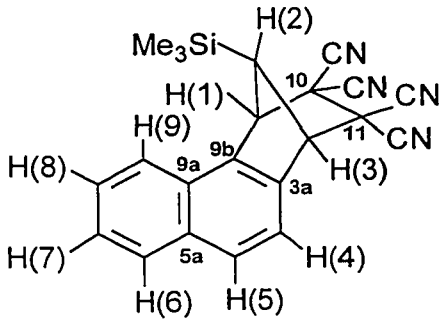

63

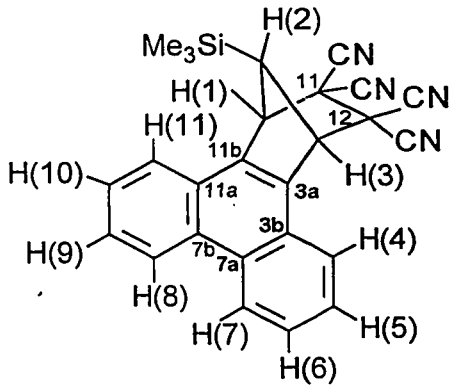

64

Table 3.3 ^{1}H, ^{13}C and ^{29}Si NMR Data (ppm) for the Angular Trimethylsilylbenzindene + TCNE Adduct **63**

		Chemical Shift (ppm)
$SiMe_3$	^{1}H	-0.26 (s)
	^{13}C	-1.8
	^{29}Si	-2.5
1	^{1}H	4.90 (m)
	^{13}C	58.9
2	^{1}H	2.23 (m)
	^{13}C	51.6
3	^{1}H	4.47 (m)
	^{13}C	61.7
3a	^{13}C	137.0
4	^{1}H	7.60 (d, 8.4 Hz)
	^{13}C	121.1
5	^{1}H	7.96 (d, 8.4 Hz)
	^{13}C	122.7
5a	^{13}C	128.7
6	^{1}H	7.96 (d, 8.4 Hz)
	^{13}C	131.4

7	^{1}H	7.67 (tr, 7.3 Hz, of d 1.3 Hz)
	^{13}C	128.6
8	^{1}H	7.57 (tr, 7.5 Hz, of d 1.1 Hz)
	^{13}C	127.5
9	^{1}H	7.94 (d, 8.2 Hz, of d 1.4 Hz)
	^{13}C	129.4
9a	^{13}C	133.9
9b	^{13}C	136.0
10	^{13}C	50.0
11	^{13}C	49.5
ax CN	^{13}C	110.3, 110.1
eq CN	^{13}C	112.5, 112.4

Table 3.4 ^{1}H, ^{13}C and ^{29}Si NMR Data (ppm) for the Trimethylsilylcyclopenta[*l*]phenanthrene + TCNE Adduct **64**

		Chemical Shift (ppm)
$SiMe_3$	^{1}H	-0.31
	^{13}C	-1.7
	^{29}Si	2.1
1	^{1}H	5.39 (d, 1.1 Hz)
	^{13}C	60.5
2	^{1}H	2.32 (tr, 1.1 Hz)
	^{13}C	52.3
3	^{1}H	5.39 (d, 1.1 Hz)
	^{13}C	60.5
3a	^{13}C	138.1
3b	^{13}C	131.8
4	^{1}H	8.29 (m)
	^{13}C	125.8
5	^{1}H	7.81 (m)
	^{13}C	129.3
6	^{1}H	7.81 (m)
	^{13}C	129.0
7	^{1}H	8.87 (m)
	^{13}C	124.9
7a	^{13}C	128.0
7b	^{13}C	128.0

8	^{1}H	8.87 (m)
	^{13}C	124.9
9	^{1}H	7.81 (m)
	^{13}C	129.0
10	^{1}H	7.81 (m)
	^{13}C	129.3
11	^{1}H	8.29 (m)
	^{13}C	125.8
11a	^{13}C	131.8
11b	^{13}C	138.1
12	^{13}C	51.3
13	^{13}C	51.3
ax CN	^{13}C	112.5
eq CN	^{13}C	114.2

CHAPTER FOUR

η^5-Transition Metal Complexes of Cyclopenta[*d*]phenanthrene

4.1 Introduction

The availability of cyclopenta[*d*]phenanthrene, **55**, prompted us to prepare a series of transition metal complexes of this ligand with a view to comparing its organometallic chemistry with that of indene.

Indenyl-metal complexes continue to attract considerable attention. The "indenyl effect' is predicated on the ability of the ML_n moiety to adopt an η^3-structure, **21**, with concomitant development of aromatic character in the transition state.

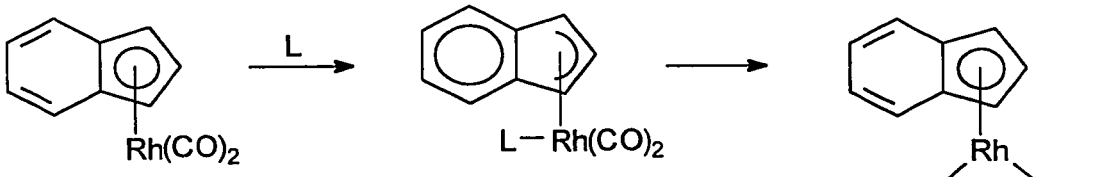

20 **21**

In similar fashion, η^6- to η^5- haptotropic shifts in the cyclopenta[*def*]phenanthrene system are greatly facilitated by the development of a 10π aromatic (naphthalene-type) transition state, **66**.

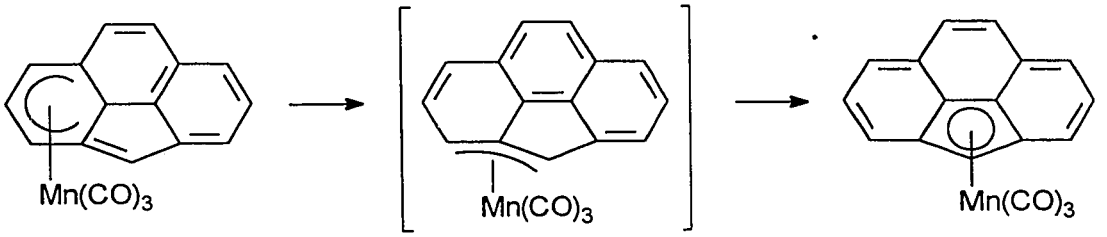

65 **66** **67**

We wondered whether η^5-transition metal complexes of cyclopenta[l]phenanthrene would show a "super-indenyl" effect. Would the ML_n moiety be able to adopt an η^3- structure, **69**, with the stability of phenanthrene, as an intermediate in ligand substitution reactions?

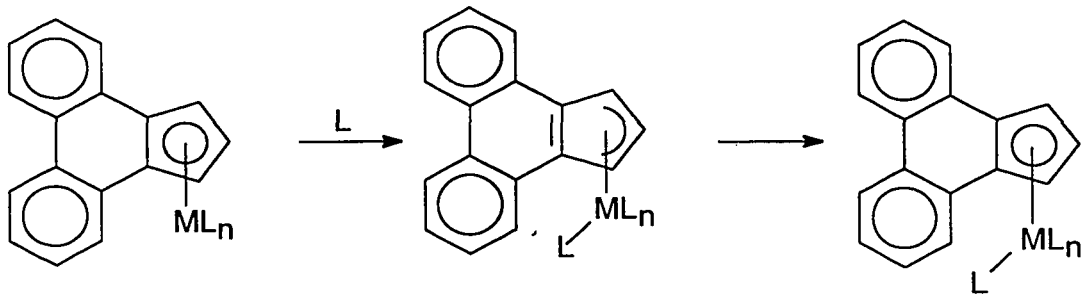

68 **69** **70**

4.2 Results and Discussion

We have prepared complexes of titanium, manganese, iron and rhodium derivatives of **55**, and contrasted their behavior with that of the analogous indenyl complexes.

The complexes (η^5-indenyl)ML_n, where ML_n = $TiCl_3$, **71**, $Mn(CO)_3$, **72**, $Fe(C_5H_5)$, **73**, $Rh(C_2H_4)_2$, **74**, and also $(\eta^5\text{-indenyl})_2Fe$, **75**, have been described previously, and their reactivity towards phosphines and acids has been reported. The chemistry of the molecules **71** through **75** differs markedly from that of the corresponding cyclopentadienyl complexes.

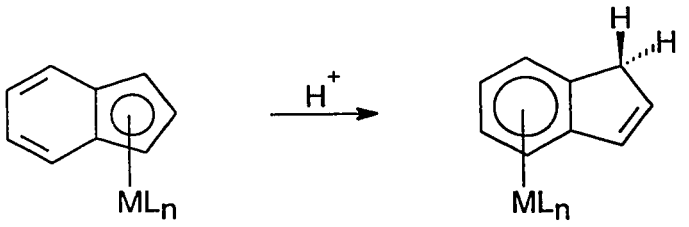

71 $ML_n = TiCl_3$

72 $ML_n = Mn(CO)_3$

73 $ML_n = Fe(C_5H_5)$

74 $ML_n = Rh(C_2H_4)_2$

75 $ML_n = Fe(C_9H_7)$

Thus, protonation of $(C_5H_5)Rh(C_2H_4)_2$ involves a complex series of reactions culminating in the formation of 1-butene via coupling of the two ethylene ligands on rhodium. In contrast, treatment of (η^5-indenyl)$Rh(C_2H_4)_2$, **74**, with trifluoroacetic acid yields [(η^6-indene)$Rh(C_2H_4)_2]^+$, **76**. This reaction must proceed with initial protonation at rhodium since use of CF_3CO_2D also deuterates the alkenes, presumably *via* a rhodium-ethyl intermediate.

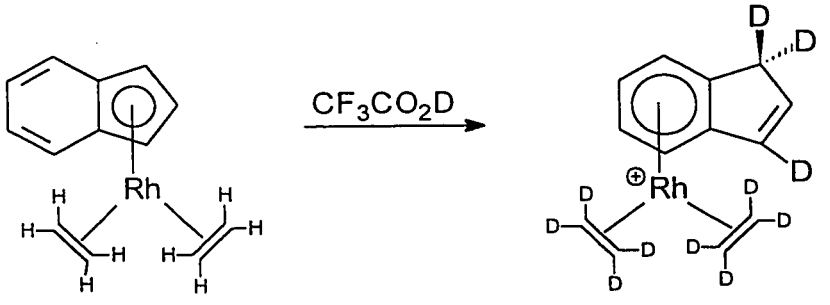

74 **76**

Analogously, (η^5-indenyl)$Mn(CO)_3$, **72**, and also the benzoferrocenes, **73** and **75**, undergo an η^5- to η^6- haptotropic shift upon protonation. Moreover, both **72** and **74** react readily with phosphines with loss of CO or C_2H_4 ligands, respectively.

4.2.1 Synthesis

Cyclopenta[*l*]phenanthrene, **55**, may be prepared *via* the multistep sequence outlined in Chapter Three. The ^{1}H and ^{13}C NMR spectra of the anion **77** are in accord with the overall aromatic character of this species. As shown in Figure 4.1, treatment of the anion **77** with $BrMn(CO)_5$, $[Rh(C_2H_4)_2Cl]_2$, or $FeCl_2$ yields the complexes **78** through **80**. The anion also reacts with $(C_5H_5)Fe(CO)_2I$ to give, after decarbonylation, the unsymmetrical sandwich compound **81**.

The molecules **78** through **81** were characterized by mass spectrometry and NMR spectroscopy. In each case, the ^{1}H NMR spectrum exhibited the expected doublet (2H) and triplet (1H) patterns for the complexed five-membered ring. The aromatic protons and carbons were assigned by means of 2D ^{1}H-^{1}H COSY, ^{1}H-^{13}C shift-correlated, and ^{1}H-^{1}H NOESY spectra; these data are collected in Table 4.1. The trimethylsilyl derivative, **82**, reacts with titanium tetrachloride to give the $TiCl_3$ complex **83**.

The rhodium complex **79** showed some fluxional behaviour. The ^{1}H spectrum shows two broad resonances of equal intensity, arising from the ethylene signals, at 6.4°C. When the sample was cooled to -35.6°C in an NMR probe, the ethylene signals are split into two pairs of doublets. When the sample was heated to 16.7 °C, the ethylene signals coalesced into one signal, which became a fairly sharp signal by 38.4°C. The protons equilibrate *via* rapid rotation of the coordinated ethylene about the Rh-alkene centroid axis.

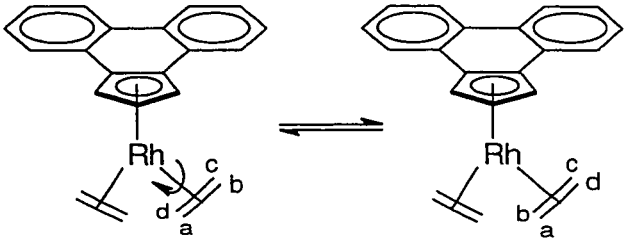

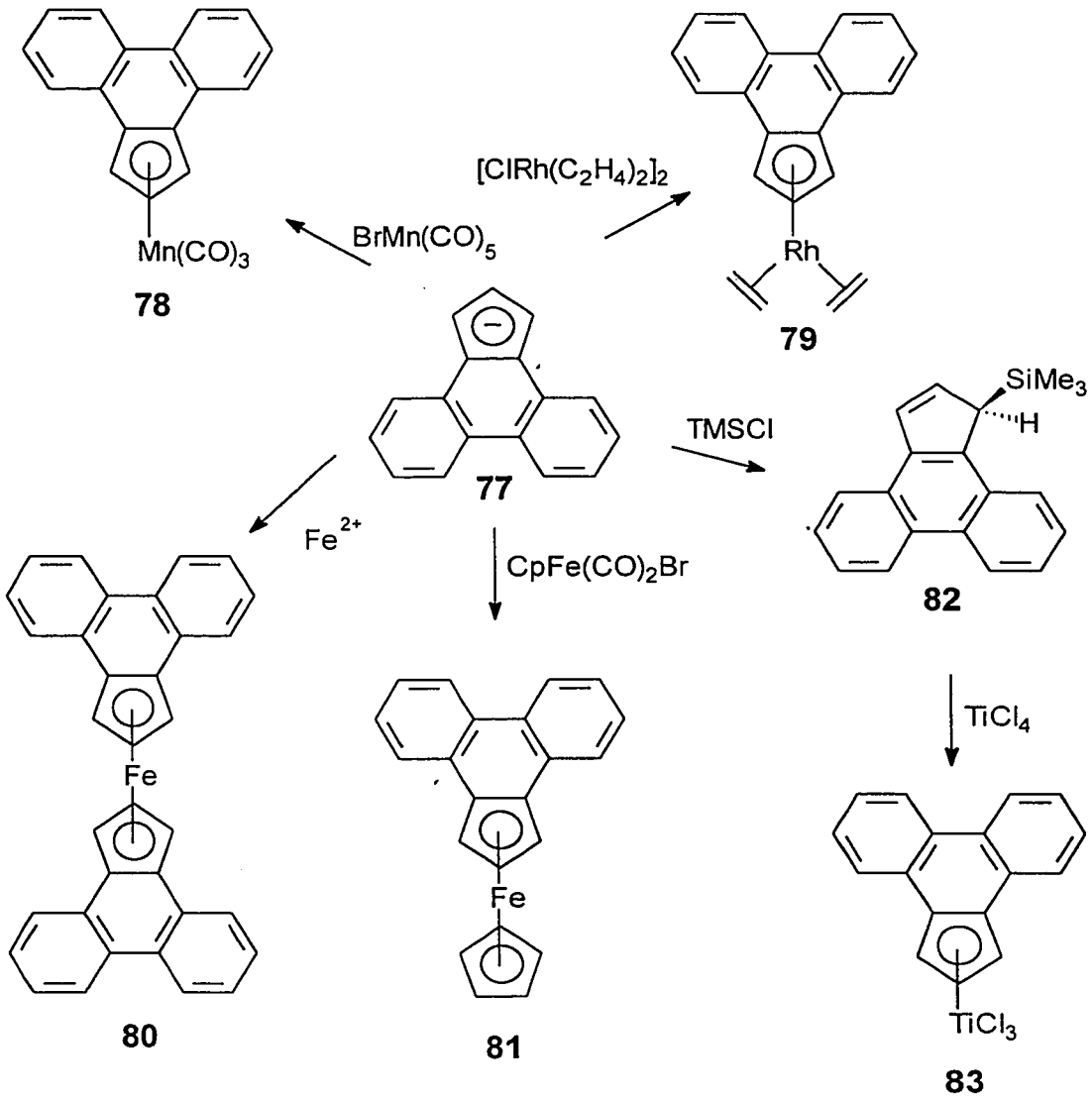

Figure 4.1 Synthesis of η^5-transition metal complexes of cyclopenta[*l*]phenanthrene

Compound		1,3	2	3a	3b	4	5,6	7,8	7a,7
(η^5-cpp)Mn(CO)$_3$	^{1}H	5.60(d,2.8Hz)	5.17(tr,2.8Hz)			7.97(m)	7.62(m)	8.49(m)	
†	^{13}C	73.3	86.3	99.0	130.5	124.6	128.4,128.3	124.5	130
(η^5-cpp)TiCl$_3$	^{1}H	7.62(d,3.3Hz)	7.25(tr,3.3Hz)				7.74-7.67(m)	8.56(d,8.5Hz)	8.23(d,7 of d,1.
	^{13}C	115.4	123.1	131.1	127.6	125.5	128.3,130.1	124.1	131
(η^5-cpp)Rh(C_2H_4)$_2$ *	^{1}H	5.68(d,2.8Hz)	6.16(d,1.5Hz, of tr, 2.8Hz)			7.83-7.81(m)	7.58-7.56(m)	8.61-8.59(m)	
	^{13}C	80.2(d,3 Hz)	89.2(d,4.5 Hz)	102.8	129.0	123.7	127.7, 126.0	124.2	127
(η^5-cpp)$_2$Fe	^{1}H	4.66(d,2.5Hz)	4.14(tr,2.5Hz)			7.12(d,1.2 Hz, of d, 7.8 Hz)	6.96(d,1 Hz, of tr, 7.4 Hz) 7.17(d,1.1 Hz of tr, 7.6 Hz)	7.68(d, 8.1 Hz)	
	^{13}C	63.5	69.9	82.9	130.8	123.7	126.9, 124.9	123.5	129
(η^5-cpp)Fe(η^5-Cp)	^{1}H	5.28(d,6.3Hz)	4.39(tr,6.3Hz)			7.97(m)	7.44(m)	8.42(m)	
‡	^{13}C	63.3	69.9	82.2	135.5	124.7	128.1, 126.4	124.4	131

† 221.0 CO

* 1.84 (s, broad) ethylene H's, 44.3 ethylene C.

‡ 3.59 (s, broad) Cp H's, 70.6 Cp C's.

Table 4.1 ^{1}H and ^{13}C Chemical Shifts for η^5-complexes of Cyclopenta[*l*]phenanthrene

The Gutowsky-Holm approximation[79] yields a $\Delta G^{\ddagger}_{290}$ value of 13.0 ± 0.5 kcal/mol for the fluxional process. This activation energy lies closer to that for the analogous cyclopentadienyl system of 15 kcal/mol,[82] than to the indenyl system at 10.5 kcal/mol.[63]

4.2.2 Protonation of Complexes of cyclopenta[*l*]phenanthrene

In an attempt to promote η^5- to η^6- haptotropic shifts of the type previously noted for the indenyl complexes **72** through **75**, the cyclopenta[*l*]phenanthrenyl systems **78** through **81** were protonated. The NMR spectra of the manganese and iron complexes **78**, **80**, and **81** were essentially unchanged on protonation.

Conversely, when the rhodium complex **79** was acidified, changes in the NMR spectra were observed. However, the results indicated that protonation of **79** led to decomposition and formation of 1-butene, not to migration of the metal into a six-membered ring as in the corresponding indenyl system.

4.2.3 Ligand Substitution Reactions

In an attempt to observe an enhanced rate for ligand substitution reactions, which could indicate the intermediacy of an η^3- structure, (η^5-cyclopenta[*l*]phenanthrenyl)$Mn(CO)_3$, **78,** was refluxed with triethylphosphine in dry hexane. Instead of the immediate colour change that is observed in analogous indenyl systems, no ligand substitution occurred even after two weeks. Similarly, no ligand substitution occurred when (η^5-cyclopenta[*l*]phenanthrenyl)$Rh(C_2H_4)_2$, **79**, was reacted with either diphos or trimethylphosphine.

4.3 Conclusion

These results all indicate that the molecules **78** through **81** possess the characteristics of complexes of cyclopentadienyl rather than indenyl ligands. That is, the anion **77** behaves as

though it is comprised of three independent 6π aromatic systems and not as a dibenzo-indenide ligand.

CHAPTER FIVE

Attempted Preparation of η^6-complexes of Cyclopenta[*l*]phenanthrene

5.1 Introduction

Since most haptotropic rearrangements that have been studied result from deprotonating an η^6-metal complex, we attempted to prepare organometallic complexes of cyclopenta[*l*]phenanthrene in which the metal is bonded to a six-membered ring of the ligand as in **84**.

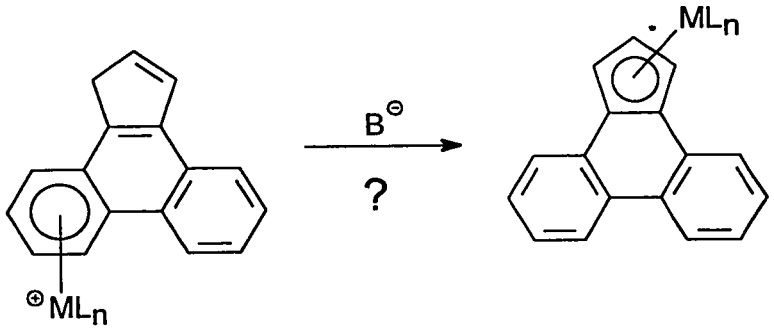

84

5.2 Results and Discussion

5.2.1 Reaction with Ferrocene, Al, and $AlCl_3$

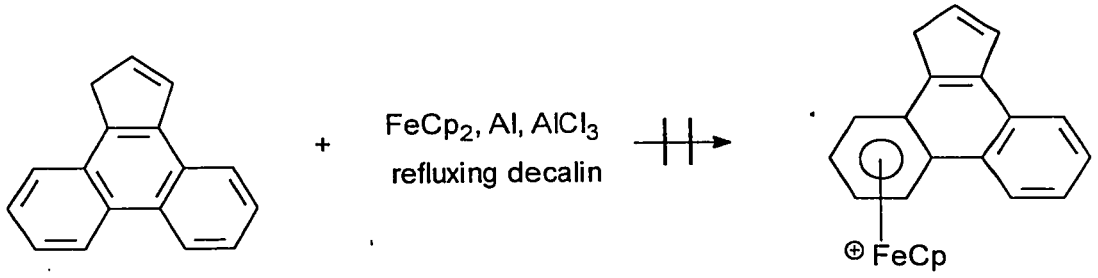

85

Reaction of cyclopenta[*l*]phenanthrene with ferrocene, Al and $AlCl_3$ in refluxing decalin did not yield the desired product, **85**, and the organic layer contained only ligand.

5.2.2 Reaction with $BrMn(CO)_5$ and $AlCl_3$

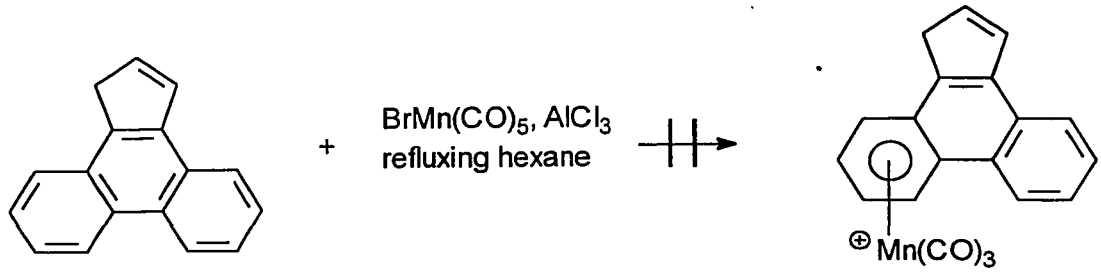

86

Reaction of cyclopenta[*l*]phenanthrene with $BrMn(CO)_5$ and $AlCl_3$ in refluxing hexane did not yield the desired product, **86**, and the organic layer contained only ligand.

5.2.3 Attempts to Prepare $Cr(CO)_3$ Complexes

Standard methods of synthesizing $Cr(CO)_3$ complexes of arenes did not yield (cyclopenta[*l*]phenanthrene)$Cr(CO)_3$, **87**. The relatively low temperature reaction of $(NH_3)_3Cr(CO)_3$ with cyclopenta[*l*]phenanthrene in refluxing hexane yielded only ligand and inorganic salts.

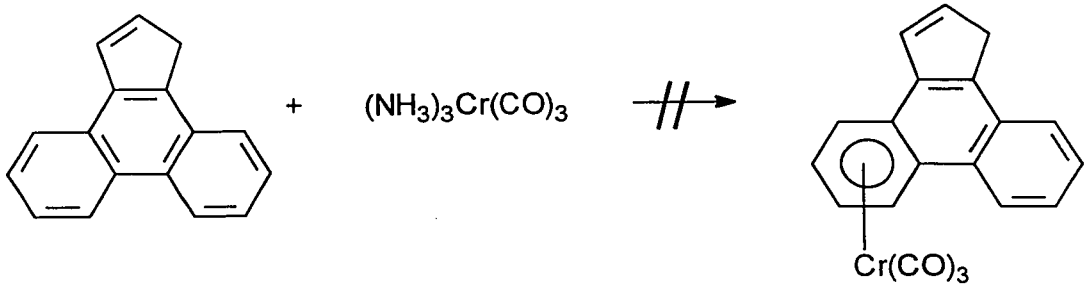

87

Reaction of $Cr(CO)_6$ in refluxing *n*-butyl ether did not yield (cyclopenta[*l*]phenanthrene)$Cr(CO)_3$ either. However, when the ligand had not been carefully

dried prior to reaction with $Cr(CO)_6$, the $Cr(CO)_3$ complex, **88**, in which the double bond of the 5-membered ring had been hydrogenated, was obtained along with partially hydrogenated ligand, **89**.

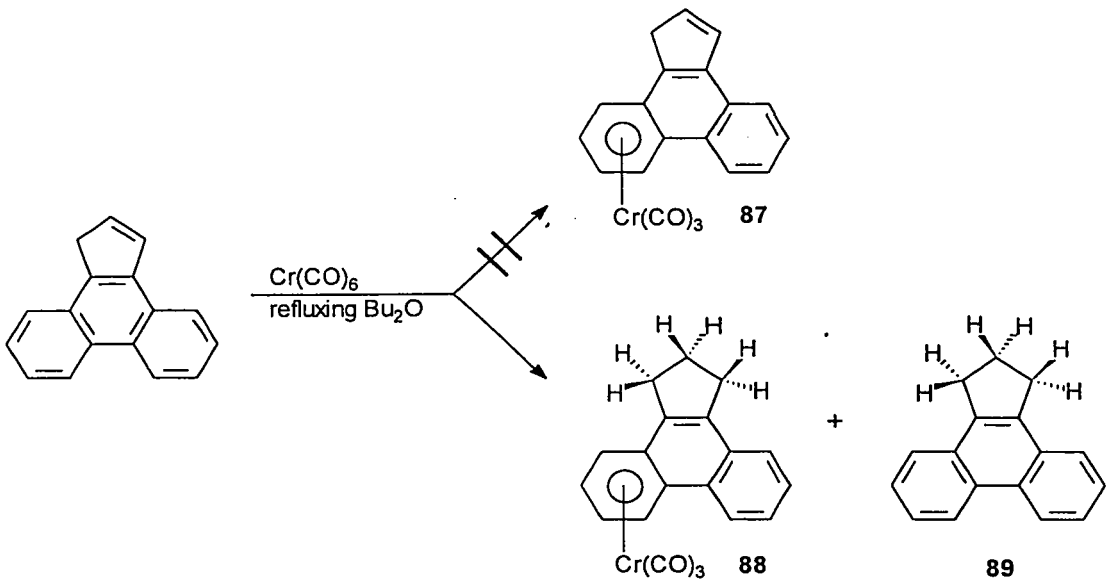

The structure of **88** was easily deduced from its 1-D ^1H and ^{13}C NMR spectra and ^1H - ^1H 2-D COSY spectrum, along with ^1H - ^{13}C 2-D shift-correlated and ^1H - ^{13}C long-range 2-D shift-correlated spectra. Formation of the complex in which the $Cr(CO)_3$ group is bonded to a terminal 6-membered ring, rather than the central six-membered ring is in accord with other complexes of polycyclic aromatic ligands.[83,84]

In order to establish the orientation of the $Cr(CO)_3$ tripod, an X-ray crystal structure was obtained. In the analogous system, (phenanthrene)$Cr(CO)_3$, x-ray data[84] confirm the molecular orbital prediction[43] that the $Cr(CO)_3$ unit adopts the *exo* conformation **90a**, as opposed to the *endo* conformation **90b**.

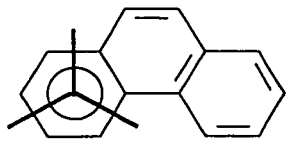

90a

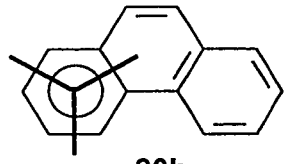

90b

A crystal structure of the related compound (triphenylene)$Cr(CO)_3$ **91**, reveals that it also adopts the *exo* conformation,[83] as does (η^6-cyclopenta[*def*]phenanthrene)$Cr(CO)_3$ **92**.[73] In fact, possibly the only known (arene)$Cr(CO)_3$ in which the $Cr(CO)_3$ group adopts the *endo* conformation is (biphenylene)Cr(CO) **93**.[83]

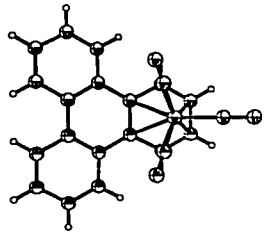

91

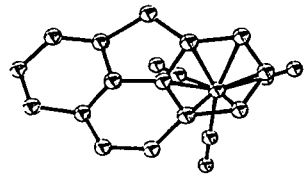

92

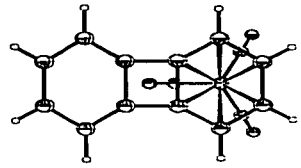

93

The crystal structure of (cyclopenta[*l*]dihydrophenanthrene)$Cr(CO)_3$, **88**, is shown below.

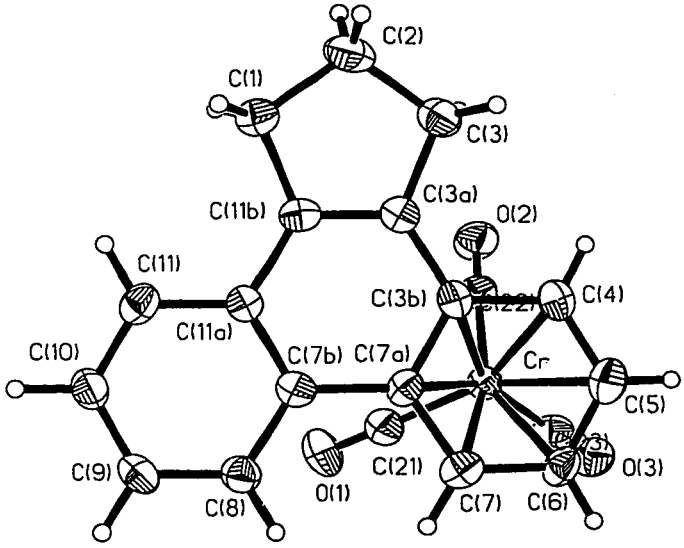

Crystal Structure of (cyclopenta[*l*]dihydrophenanthrene)Cr(CO)$_3$, 88

Note that the Cr(CO)$_3$ unit does adopt the expected *exo* conformation.

The geometry of the Cr(CO)$_3$ unit is similar to that found in other (arene)Cr(CO)$_3$ complexes.[83-85] Also, the Cr-arene distances found for (cyclopenta[*l*]dihydrophenanthrene)Cr(CO)$_3$, **88**, are typical of those found for other polynuclear (benzenoid)Cr(CO)$_3$ complexes.[85] The Cr(CO)$_3$ group is shifted away from an idealized η^6 position, with the Cr-C distances for the ring junction carbons being significantly longer than for the other carbons in the six-membered ring. According to calculations done by Hoffmann,[43] the reason these compounds adopt this geometry is because there is a very high potential energy region around the C(1) - C(2) η^2 position for the Cr(CO)$_3$ moiety. This is not counterbalanced by an equally high energy for moving the Cr(CO)$_3$ group to an η^2 geometry in the opposite direction, over the C(5) - C(4) bond, because there is some overlap here between the orbitals of the Cr(CO)$_3$ group and the ligand. The ground state geometry is therefore shifted away from C(1) -

C(2) toward C(5) -C(4).[43] Chromium-carbon distances for (cyclopenta[*l*]dihydrophenanthrene)$Cr(CO)_3$ **88**, (cyclopenta[*def*]phenanthrene)$Cr(CO)_3$ **92**, (phenanthrene)$Cr(CO)_3$ **90**, and (triphenylene)$Cr(CO)_3$ **91**, are compared in the table below. The non-standard numbering scheme below is adopted for simplification:

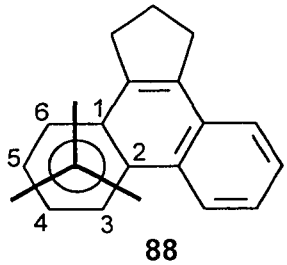

88

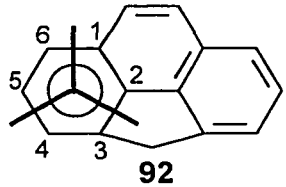

92

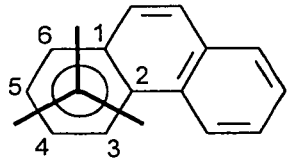

90

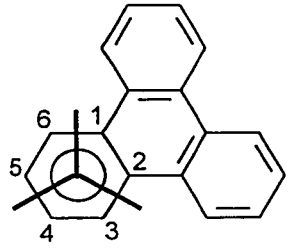

91

Compound			Bond	Length [Å]		
	Cr-C(1)	Cr-C(2)	Cr-C(3)	Cr-C(4)	Cr-C(5)	Cr-C(6)
88	2.295(6)	2.296(6)	2.212(7)	2.213(6)	2.198(7)	2.203(7)
92	2.261(4)	2.314(4)	2.224(4)	2.252(4)	2.251(4)	2.197(5)
90	2.278(5)	2.289(4)	2.208(5)	2.213(5)	2.214(5)	2.207(5)
91	2.258(3)	2.258(3)	2.198(3)	2.209(3)	2.209(3)	2.198(3)

The tetracyclic ring system is not planar, but slightly arced away from the organometallic moiety. The interplanar angle between the two external six-membered rings is 9.2°. A crystal structure of the ligand was not available for comparison.

The molecules are arranged in a head-to-head manner such that closest neighbors have their tetracyclic ligands aligned parallel to each other at an inter-plane distance of 3.674 Å.

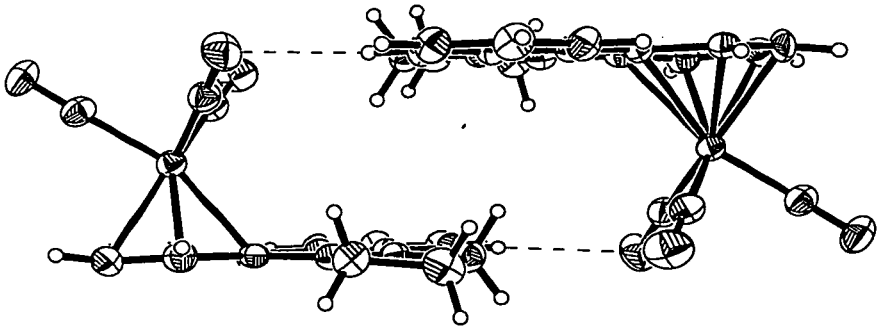

Figure 5.1 (Cyclopenta[*l*]dihydrophenanthrene)$Cr(CO)_3$, 88

When the ligand had been carefully dried prior to reaction with $Cr(CO)_6$, no organometallic complex was obtained. Instead, the reaction yielded inorganic salts and an organic molecule whose mass spectrum yields the dimeric formula $C_{34}H_{24}$.

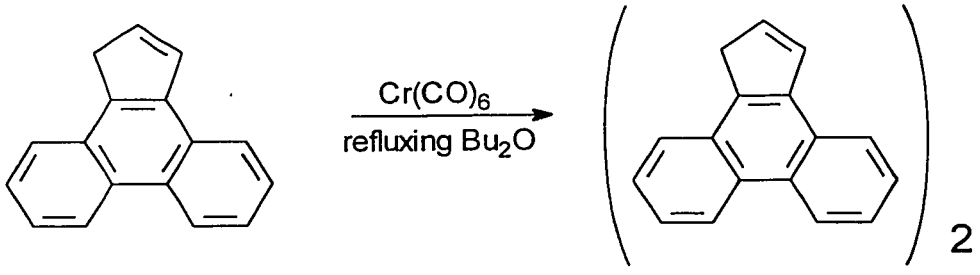

^1H NMR of the compound revealed that there were four distinct aromatic rings. A ^1H - ^1H 2-D COSY spectrum (Figure 5.2), along with ^1H - ^{13}C 2-D shift-correlated and ^1H - ^{13}C long-range 2-D shift-correlated spectra led us to believe that the dimer had the following structure.

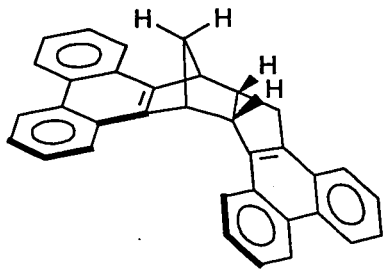

94

This molecule could arise if a [1,5]-hydrogen migration occurred, generating an *iso*-indene type intermediate. This intermediate could then trap another molecule of cyclopenta[*l*]phenanthrene, *via* a Diels-Alder reaction.

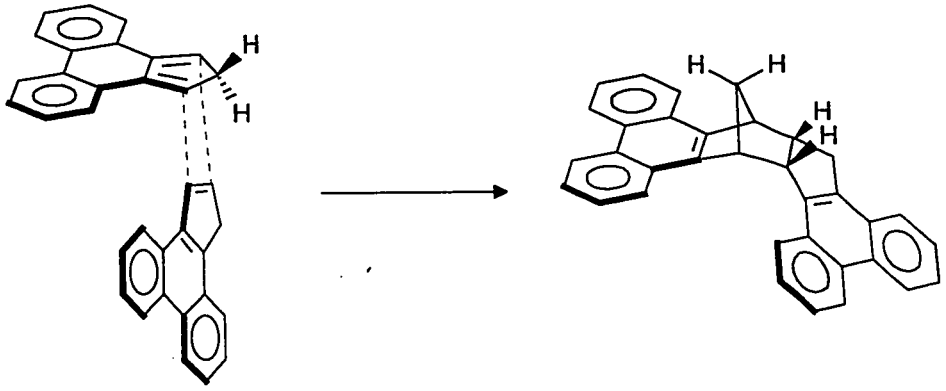

We suspected that the dimer was the *endo* Diels-Alder adduct, because its ^{1}H - ^{1}H 2-D NOESY spectrum was essentially the same as that for cyclopentadiene dimer, which is known to adopt the *endo* conformation. The NOESY spectrum allowed for the complete assignment of the proton spectrum. All of the NOE enhancements observed are shown in Figure 5.4.

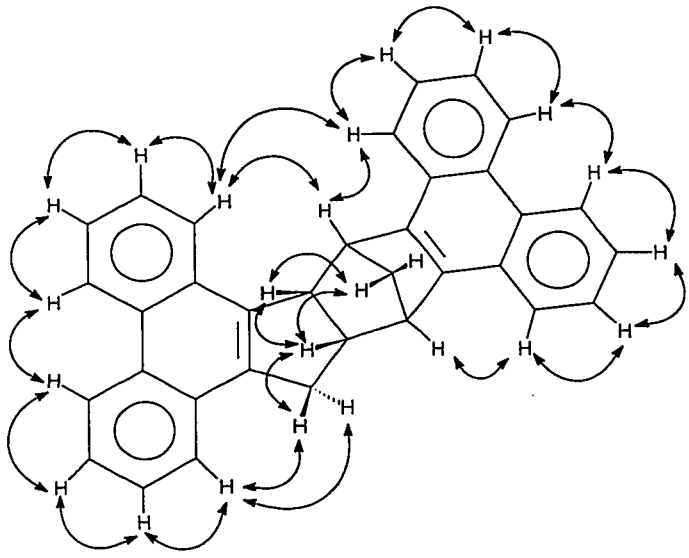

Figure 5.4 NOE enhancements for the dimer of cyclopenta[*l*]phenanthrene, 94.

^{1}H and ^{13}C chemical shifts for the molecule are shown in Figures 5.5 and 5.6, and are listed in Table 5.1. The numbering scheme for the molecule is shown in Figure 5.7.

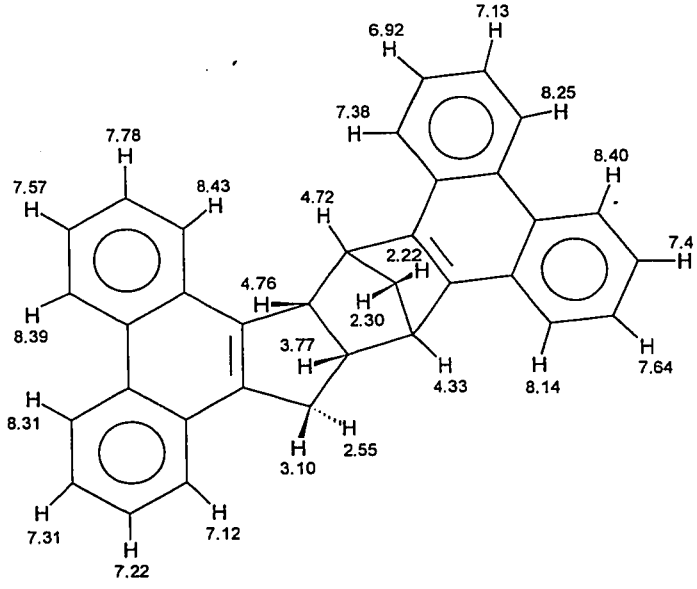

Figure 5.5 ^{1}H Chemical Shifts for the dimer of cyclopenta[*l*]phenanthrene, 94.

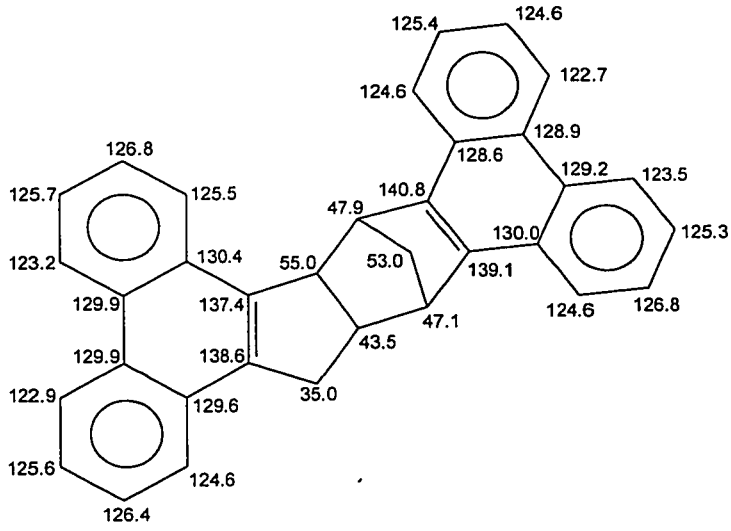

Figure 5.6 ^{13}C Chemical shifts for the dimer of cyclopenta[*d*]phenanthrene, 94.

Table 5.1 ^{1}H and ^{13}C Chemical shifts for the dimer of cyclopenta[*d*]phenanthrene, **94**.

	^{1}H	^{13}C
1a	3.10 (d, 16.9 Hz of d, 10.1 Hz)	35.0
1b	2.55 (d, 16.6 Hz)	"
2	3.77 (m)	43.5
3	4.76 (d, 8.7 Hz)	55.0
3a		137.4
3b		130.4
4	8.43 (d, 8.0 Hz)	125.5
5	7.78 (tr, 7.6 Hz)	126.8
6	7.57 (tr, 7.3 Hz)	125.7
7	8.39 (d, 8.2 Hz)	123.2
7a		129.9
7b		129.9
8	8.31 (d, 8.3 Hz)	122.9
9	7.31 (tr, 7.1 Hz)	125.6
10	7.22 (tr, 7.4 Hz)	126.4
11	7.12 (d, 7.4 Hz)	124.6
11a		129.6
11b		138.6
12	4.33 (d, 3.5 Hz)	47.1
13	2.30 (d, 8.1 Hz)	53.0
13'	2.22 (d, 8.1 Hz of d, 1.6 Hz)	53.0
14	4.72 (s)	47.9
14a		140.8

14b		128.6
15	7.38 (d, 8.0 Hz)	124.6
16	6.92 (tr, 7.5 Hz)	125.4
17	7.13 (tr, 7.1 Hz)	124.6
18	8.25 (d, 8.3 Hz)	122.7
18a		128.9
18b		129.2
19	8.40 (d, 8.3 Hz)	123.5
20	7.48 (tr, 7.2 Hz)	125.3
21	7.64 (tr, 7.3 Hz)	126.8
22	8.14 (d, 8.0 Hz)	124.6
22a		130.0
22b		139.1

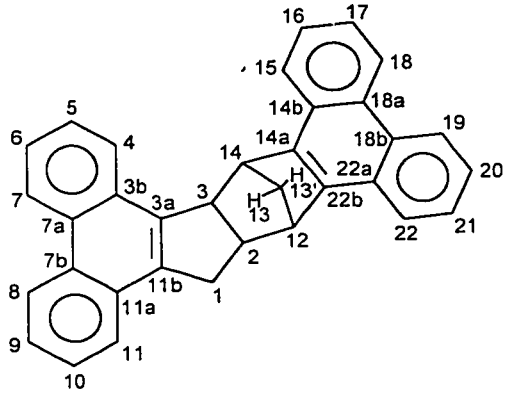

Figure 5.7 Numbering scheme for the dimer of cyclopenta[*l*]phenanthrene, 94.

Verification of this came when we were able to grow X-ray quality crystals by slow evaporation of the solvent from a solution of the dimer in acetone and *n*-heptane.

X-ray crystal structure of the dimer of cyclopenta[*l*]phenanthrene, 94.

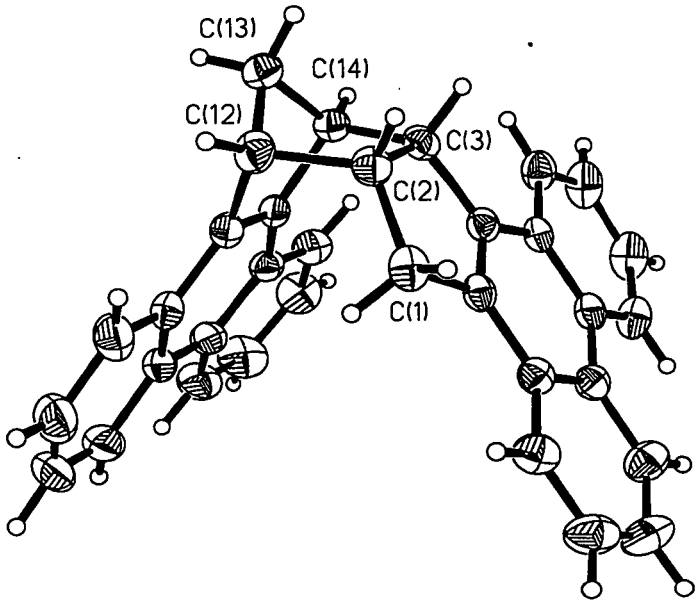

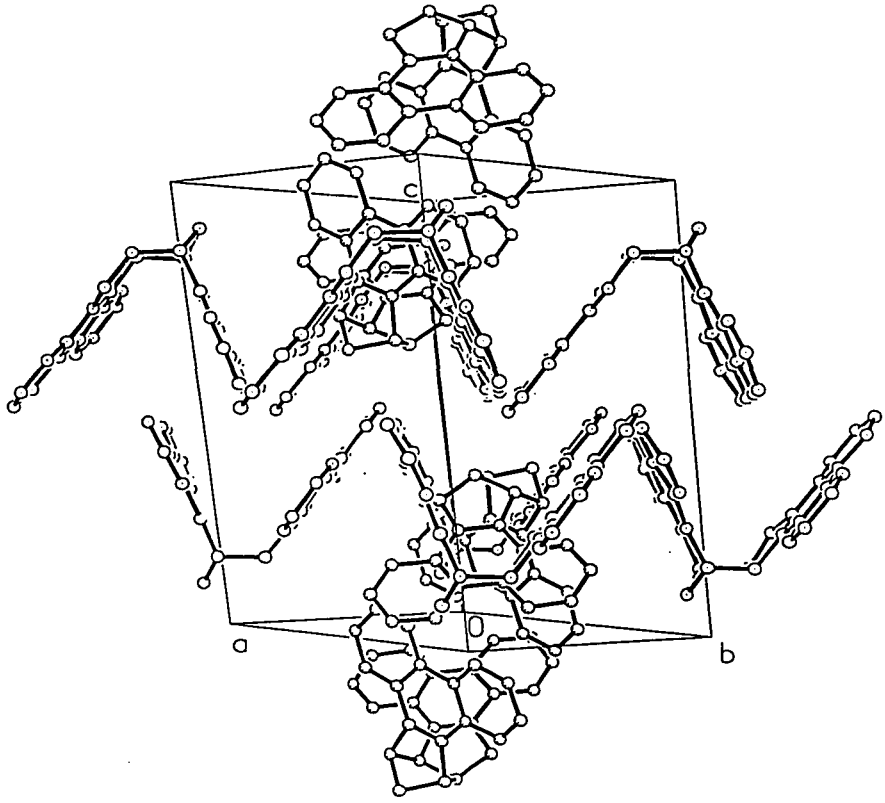

Note that there are two crystallographically distinct molecules in the assymetric unit.

Two important questions arose concerning the mechanism of the reaction. Was the hydrogen shift somehow mediated by the Cr in solution? To answer this question, cyclopenta[*l*]phenanthrene was refluxed in *n*-butyl ether, and gave the same dimer.

The other question related to the occurrence of the Diels-Alder reaction, since indene itself does not dimerize. The related molecule trimethylsilylindene, undergoes [1,5]-silatropic shifts *via* an *iso*-indene, with a much lower barrier for silicon migration than for hydrogen migrations.[86] However, the intermediate is trapped only with dienophiles that have electron-withdrawing groups, such as tetracyanoethylene. Why would the *iso*-indene-type intermediate for

cyclopenta[*l*]phenanthrene be trapped by the relatively unreactive dienophile cyclopenta[*l*]phenanthrene?

To answer this question we performed some molecular orbital calculations at the unrestricted Hartree-Fock (UHF) level using the programs AMPAC[77] and MOPAC.[78] The energy-minimized structures for cyclopenta[*l*]phenanthrene, **55**, and the intermediate *iso*-indene resulting from a hydrogen migration, and the transition state that connects the two are shown in Figure 2.5. The transition state lies 43.3 kcal/mol above the energy of the starting material, *i.e.* cyclopenta[*l*]phenanthrene, while the *iso*-indene intermediate lies in a potential well only 4.3 kcal/mol above the ground state. For comparison, in the analogous indene system, **54**, the transition state is 46.5 kcal/mol above the ground state, while the intermediate *iso*-indene 9.0 kcal/mol above the ground state. While the barrier to the [1,5]-hydrogen migration is high (thus the need to heat under reflux in *n*-butyl ether to form the dimer), the intermediate is rather stable and probably relatively long-lived in solution.

Cyclopenta[*l*]phenanthrene traps tetracyanoethylene at room temperature, but not through a Diels-Alder reaction. The product results from a 2 + 2 cycloaddition:

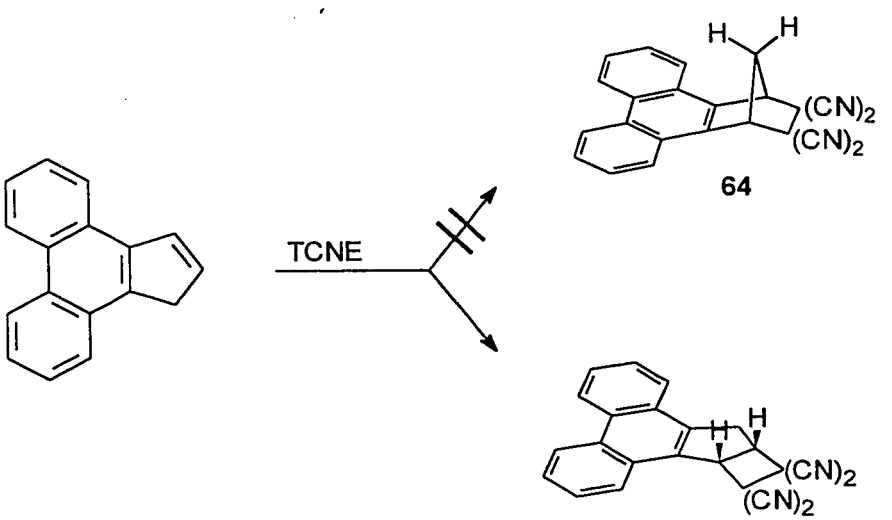

64

95

Indene is reported to trap TCNE in a similar manner.

In conclusion, although we have not yet been able to place a π-bonded metal on a six-membered ring of cyclopenta[*l*]phenanthrene, the fact that cyclopenta[*l*]phenanthrene dimerizes provides further evidence that the ligand behaves chemically like cyclopentadiene, rather than indene.

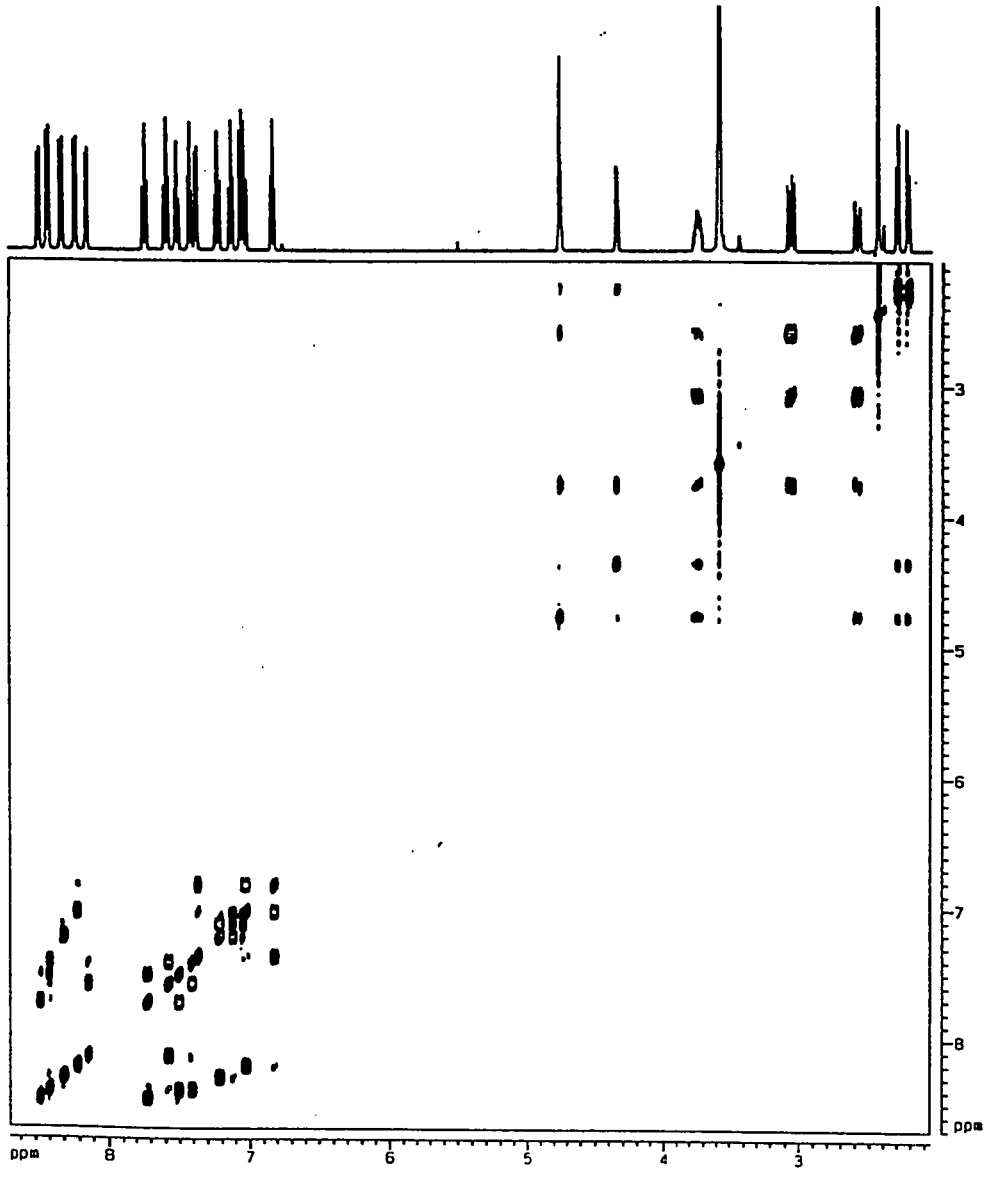

Figure 5.2 ^{1}H - ^{1}H COSY Spectrum of the dimer of Cyclopenta[*l*]phenanthrene

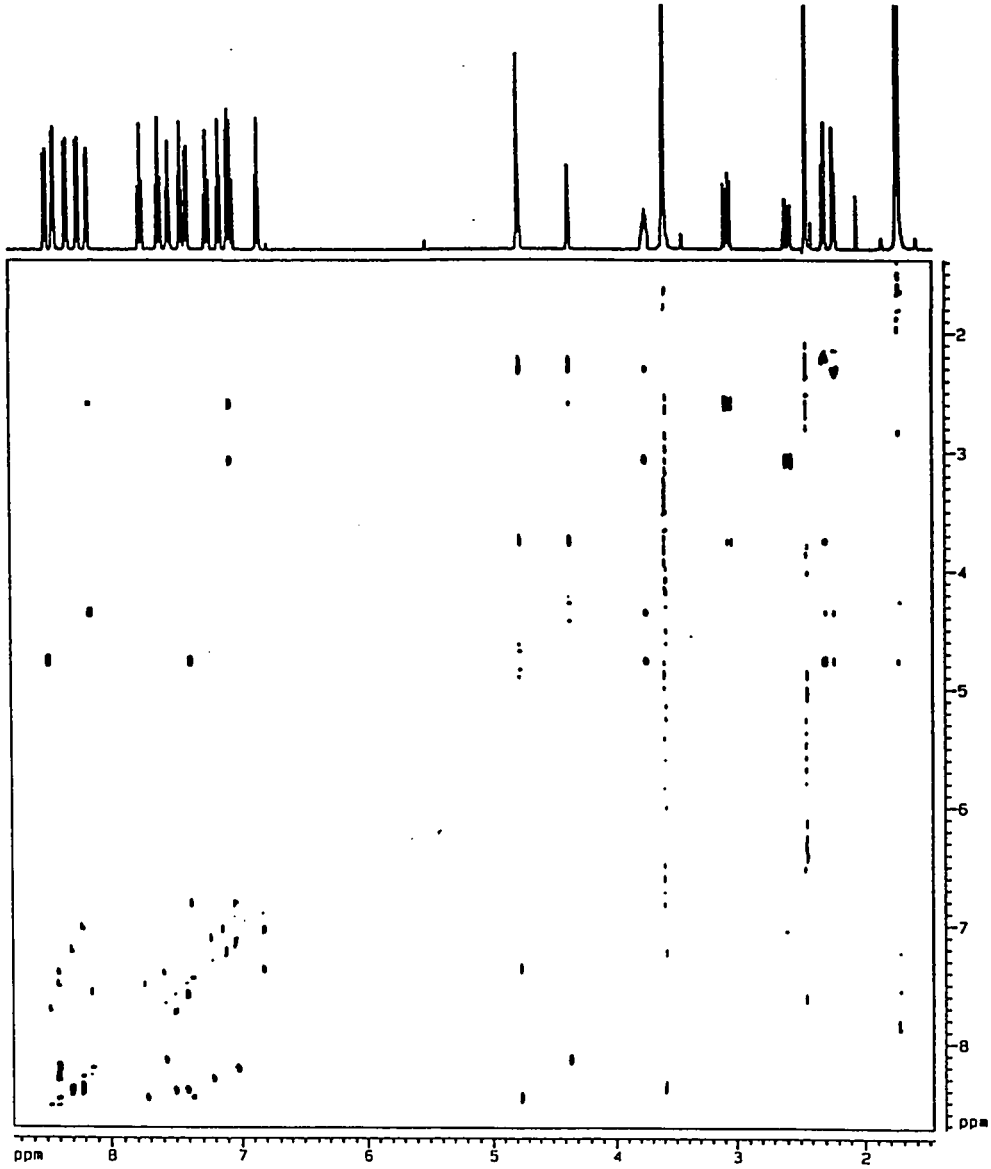

Figure 5.3 ^{1}H - ^{1}H NOESY Spectrum of the dimer of cyclopenta[*l*]phenanthrene.

CHAPTER SIX

Nmr Study of a Metal-cluster Stabilized Cyclopentenyl Cation

6.1 Introduction

The general reaction of trimethylsilylethynyl anion with ketones yields trimethylsilylethynyl alcohols. Reaction of these alcohols with $Co_2(CO)_8$ yields tetrahedral di-cobalt clusters, which can be protonated to give cations. These clusters are known to provide enormously enhanced stability to neighbouring cationic centres.[87] For example, the fluorenyl cation itself remains unobtainable, but recently a metal-cluster stabilized fluorenyl cation, **96**, has been characterized.[88]

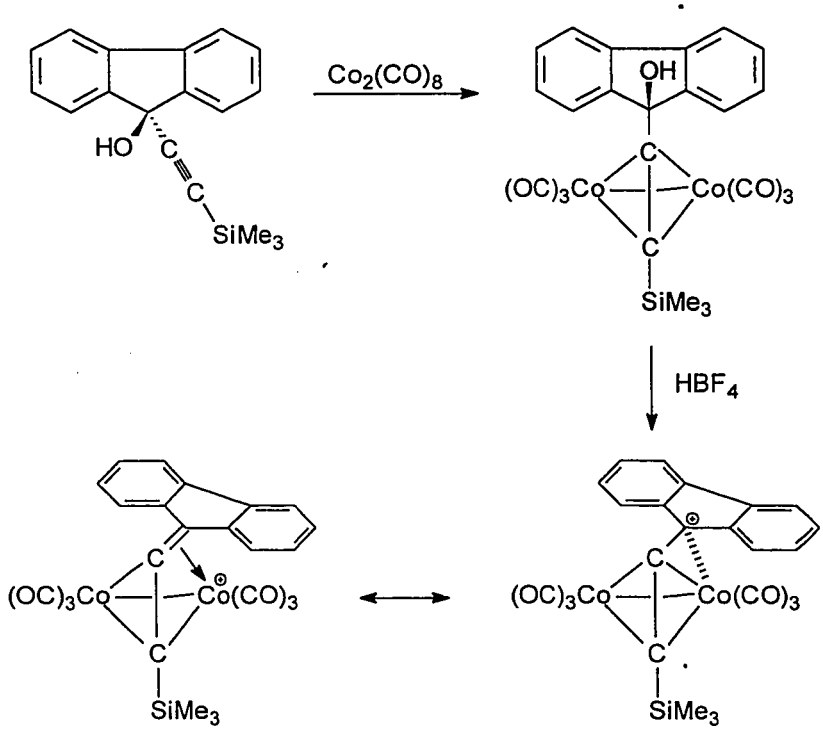

96

Scheme 6.1

With the ketone 2,3-dihydro-2-oxo-1H-cyclopenta[*l*]phenanthrene, **97**, readily available, we attempted to prepare a metal-cluster stabilized substituted cyclopentenyl cation.

6.2 Results and Discussion

All efforts to obtain X-ray quality crystals of cobalt-stabilized cations have been unsuccessful, to date. However, extended Hückel molecular orbital (EHMO) calculations provide a reasonable model for the molecular geometry of these cations. These calculations indicate that the vinylidene capping group is inclined through an angle θ towards one of the metal vertices, as in **98**. In the parent system, $[Co_2(CO)_6(HC{=}C{=}CH_2)]^+$, the total electronic energy is minimized at a bend angle, θ, of approximately 55°.[87,89,90] The bent structure predicted by EHMO calculations is supported by NMR data for this molecule.[91] The data indicate that the methylene protons are inequivalent, one being *syn* with respect to the Co-Co vector, the other being *anti* relative to this bond.

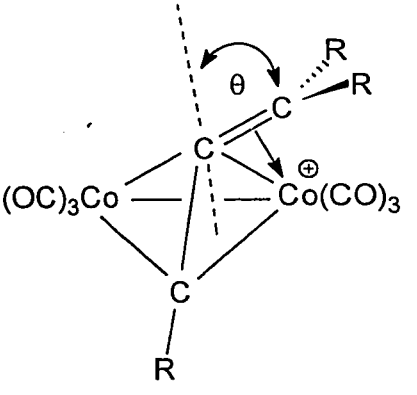

98

Two fluxional processes have been observed in these systems.[92] The lower energy process interconverts enantiomers of the cation *via* antarafacial migration of the vinylidene

group. The higher energy process which is equivalent to a suprafacial migration involves rotation about the double bond in the vinylidene group.

From the ketone **97** (Figure 7.1), it was possible to obtain 2,3-dihydro-2-hydroxy-2-trimethylsilylethynyl-1H-cyclopenta[*l*]phenanthrene, **99**, upon reaction with the lithium salt of trimethylsilylethyne. Treatment of the cyclopentaphenanthrenol with $Co_2(CO)_8$ produced the tetrahedral di-cobalt cluster, **100**. Protonation of **100** with HBF_4 in CD_2Cl_2 at -93°C resulted in the immediate formation of a deep red coloured solution, indicating the formation of cation **101**.

The substituted cyclopentenyl cation was identified spectroscopically. One would expect a bent structure, as in **96** and **98**, for the metal-stabilized cyclopentenyl cation and the NMR data bear this out. The ^{13}C NMR spectrum of **101** at -93°C shows 14 signals attributable to the tetracyclic ligand. One would expect seventeen signals for an unsymmetrical structure, but the chemical shifts of three are degenerate; this compares with the nine observed for the symmetrical cluster. The aromatic region of the ^{1}H spectrum is broadened compared with the symmetrical spectrum of the cluster. The signals arising from the methylene protons exhibit an AB pattern in the cluster **100**, while four separate signals are observed in the spectrum of the cation **101**. The observation of two methylene carbons and four protons below -33°C, is not consistent with a symmetrical structure. Figure 7.2 shows the ^{1}H methylene region for the cluster **100** (lower spectrum) and the cation **101** (upper spectrum) at -93 °C. It is clear from these data that the two sides of the tetracyclic ligand are inequivalent, as expected for the unsymmetrical structure **101**.

Certain aspects of the NMR spectra are unique. The presence of paramagnetic cobalt impurities usually limits one to observation of ^{13}C nuclei, which require long acquisition times to achieve acceptable signal/noise ratios because of the fairly poor solubility of the cation in CD_2Cl_2. The very clean sample used to observe the cyclopentenyl cation in this work allowed for observation of the proton signals, with resolution of all four methylene protons. We were able to discern which two protons of the four were attached to each of the two methylene carbons by

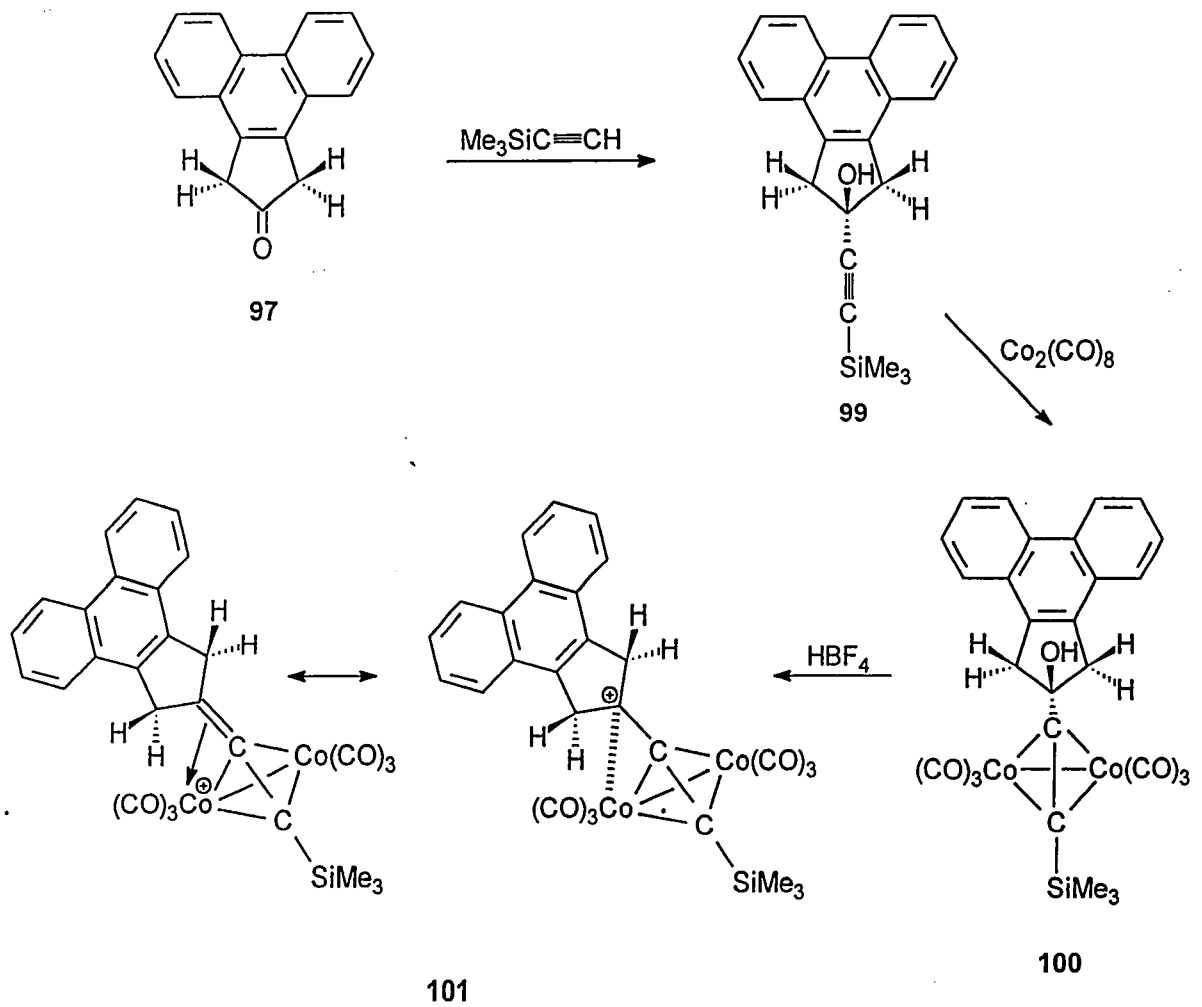

Figure 6.1 Synthesis of the cobalt-stabilized substituted-cyclopentenyl cation, 101.

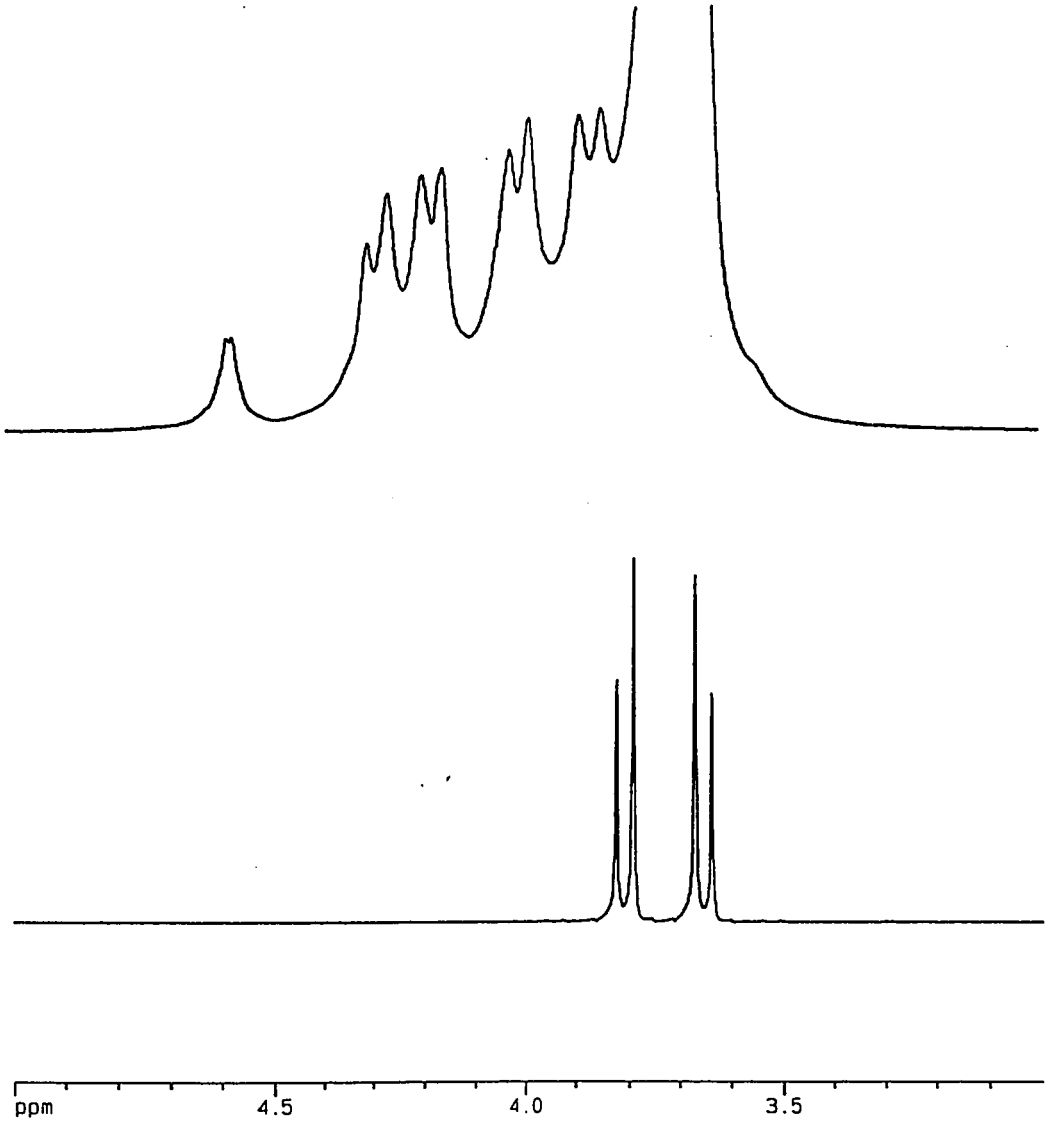

Figure 6.2 ^{1}H methylene region for the cluster, 100, (lower spectrum) and the cation, 101, (upper spectrum) at -93 °C.

performing a ^{1}H - ^{13}C shift correlated experiment (HSQC) at -93 °C. The methylene region of this HSQC spectrum is shown in Figure 7.3. In addition to the unusual resolution achieved in the ^{1}H NMR spectra, we were able to freeze out carbonyl migrations at low temperature. At -93 °C, we detected six carbonyl resonances, which had not been observed previously in a cobalt-stabilized cation. Upon warming to -83 °C, three resonances are observed, and by -63 °C, the carbonyl signals have broadened so as to be indistinguishable from the spectral baseline.

The temperature-dependent NMR spectra of the cation are consistent with a lower energy antarafacial migration of a vinylidene ligand from one cobalt tricarbonyl unit to the other. The antarafacial migration should be distinguishable from the suprafacial migration for this molecule because the proton spectrum is resolved. The antarafacial process equilibrates methylene protons on the same carbon, whereas the suprafacial process equilibrates protons on different carbon atoms. The two processes are illustrated in Figure 7.4. The 2-D EXSY (Figure 6.5) spectrum at -68 °C shows exchange between two protons on the same carbon, consistent with antarafacial migration. The cation started to decompose at -33°C, before we could observe any exchange between protons on different carbons, or between the two carbon signals themselves. Tertiary cations are typically stable below -30°C.[92] One can estimate the activation energy for the observable antarafacial migratory process from the coalescence temperatures for the two sets of methylene protons. The barriers obtained, 10.0 ± 0.5 and 10.7 ± 0.5 kcal/mol are in the normal range for cobalt-stabilized tertiary cations.[91,92]

The mechanism of carbonyl migrations in these metal-stabilized cations remains open to discussion. The resolution of six carbonyl signals for this cation makes it possible to determine the mechanism for carbonyl scrambling by acquiring 2-D ^{13}C EXSY spectra. In order to be practicable, however, one would have to enrich the cluster in ^{13}CO.

It has been shown that isolobal substitution of a $Co(CO)_3^+$ vertex in [(TMS-C≡C= fluorenyl)$Co_2(CO)_6$] by an $Fe(CO)_3$ unit yields the stable iron-cobalt cluster [(TMS-C≡C=

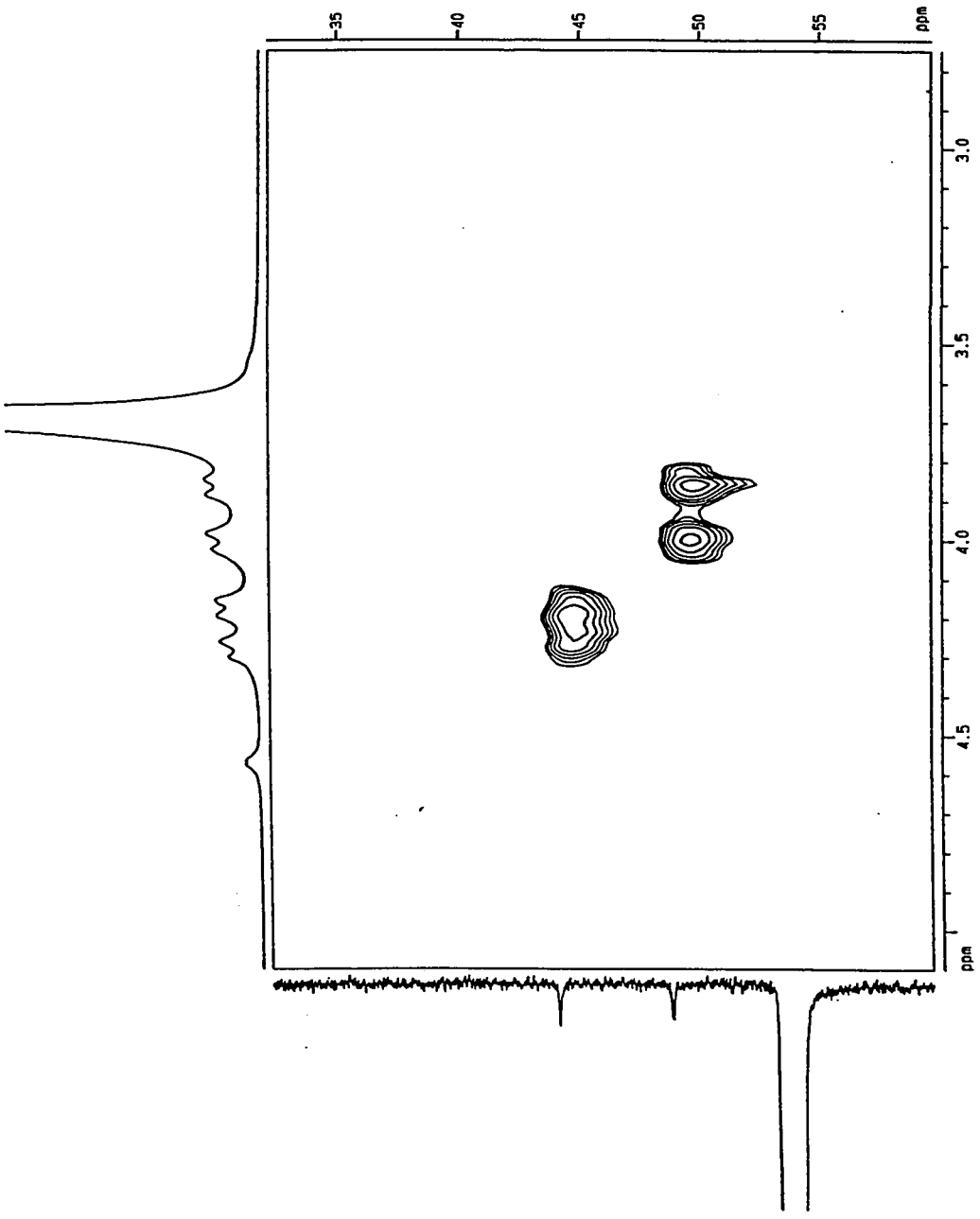

Figure 6.3 The methylene region of the HSQC spectrum of the cation, 101, at 180 K.

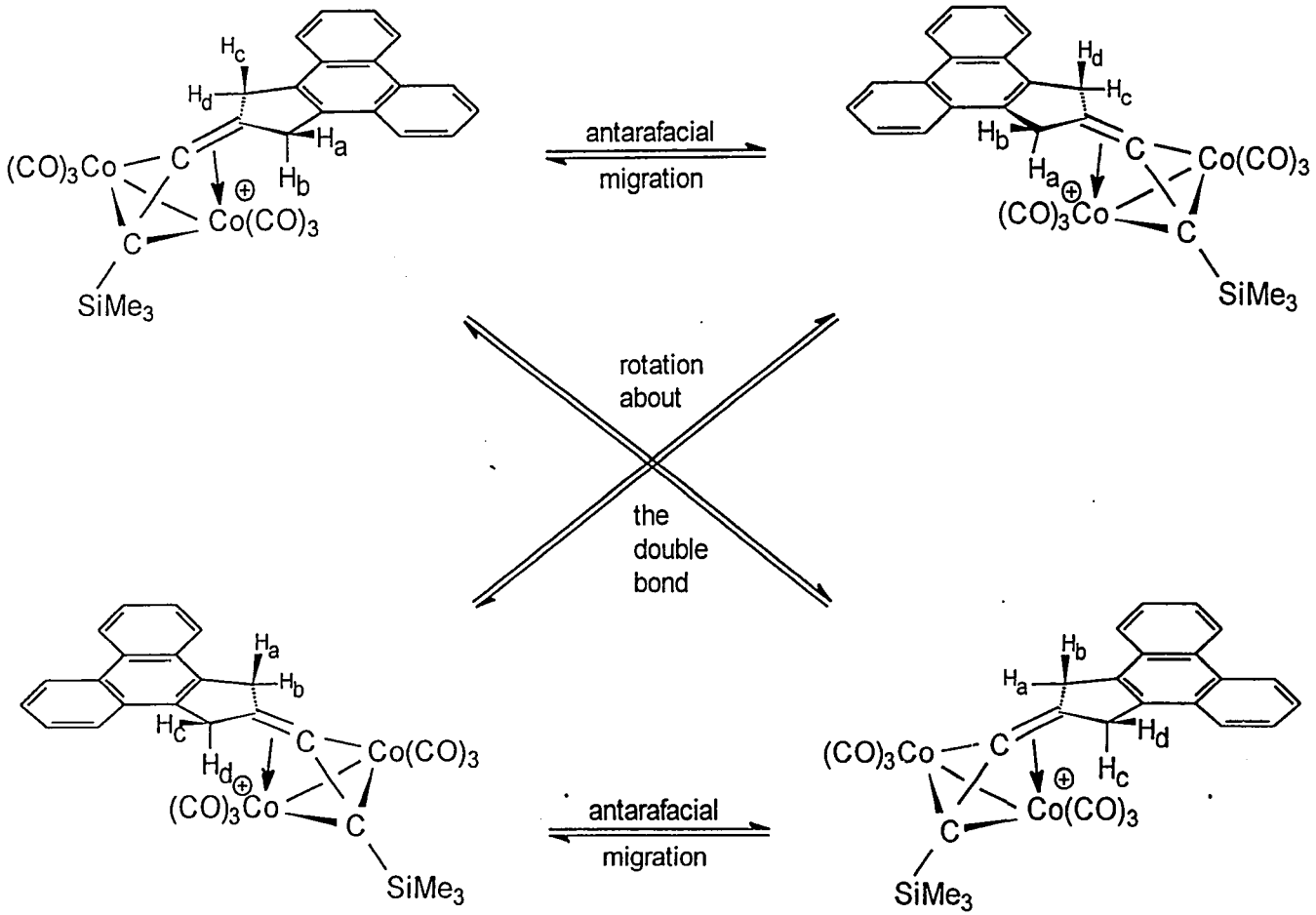

Figure 6.4 Fluxional processes in $[Co_2(CO)_6(Me_3SiC{\equiv}C\text{-}C_{17}H_{12})]^+$, 101.

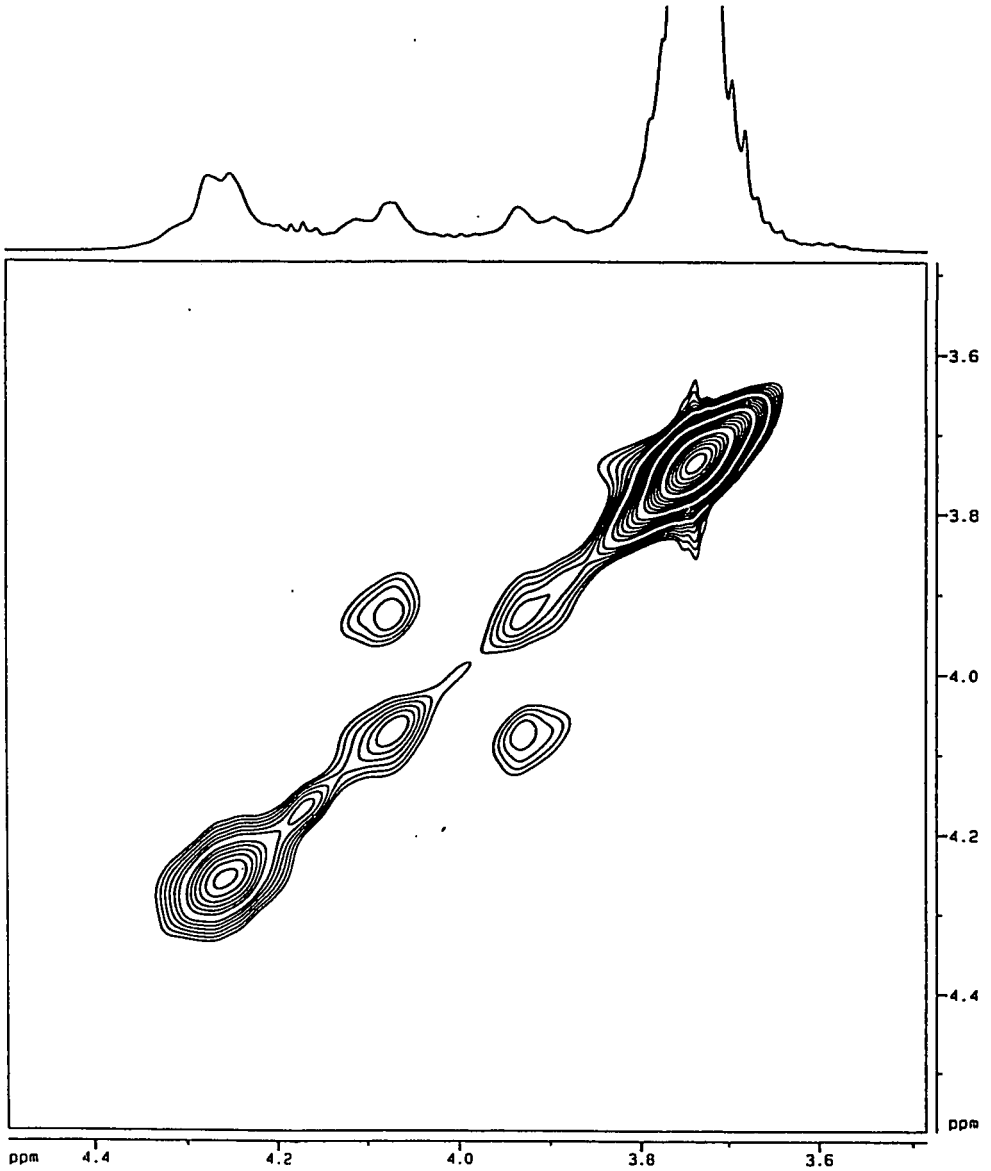

Figure 6.5 2-D EXSY spectrum of the methylene region of the cobalt-stabilized substituted-cyclopentenyl cation, 101, at 205 K , with a mixing time of 0.1 s.

fluorenyl)CoFe$(CO)_6$] whose X-ray structure corresponds very well to the energy-minimized geometry predicted from EHMO calculations. It would be interesting to substitute $Fe(CO)_3$ for one of the $Co(CO)_3^+$ vertices in the cyclopentenyl cation in this work.

^{13}CO chemical shifts at 190 ppm show that a cation has indeed been obtained, while the 2-D NMR data allow the assignments of the four methylene protons. Exchange between protons on the same carbon atoms is consistent with an antarafacial migration process.

CHAPTER SEVEN

Conclusions

The migration of organosilyl groups and transition metals over molecular surfaces has received much attention recently.[1] Molecules of the type L_2ZrX_2, where L = cyclopentadienyl, indenyl or fluorenyl, are important because of their relevance to stereospecific polymerizations of alkenes.[2] When the metallocene rings are linked via alkyl or silyl bridges, the resulting complexes can be chiral catalysts. Any processes such as [1,5]-silicon migrations which might bring about loss of stereochemical integrity in the catalytic species, need to be understood at a fundamental level.

R_3E groups (E = Si, Ge, Sn) migrate around cyclopentadienyl groups through successive [1,5]-metal shifts with barriers of 15 kcal/mol for Me_3Si, 13 kcal/mol for Me_3Ge and 7 kcal/mol for Me_3Sn. Incorporation of a six-membered ring into these molecules gives the corresponding indenyl systems, **1**, in which barriers to Me_3E migrations increase to 24 kcal/mol for Me_3Si, 22 kcal/mol for Me_3Ge and 15 kcal/mol for Me_3Sn. The increased barriers in the indenyl systems relative to the cyclopentadienyl systems have been attributed to a decrease in aromaticity of the six-membered ring during the migration process. It has been unequivocally demonstrated that the Me_2Si group migrates from C-1 to C-3 in bis(indenyl)dimethylsilane, **5**.[18] In addition, the intermediate *iso*-indenes for trimethylsilylindene, **2**, bis(indenyl)dimethylsilane, **6**, and tris(indenyl)methylsilane, **9**, have all been trapped as their tetracyanoethylene Diels-Alder adducts.[17,18]

The results obtained in this thesis further support the notion of increased barriers in indenyl systems through reduction of aromaticity in *iso*-indene intermediates. It has been hypothesized that one could reduce the barrier to silicon migration by successively adding, first one aromatic ring, then two aromatic rings to the trimethylsilylindene system. We calculated barriers for silicon migrations in these systems and our results indicated that the barrier to silicon

migration should be reduced by adding one ring to the system, with a further reduction in activation energy when a second ring was added.

The two new molecules, angular trimethylsilylbenzindene, **50**, and trimethylsilylcyclopenta[*l*]phenanthrene, **53**, were synthesized. The two molecules were found to be fluxional, and the addition of first one ring, then two rings to the trimethylsilylindene system did successively lower the barrier to silicon migration around the five-membered ring. In addition, *iso*-indene type intermediates for both molecules have been trapped as their tetracyanoethylene Diels-Alder adducts.

Transition-metal complexes of the tetracyclic system cyclopenta[*l*]phenanthrene, **55**, have been prepared for a series of metals, *i.e.* (η^5-cyclopenta[*l*]phenanthrenyl)$Mn(CO)_3$, **78**, (η^5-cyclopenta[*l*]phenanthrenyl)$Fe(C_5H_5)$, **81**, (η^5-cyclopenta[*l*]phenanthrenyl)$_2Fe$, **80**, (η^5-cyclopenta[*l*]phenanthrenyl)$TiCl_3$, **83**, and (η^5-cyclopenta[*l*]phenanthrenyl)$Rh(C_2H_4)_2$, **79**; in all cases the metal is bonded to the five-membered ring. Upon protonation, none of the above compounds were found to undergo haptotropic shifts, mirroring the behaviour of the analogous cyclopentadienyl complexes. Furthermore, the molecule (η^5-cyclopenta[*l*]phenanthrenyl)$Rh(C_2H_4)_2$ rearranges to produce butene at low temperatures, as does the corresponding cyclopentadienyl complex. Transition-metal indenyl complexes undergo ligand substitution reactions at a much greater rate than cyclopentadienyl compounds, owing to the well known "indenyl effect".[45] Neither (η^5-cyclopenta[*l*]phenanthrenyl)$Mn(CO)_3$ nor (η^5-cyclopenta[*l*]phenanthrenyl)$Rh(C_2H_4)_2$ underwent ligand substitution reactions, as is the case with the analogous cyclopentadienyl complexes.

We hypothesized that we might be able to induce haptotropic shifts in complexes in which the transition-metal is bound to a six-membered ring of cyclopenta[*l*]phenanthrene, by deprotonating such complexes. However, attempts to bond transition-metals to a six-membered ring of the ligand were unsuccessful. When the ligand was not carefully dried, the result was to

hydrogenate the double bond of the five-membered ring and yield a complex with $Cr(CO)_3$ attached to a terminal six-membered ring. This molecule, (cyclopenta[*l*]dihydrophenanthrene)$Cr(CO)_3$, **88**, was characterized by X-ray crystallography.

In an attempt to bond $Cr(CO)_3$ to a six-membered ring by using carefully dried ligand, we isolated the Diels-Alder dimer, **94**, of the ligand cyclopenta[*l*]phenanthrene. It was also possible to synthesize this molecule by heating it under reflux in *n*-butyl ether, and we obtained an X-ray crystal structure of the molecule. Of course, it is well-known that cyclopentadiene dimerizes at relatively low temperature; in contrast, indene itself does not dimerize, but instead yields a styrene-type polymer. Theoretical studies on indene and cyclopenta[*l*]phenanthrene revealed that both have a high barrier (≈ 43 kcal/mol for cyclopenta[*l*]phenanthrene and 46 kcal/mol for indene) to hydrogen migration, but that the *iso*-indene type intermediate structure for cyclopenta[*l*]phenanthrene is only 4.3 kcal/mol above the ground state, while the intermediate for indene is 9.0 kcal/mol above the ground state.

CHAPTER EIGHT

Future Work

8.1 Haptotropic shifts in complexes of the angular benzindene.

One of the goals of this thesis was to prepare η^6-metal complexes of cyclopenta[*l*]phenanthrene which would undergo haptotropic shifts. Such multiple inter-ring migrations have not been investigated so far. Had this been achieved, the research would have involved determining the pathway followed by the organometallic moiety over the polycyclic ligand. Specifically, trapping experiments would have been attempted, as well as locating a trajectory using extended Hückel molecular orbital calculations.

It was not possible to prepare η^6-metal complexes of cyclopenta[*l*]phenanthrene. Moreover, η^5-metal complexes behaved as cyclopentadienyl complexes, rather than indenyl systems. Attempts to protonate these complexes did not induce metal migrations into the six-membered ring, as in the analogous indenyl systems.

It may be possible to investigate multiple inter-ring rearrangements by preparing organometallic complexes of the angular benzindene **49**. Would it behave as an indenyl system, a cyclopentadienyl system, or something intermediate between the two? Although the preparation of this ligand is non-trivial, there is apparently a much improved synthesis.[93] The ligand has been used recently to make catalyst precursors,[74,94,95] but no organometallic complexes in which the metal is bonded to a six-membered ring have appeared in the literature as yet.

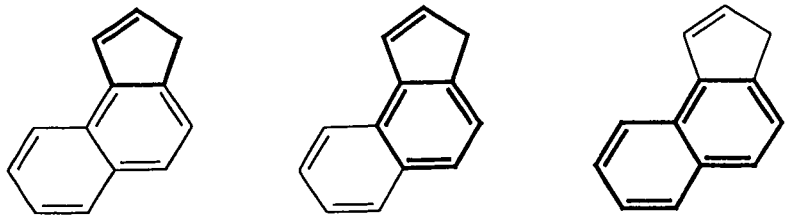

Would it be possible to prepare η^6-complexes of this ligand, and if so, which six-membered ring would the metal bind to? If it bonded to the terminal six-membered ring, it would be interesting to see if the metal would migrate from the terminal six-membered ring, through the central six-membered ring and into the five-membered ring upon deprotonation of the complex. Alternatively, if the metal is bonded to the central six-membered ring, would it migrate to the five-membered ring on deprotonation?

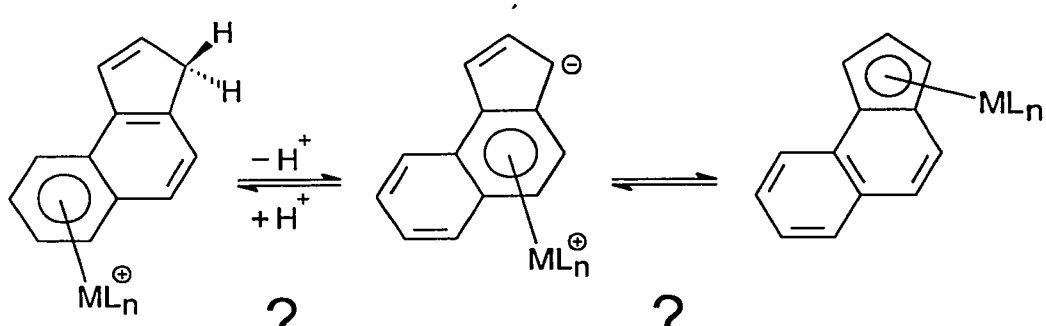

102

One can speculate that η^5-complexes of the angular benzindene would not behave like a cyclopentadienyl-metal complex because the angular (η^5-benzindenyl)$TiCl_3$ complex is a catalyst precursor for the polymerization of styrene. Presumably the η^5-$TiCl_3$ group can "slip" to η^3-$TiCl_3$ allow a vacant coordination site for an incoming styrene molecule. If this is the case, complexes of the angular benzindene in which the metal is bonded in an η^5- fashion may well undergo haptotropic shifts upon protonation, with the metal moving into a six-membered ring.

On the other hand, since η^5-metal complexes derived from cyclopenta[*l*]phenanthrene do not undergo haptotropic shifts, or rapid ligand substitution reactions, one can speculate that they would also not behave as catalyst precursors for polymerization reactions. Since the η^5-$TiCl_3$ complex **83** has now been prepared, it would be interesting to test this hypothesis.

Aside from haptotropic shifts in metal complexes, there is still much interesting chemistry of cyclopenta[*l*]phenanthrene to be investigated. We here suggest some avenues that lend themselves to further study.

8.2 Cyclopenta[*l*]phenanthrenyl cation.

The anion of cyclopenta[*l*]phenanthrene has been prepared and characterized by NMR spectroscopy.[76] Another interesting area to explore would be the preparation of a cyclopentadienyl-type cation of the ligand. Bromination of the ligand with *N*-bromosuccinimide would yield 1-Br-cyclopenta[*l*]phenanthrene. Abstraction of bromide ion could produce the cyclopenta[*l*]phenanthrenyl cation **103**.

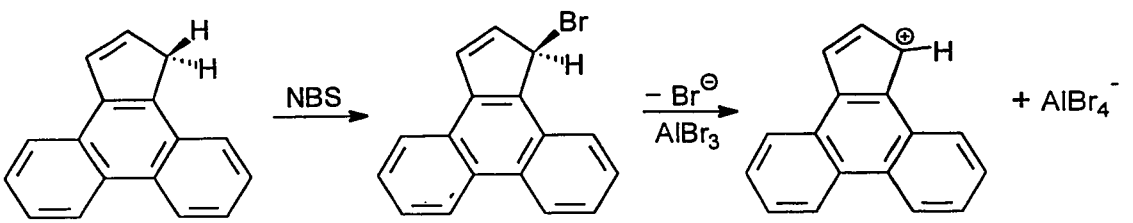

103

If this proves unsuccessful, it may be possible to stabilize the cation on a metal cluster, as outlined in the following synthetic scheme:

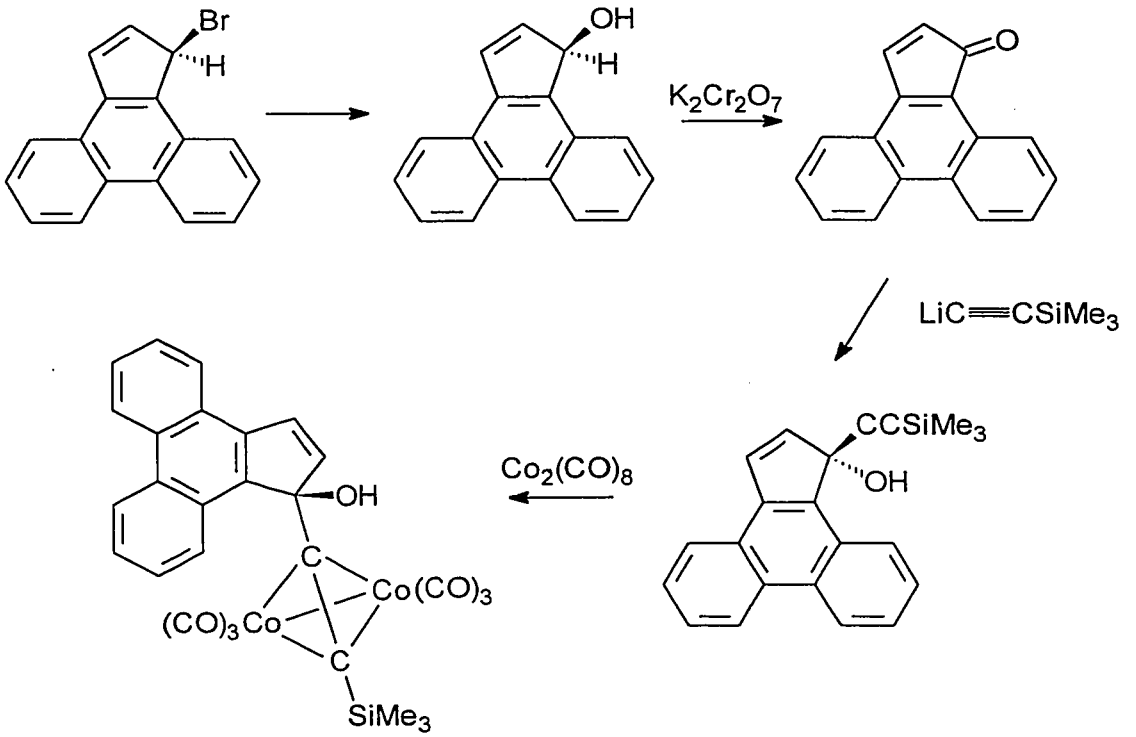

104

Protonation of the metal cluster should yield the metal-stabilized cyclopenta[*l*]phenanthrenyl cation.

8.3 η^5- complexes of cyclopenta[*l*]phenanthrene.

There is also more structural information to be learned about the η^5 complexes of cyclopenta[*l*]phenanthrene. Although we have established that the molecules behave as their cyclopentadienyl analogues, it would be important to grow X-ray quality crystals of one of these systems. This would allow us to determine if the metal is in the centre of the ring, as one expects if it is a cyclopentadienyl analogue, or closer to the three C-H carbons than the two ring junction carbons, as in the indenyl systems.

It would also be interesting to prepare 1-methyl cyclopenta[*l*]phenanthrene, to make the corresponding $Rh(C_2H_4)_2$ complex **106**. Such a substitution would render chiral the metal complexes and therefore the ethylene ligands diastereotopic. Thus the barrier to ML_2 rotation about the metal-polycyclic axis could be determined.

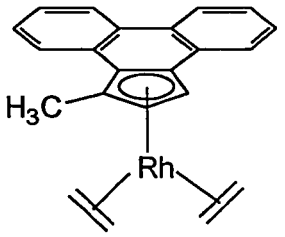

106

The molecule could be made in an analogous manner to the non-methylated complex:

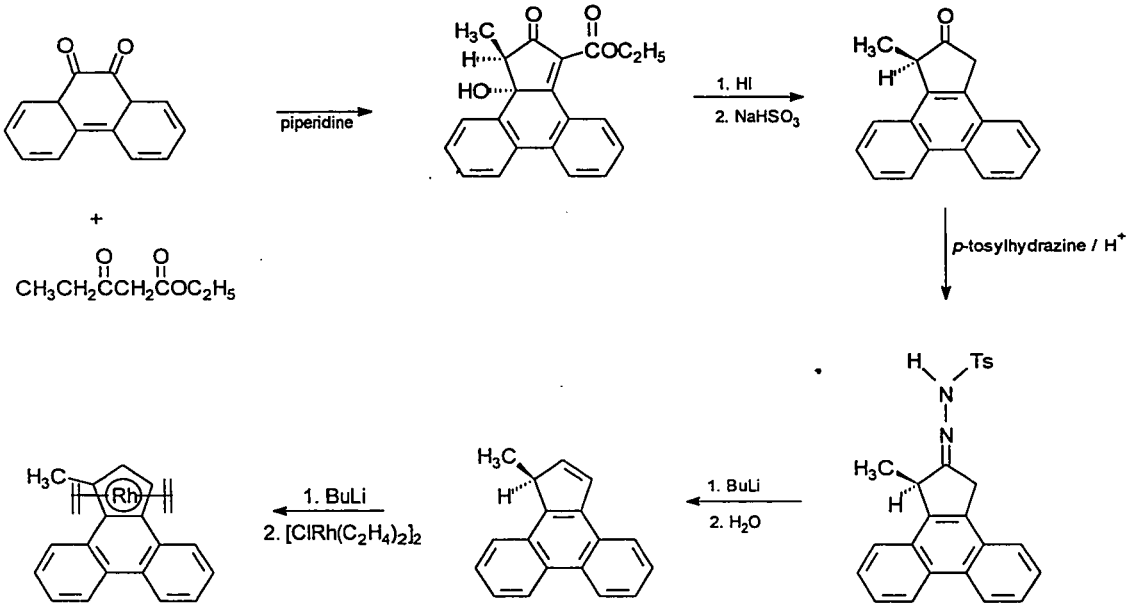

In summary, although several syntheses of cyclopenta[*l*]phenanthrene have appeared in the literature, none of them are trivial. Consequently, the chemistry of this fascinating ligand is almost entirely unexplored. We have made a start, but there is still much to learn about it.

CHAPTER NINE

Experimental

9.1 General Procedures

All syntheses were carried out under a dry nitrogen atmosphere utilizing conventional benchtop and glovebag techniques. Solvents were dried and distilled according to standard procedures.[96] $BrMn(CO)_5$,[97] $[ClRh(C_2H_4)_2]_2$[98] and angular benzindenes, **13**,[99-101] were prepared according to standard procedures. Melting points were measured in open glass capillaries using a Thomas Hoover Unimelt capillary melting point apparatus. The melting points were not corrected.

9.2 NMR Spectra

All NMR spectra were recorded on a Bruker DRX-500 or AC-300 spectrometer.

All spectra used for characterization of molecules were recorded on a Bruker Avance DRX-500 spectrometer, with an 11.74 T superconducting magnet. These experiments included 1-D ^1H, ^{13}C and ^{29}Si NMR spectra as well as 2-D ^1H -^1H COSY, 2-D ^1H -^1H NOESY ^1H -^{13}C shift-correlated and long range ^1H -^{13}C shift-correlated spectra. Single selective inversion ^1H experiments, a 2-D ^1H EXSY spectrum, and variable temperature ^1H and ^{13}C 1-D NMR spectra for trimethylsilylcyclopenta[*l*]phenanthrene, **53**, were recorded on the above system. Following protonation of all organometallic complexes, spectra were acquired on the DRX-500.

Sample temperature was maintained by a Bruker Eurotherm variable temperature unit. Spectra were recorded on spinning samples (except during the acquisition of 2-D spectra), locked to a solvent signal. Peaks were referenced to a residual proton signal of the solvent, or to a ^{13}C solvent signal. Each temperature was measured by placing a copper-constantan thermocouple, contained in an NMR tube, into the probe.

In order to obtain accurate chemical shifts and coupling constants for trimethylsilylcyclopenta[*l*]phenanthrene, **53**, a spectral simulation was performed using the commercially available Bruker Aspect 300 PANIC program.

Proton spectra were acquired at 500.130 MHz using a 5 mm broadband inverse probe with triple axis gradient capability. Typically, spectra were obtained with 8 scans in 32K data points over a 3.931 KHz spectral width (4.168 s acquisition time). The free induction decay (FID) was processed using exponential multiplication (line broadening: 0.15 Hz) and was zero-filled to 64K before Fourier transformation. Carbon-13 NMR spectra were recorded at 125.758 MHz using the 5 mm broadband inverse probe with triple axis gradient capability. The spectra were acquired over a 28.986 KHz spectral width in 32K data points (0.557 s acquisition time). The ^{13}C 90° pulse width was 4.4 μs (31° flip angle). Typically, relaxation delays of 1.0 s were used. The FIDs were processed using exponential multiplication (line broadening: 4.0 Hz) and zero-filled to 64K before Fourier transformation. ^{29}Si NMR spectra were acquired at 99.354 MHz.

Proton COSY 2-D NMR spectra were recorded in the absolute value mode using the pulse sequence: 90° - t_1 - 45° - ACQ and including pulsed field gradients for coherence selection. Typically, spectra were acquired in 2 scans for each of the 256 FIDs that contained 2K data points in F2 over a spectral width of 3930.82 Hz. The 90° ^1H pulse width was 6.6 μs. A 1.0 s relaxation delay was employed between acquisitions. Zero-filling in F1 produced a 1K x 1K data matrix with digital resolution of 3.84 Hz/point in both dimensions. During 2-D Fourier transformation a sine-bell squared window function was applied to both dimensions.

Inverse detected ^1H - ^{13}C 2-D chemical shift correlation spectra were acquired in the phase sensitive mode using the pulsed field gradient version of the HSQC pulse sequence. Typically, the FIDs in the F2 (^1H) dimension were recorded over a 3.655 KHz spectral width in 1K data points. The 128 FIDs in the F1 (^{13}C) dimension were obtained over a 21.368 KHz spectral width. Each FID was acquired in 2 scans. The fixed delays during the pulse sequence were a 1.0

s relaxation delay and a polarization transfer delay of 0.00178 s (corresponding to $1/[4^1J_{CH}]$ = 140 Hz). The 90° ^1H pulse was 6.6 μs while the ^{13}C 90° pulse was 11.6 μs. The data were processed using a sine-bell squared window function shifted by π/2 in both dimensions and linear prediction to 256 data points in F1 followed by zero-filling to 1K.

Inverse detected ^1H - ^{13}C 2-D chemical shift correlation spectra through two- and three-bond coupling interactions were acquired in the absolute value mode using the pulsed field gradient version of the HMBC pulse sequence. Typically, the FIDs in the F2 (^1H) dimension were recorded over a 3.6558 KHz spectral width in 1K data points. The 128 FIDs in the F1 (^{13}C) dimension were obtained over a 21.368 KHz spectral width. Each FID was acquired in 2 scans. The fixed delays during the pulse sequence were a 1.0 s relaxation delay, a 0.0033 s delay for the low pass J-filter and 0.08 s delay to allow evolution of the long-range coupling. The 90° ^1H pulse was 6.6 μs while the ^{13}C 90° pulse was 11.6 μs. The data were processed using a sine-bell squared window function shifted by π/2 in both dimensions and linear prediction to 256 data points in F1 followed by zero-filling to 1K.

A 2-D NOESY spectrum was acquired in the phase-sensitive mode using the pulse sequence: 90° - t_1 - 90° - t_m - 90° - ACQ. 256 FID's were recorded in 2K data points, in the F2 dimension. Each FID was acquired in 8 scans over a 3.931 KHz spectral width. The FIDs were Fourier transformed with sine-bell squared window functions shifted by π/2 in both F1 and F2. The relaxation delay was set to 1.0 s, and the initial value for the 2-D evolution was set to 10 μs. The 90° ^1H pulse was 6.6 μs. At ambient temperature, the mixing time, t_m, for the dimer of cyclopenta[*l*]phenanthrene, **94**, was 800 ms.

Single selective inversion ^1H relaxation experiments and 2-D EXSY spectra (^1H and ^{13}C) for the angular trimethylsilylbenzindene system **50**, were also recorded on a Bruker AC-300 spectrometer, equipped with a 7.65 T superconducting magnet. 1-D NOE difference spectra for

trimethylsilylcyclopenta[*l*]phenanthrene **53**, were recorded on this instrument. In addition, variable temperature spectra for (cyclopenta[*l*]phenanthrenyl)Rh(C_2H_4)$_2$ were acquired on the AC-300.

Proton spectra were acquired at 300.135 MHz using a 5 mm QNP probe. Carbon-13 spectra were recorded at 75.469 MHz using the same probe. Sample temperature was maintained by a Bruker Eurotherm B-VT 2000 variable temperature unit.

Proton-proton NOE difference spectra were acquired by subtraction of a control FID from an on-resonance FID. The decoupler in the control FID irradiated a position in the spectrum where there were no proton signals. The on-resonance FID was obtained with the proton of interest being selectively saturated. In both cases the same decoupler power and duration of saturation (5.0 s) were used. This saturation period also served as the relaxation delay for both the control and on-resonance FIDs. The decoupler was gated off during acquisition. Eight scans were acquired for both the control and on-resonance FIDs. This cycle of alternate acquisition of control and on-resonance FIDs was repeated 4 times for a total of 32 scans for the final difference FID. A 90° ^{1}H pulse width of 7.8 μs was used. The difference FID was processed using exponential multiplication (line broadening: 4.0 Hz) and was zero-filled to 32K before Fourier transformation.

2-D EXSY spectra were acquired in the phase-sensitive mode using the pulse sequence: 90° - t_1 - 90° - t_m - 90° - ACQ. In a typical ^{1}H EXSY experiment, 1024 FID's were recorded in 2K data points, in the F2 dimension. Each FID was acquired in 4 scans over a 3.125 KHz spectral width. The FIDs were Fourier transformed with Gaussian window functions in both F1 and F2, with a line broadening of 3.0 Hz. The relaxation delay was set to 2.0 s, and the initial value for the 2-D evolution was set to 10 μs. The 90° ^{1}H pulse was 8.4 μs. At 106.6 °C, the mixing time, t_m, for the angular trimethylsilylbenzindene system, **50**, was 0.5 s.

The exchange rates in the slow exchange limit were measured by selective inversion relaxation experiments. One part of the spectrum was perturbed using a 90° - τ - 90° pulse

sequence, and then the return to equilibrium was monitored as in an inversion-recovery T_1 experiment. In the systems studied here, selective inversion of a single line proved to be the best way of probing the relaxation, but this is by no means generally true.[25] A C programming language version of McClung's program SIFIT [24] was used to do a non-linear least-squares fit to the experimental results, and to extract values for the rates. Typical errors in the rates are ±10%.

9.3 Mass Spectra

Mass spectra were (DEI) were obtained on a VG Analytical ZAB-SE spectrometer with an accelerating potential of 8kV and a resolving power of 10,000.

9.4 IR Spectra

All infrared spectra were obtained on a Bio Rad FTS-40 FT-IR spectrometer and a SPC 3200 work station using NaCl 0.1 mm solution cells.

9.5 Microanalyses

Microanalyses were performed by Guelph Chemical Laboratories in Guelph, Ontario.

9.6 X-ray Crystallography

Crystals of (η^6-cyclopenta[*l*]dihydrophenanthrene)$Cr(CO)_3$, **88**, were grown by slow evaporation of the solvent from a solution of (η^6-cyclopenta[*l*]dihydrophenanthrene)$Cr(CO)_3$ in methylene chloride and *n*-hexane at -20°C. Crystals of the dimer, **94**, were grown by slow evaporation of the solvent from a solution of the dimer in acetone and *n*-heptane at ambient temperature.

Crystal Structure Determination for (η^6-cyclopenta[*l*]dihydrophenanthrene)$Cr(CO)_3$, 88:

X-ray crystallographic data for (η^6-cyclopenta[*l*]dihydrophenanthrene)$Cr(CO)_3$ were collected from a single crystal which was mounted on a glass fiber and transferred to an Enraf Nonius CAD4 diffractometer, equipped with graphite-monochromated Mo-Ka radiation (λ = 0.71073 Å). Three standard reflections that were measured after every 30 minutes of X-ray exposure time showed neither instrument instability nor crystal decay. The structure was solved using the Patterson Methods procedure in the SHELXTL-PLUS program library.[102] Carbon and oxygen atoms were found in a Fourier difference map. The hydrogen atoms were included in calculated positions and refined isotropically. Aromatic hydrogens and CH_2 hydrogen atoms have a common thermal parameter U. Crystallographic collection parameters, atomic coordinates and bond lengths for (η^6-cyclopenta[*l*]dihydrophenanthrene)$Cr(CO)_3$ are presented in the appendix. Additional information has been stored on a 5.25" disk (departmental thesis copy). The file A.SFT contains the tables of observed and calculated structure factors according to the numbering scheme shown below. The files can be loaded into Microsoft Word.

Crystal Structure Determination for the dimer of cyclopenta[*l*]phenanthrene, 94:

X-ray crystallographic data for the dimer of cyclopenta[*l*]phenanthrene were collected from a single crystal sample, which was mounted in a 0.2 mm sealed glass capillary. Data were collected using a P4 Siemens diffractometer, equipped with a Siemens SMART 1K Charge-Coupled Device (CCD) Area Detector (using the program SMART[103]) and a rotating anode using graphite-monochromated Mo-Ka radiation (λ = 0.71073 Å). The crystal-to-detector distance was 3.991 cm, and the data collection was carried out in 512 x 512 pixel mode, utilizing 2 x 2 pixel binning. The initial unit cell parameters were determined by a least-squares fit of the angular settings of the strong reflections, collected by a 4.5 degree scan in 15 frames over three different parts of reciprocal space (45 frames total). One complete hemisphere of data was collected, to better than 0.8 Å resolution. Upon completion of the data collection, the first 50

frames were recollected in order to improve the decay corrections analysis (if required). Processing was carried out by use of the program SAINT,[104] which applied Lorentz and polarization corrections to three-dimensionally integrated diffraction spots. The program SADABS[105] was utilized for the scaling of diffraction data, the application of a decay correction, and an empirical absorption correction based on redundant reflections. The structure was solved by using the direct methods procedure in the Siemens SHELXTL program library,[106] and refined by full-matrix least squares methods with anisotropic thermal parameters for all non-hydrogen atoms. Crystallographic collection parameters, atomic coordinates and bond lengths for the dimer of cyclopenta[*l*]phenanthrene, **94**, are presented in the appendix. Additional information has been stored on a 5.25" disk (departmental thesis copy). The file B.SFT contains the tables of observed and calculated structure factors according to the numbering scheme shown below. The files can be loaded into Microsoft Word.

9.7 Molecular Orbital Calculations

Optimized equilibrium geometries and transition states were calculated with AM1 of AMPAC [77] (version 2.1) and MOPAC [78] (version 6.0) at the UHF level of theory. The keyword PRECISE was used to tighten the convergence criteria. Molecular mechanics calculations with the MMX force-field of PCMODEL [107] provided the optimized geometries used as input for the AM1 calculations, which gave optimized equilibrium geometries and the heats of formation for **1**, **50a**, **51a**, and **53a**, and for their *iso*-indene analogues **2**, **50b**, **51b**, and **53b**, respectively. Similarly, optimized equilibrium geometries and the heats of formation for the hydrocarbons **54a, and 55a**, along with their *iso*-indene analogues **54b and 55b** were obtained.

To locate the transition state for the rearrangement of **1** into **2**, the C(1)—$SiMe_3$ bond was stretched to 2.3 Å, then the Si—C(1)—C(2) bond angle was decreased from 108.8° to 65° in 5° increments while the C(1)—$SiMe_3$ bond length was fixed at 2.3 Å. The geometry with a C(1)—

$SiMe_3$ bond length of 2.3 Å, and Si-C(1)—C(2) bond angle of 70° was used as input to calculate the transition state. SIGMA or NLLSQ calculations [the keyword SIGMA invokes the McIver-Komornicki gradient norm minimisation routines. The keyword NLLSQ invokes L.S. Bartel's nonlinear least-squares gradient norm minimisation method] were used in the case of the AMPAC calculation; in the case of the MOPAC calculation, the eigenvector following (EF) method, which is invoked with the keyword TS, was used to locate the transition state.

The AMPAC and MOPAC calculations gave identical geometries and heats of formation for the transition state. The calculated Me_3Si—C(1) and Me_3Si—C(2) bond distances for the transition state were 2.368 Å and 2.305 Å, respectively, significantly longer than the value of 1.860 Å obtained in the calculation of **1**; the C(1)—C(2) bond length in the transition state was 1.473 Å. A force calculation with AMPAC or MOPAC — the keyword FORCE is used — gave one negative force constant (frequency) as is required for a transition state.

To locate the transition state for the [1,5]-hydrogen shift from C(1) to C(2) in **1**, the C(1)—H bond was stretched to 1.5 Å, the H—C(1)—C(2) bond angle was decreased from 110.3° to 75° in 5° increments, and the 1.5 Å/75° geometry was used as the input geometry in a MOPAC EF calculation. The calculated H—C(1) and H—C(2) bond distances for the transition state were 1.417 Å and 1.368 Å, respectively, significantly longer than the value of 1.121 Å calculated for **1**; the C(1)—C(2) bond length in the transition state was 1.493 Å. A force calculation with AMPAC or MOPAC, as was the case for the Me_3Si shift, gave one negative force constant (frequency), as is required for a transition state.

To ensure that the vibrations with the negative frequencies connected the reactants and products (both for the Me_3Si- and the H-shifts), the system was viewed with CHEMSTAT, which animates normal modes of vibration calculated with semi-empirical and *ab initio* quantum chemistry programs. This computer software package was run on an IBM RS/6000 Model 530 workstation equipped with a 24-bit graphics adapter.

Calculations on the [1,5]-silatropic shifts in **50**, **51**, and **53** as well as on the hydrogen shift in both indene and cyclopenta[*l*]phenanthrene were carried out in the manner described for **1**. In the transition state for the rearrangement of **50a** to **50b**, the calculated distances were found to be: Me_3Si—C(1) 2.364 Å, Me_3Si—C(2) 2.318 Å, C(1)—C(2) 1.473 Å; for the transformation of **50b** into **50c**, the calculated distances were found to be: Me_3Si—C(1) 2.359 Å, Me_3Si—C(2) 2.316 Å, C(1)—C(2) 1.472 Å. In the transition state that connects **51a** with **51b**, the calculated distances were found to be: Me_3Si—C(1) 2.368 Å, Me_3Si—C(2) 2.309 Å, C(1)—C(2) 1.472 Å. In the transition state for the rearrangement of **53a** into **53b**, the calculated distances were found to be: Me_3Si—C(1) 2.355 Å, Me_3Si—C(2) 2.328 Å, C(1)—C(2) 1.472 Å. In the transition state for the rearrangement of **54a** into **54b**, the calculated distances were found to be: H—C(1) 1.419 Å, H—C(2) 1.385 Å, C(1)—C(2) 1.487 Å. in the ground state, the analogous distances are H(1)—C(1) 1.119 Å and C(1)—C(2) 1.511 Å. Finally, in the transition state for the rearrangement of **55a** into **55b**, the calculated distances were found to be: H—C(1) 1.407 Å, H—C(2) 1.385 Å, C(1)—C(2) 1.487 Å. In the ground state, the analogous distances are H(1)—C(1) 1.119 Å and C(1)—C(2) 1.507 Å. In each case, the transition state exhibited one negative frequency.

9.8 Synthesis and Spectral Data

Preparation of Angular Trimethylsilylbenzindene, 50.

Over a 30 min period, n-butyl lithium (1.25 mL of a 1.6 M hexane solution; 2 mmol) was added dropwise to a solution of benzindene (0.232 g, 2 mmol) in THF (10 mL) at -78°C, and the cold mixture was stirred for 1 h. Trimethylchlorosilane (0.25 mL, 0.217 g, 2 mmol) in THF (5 mL) was added dropwise at -78°C and stirred at this temperature for 1 h. The reaction was allowed to warm to room temperature, stirred for 2 h and the solvent removed *in vacuo*. The residue was washed with distilled water (10 mL) to dissolve the lithium chloride, and the silyl compound was extracted with 15 mL of ether. After drying the ethereal solution over anhydrous magnesium

sulphate, the ether was evaporated under reduced pressure to leave a yellow oil. (0.290 g, 1.22 mmol; 61%). Mass spectrum (DEI), *m/z* (%): 238 (30) ([M^+]), 223 (5) ([M - CH_3]$^+$), 73 (100) ([$SiMe_3$]$^+$). Mass spectrum (high resolution, DEI): calculated for mass $^{12}C_{16}H_{18}Si$ ([M^+]), 238.1178; observed 238.1193. The numbering scheme is shown below.

Major Isomer

^1H NMR (toluene-d_8): δ 8.08 (d, 7.6 Hz, 1H) H-9, 7.77 (d, 7.5 Hz, 1H) H-6, 7.56 (d, 8.4 Hz, 1H) H-5, 7.49 (d, 8.4 Hz, 1H) H-4, 7.44 (d, 5.1 Hz of d, 1.3 Hz, 1H) H-1, 7.36 - 7.33 (m, 1H) H-8, 7.33 - 7.29 (m, 1H) H-7, 6.63 (d, 5.1 Hz of d, 1.7 Hz, 1H) H-2, 3.48 (tr, 1.5 Hz, 1H) H-3, -0.15 (s, 9H) CH_3.

^{13}C NMR (toluene-d_8): δ 143.1 C-3a, 140.5 C-9b, 137.3 C-9a, 135.5 C-2, 132.6 C-5a, 128.8 C-6, 126.9 C-1, 125.7 C-8, 124.8 C-7, 124.5 C-5, 124.2 C-9, 122.1 C-4, 48.7 C-3, -2.4 CH_3.

^{29}Si NMR (toluene-d_8): δ 3.6.

Minor Isomer

^1H NMR (toluene-d_8): δ 8.14 (d, 8.2 Hz, 1H) H-9, 7.82 (d, 8.2 Hz, 1H) H-6, 7.59 (d, 5.0 Hz, 1H) H-5, 7.36 - 7.33 (m, 1H) H-8, 7.33 -7.29 (m, 1H) H-7, 6.93 (d, 5.2 Hz of d, 1.3 Hz, 1H) H-3, 6.69 (d, 5.0 Hz, 1H) H-4, 6.58 (d, 5.2 Hz of d, 1.8 Hz, 1H) H-2, 3.81 (tr, 1.6 Hz, 1H) H-1, -0.20 (s, 9H) CH_3.

^{13}C NMR (toluene-d_8): δ 145.2 C-9b, 141.0 C-3a (C-9b and C-3a may be interchanged), 137.9 C-4, 135.7 C-2, 132.1 C-5a, 129.3 C-3, 126.4 C-5, 125.7 C-8, 125.4 C-6, 124.8 C-7, 124.3 C-9, 48.7 C-1, -0.7 CH_3 (the signal for C-9a could not be unambiguously assigned due to low intensity cross peaks in the HMBC for the minor isomer).

^{29}Si NMR (toluene-d_8): δ 3.2.

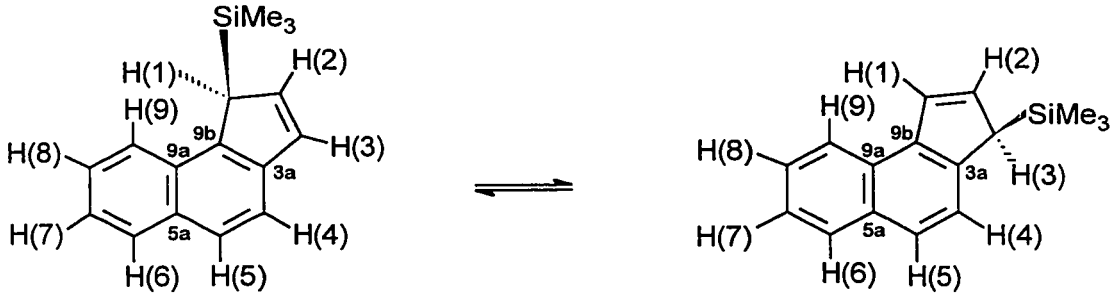

Preparation of the Diels-Alder Adduct of Trimethylsilylbenzindene with TCNE, 63.

A mixture of trimethylsilylbenzindene (1.19 g, 5 mmol) and tetracyanoethylene (0.66 g, 5 mmol) in ethyl acetate (25 mL) was stirred at room temperature, under nitrogen, for 3 days. By this time, the purple color which developed at the start of the reaction had disappeared. The solvent was removed under reduced pressure and the residue washed with hexane (5 mL) and ether (5 mL), then dried *in vacuo*. Colorless crystals (1.33 g; 72%) were obtained upon recrystallization from methylene chloride/hexane. M.p. 180°C (with decomposition). The numbering scheme is shown below.

Mass spectrum (DEI$^+$), *m/z* (%): 366 (2) ([M^+]), 351 (15) ([M - CH_3]$^+$), 310 (100) ([M - 2CH_3 - CN]$^+$), 295 (30) ([M - 3CH_3 - CN]$^+$).

^{1}H NMR ($CDCl_3$): δ 7.96 (d, 8.4 Hz, 2H) H-5, H-6, 7.94 (d, 8.2 Hz, of d, 1.4 Hz, 1H) H-9, 7.67 (tr, 7.3 Hz, of d, 1.3 Hz, 1H) H-7, 7.60 (d, 8.4 Hz, 1H) H-4, 7.57 (tr, 7.5 Hz of d, 1.1 Hz, 1H) H-8, 4.90 (unresolved multiplet) H-1, 4.47 (unresolved multiplet) H-3, 2.23 (unresolved multiplet) H-2, -0.26 (s, 9H) CH_3.

^{13}C NMR ($CDCl_3$): δ 137.0 C-3a, 136.0 C-9b, 133.9 C-9a, 131.4 C-6, 129.4 C-9, 128.7 C-5a, 128.6 C-7, 127.5 C-8, 122.7 C-5, 121.1 C-4, 112.5 equatorial CN bonded to C-11, 112.4 equatorial CN bonded to C-10, 110.3, 110.1 axial CN's, 61.7 C-3, 58.9 C-1, 51.6 C-2, 50.0, 49.5 C-10, C-11, (C-10 and C-11 may be interchanged), -1.8 CH_3.

^{29}Si NMR ($CDCl_3$): δ -2.5.

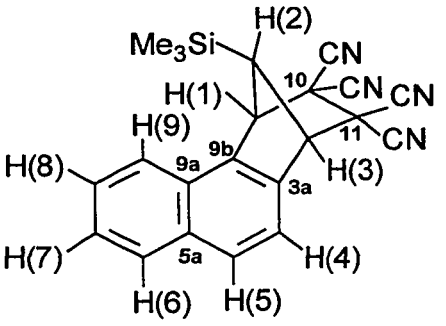

Bis(trimethylsilyl)benzindene, 58.

Over a 30 min period, n-butyl lithium (1.25 mL of a 1.6 M hexane solution; 2 mmol) was added dropwise to a solution of benzindene (0.166 g, 1 mmol) in THF (10 mL) at -78°C, and the cold mixture was stirred for 1 h. Trimethylchlorosilane (0.25 mL, 0.217 g, 2 mmol) in THF (5 mL) was added dropwise at -78°C and stirred at this temperature for 1 h. The reaction was allowed to warm to room temperature, stirred for 2 h and the solvent removed under vacuum. The residue was washed with distilled water (10 mL) to dissolve the lithium chloride, and the silyl compound was extracted with 15 mL of ether. After drying the ethereal solution over anhydrous magnesium sulphate, the ether was evaporated under reduced pressure to leave a yellow oil. (0.186 g, 0.6 mmol; 60%). Mass spectrum (DEI), *m/z* (%): 310 $[M]^+$ (35%), 295 $[M - Me]^+$ (15%), 222 $[M - Me - Me_3Si]^+$ (83%), 159 $[Me_6Si_2CH]^+$ (60%), 73 $[Me_3Si]^+$ (100%).

^1H NMR (CD_2Cl_2): δ 8.23 (d of d, 1H, *H-9*), 8.02 (d, 1H, *H-8*), 7.83 (d, 1H, *H-11*), 7.69 (d, 1H, *H-4*), 7.49 (d of d, 1H, *H-10*), 6.90 (d, 1H, *H-5*), 3.86 (d, 1H, *H-2*), 1.85 (d, 1H, *H-1*), 0.10 (s, 9H, $SiMe_3$). -0.03 (s, 9H, $SiMe_3$). [The assignments of *H-8* and *H-11* could be interchanged; likewise for *H-9* with *H-10*, and *H-4* with *H-5*.] The numbering system is shown below:

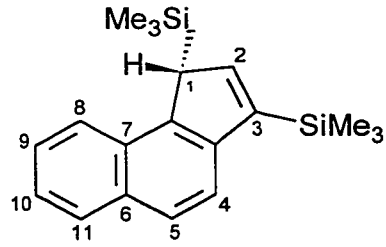

Preparation of Ethyl 3,3a-dihydro-3a-hydroxy-2-oxo-2H-cyclopenta[*l*]phenanthrene-1-carboxylate, 107.

Following the procedure of Cope *et al.*,[75] ethyl acetoacetate (37.51 g, 288.5 mmol) in 50 mL absolute ethanol was added to a suspension of 9,10-phenanthrenequinone (30.02 g, 144.4 mmol) in 25 mL absolute ethanol. Piperidine (6 drops) in 25 mL absolute ethanol was added, and the mixture was stirred and heated under reflux. After 40 min, 6 drops piperidine were added. After heating for two hours, piperidine (12 drops) in 25 mL absolute ethanol was added. After 15 min the mixture turned solid. Heating was continued for 30 min. The mixture was cooled and filtered. The solid was washed with cold ethanol, then cold benzene, leaving a yellow-brown solid. Recrystallization from acetonitrile gave yellow needles (27.75 g, 86.72 mmol, 60%, based on phenanthrenequinone), m.p. 188-189 °C. The numbering scheme is shown below.

Mass spectrum (DEI$^+$), *m/z* (%): 320 (100) ([M]$^+$), 303 (45) ([M-OH]$^+$), 274 (65) ([M - CH_2 - OH]$^+$), 247 (23) ([M-COOEt]$^+$), 202 (40) ([$C_{16}H_{10}$]$^+$).

^{1}H NMR ($CDCl_3$): δ 7.93 (d, 8.0 Hz, 1H) H-8, 7.88 (d, 7.8 Hz, 1H) H-7, 7.74 (d, 7.7 Hz of d, 0.7 Hz,1H) H-11, 7.57 (d, 1.2 Hz of tr, 7.5 Hz, 1H) H-9, 7.49-7.44 (m, 2H) H-4, H-6, 7.40-7.36 (m, 2H) H-5, H-10, 4.34 (quartet, 7.1 Hz, 2H) ethyl CH_2, 3.18 (dd, 2H) ring CH_2, 2.49 (s, 1H) hydroxyl, 1.29 (tr, 7.1 Hz, 3H) CH_3.

^{13}C NMR ($CDCl_3$): δ 199.7 C-2, 168.0 C-1, 164.0 ester CO, 136.8 C-3b, 133.5 C-7b, 132.8 C-9, 132.0 C-7a, 131.2 C-11b, 130.0 C-6, 129.9 C-11, 129.5 C-5, 128.5 C-10, 127.0 C-4, 126.1 C-11a, 125.1 C-7, 124.5 C-8, 74.7 C-3a, 61.8 ethyl CH_2, 46.9 ring CH_2, 14.0 CH_3.

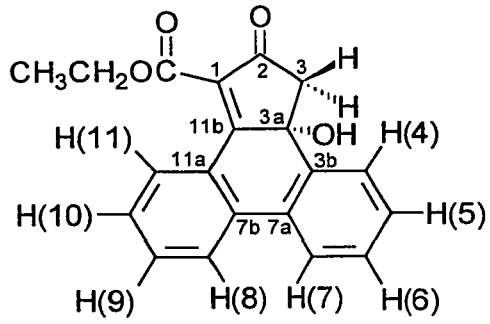

Preparation of 2,3-Dihydro-2-oxo-1H-cyclopenta[*l*]phenanthrene, 97.

Following the procedure of Cope *et al.*,[75] 24 mL hydriodic acid (47% HI) was added to ethyl 3,3a-dihydro-3a-hydroxy-2-oxo-2H-cyclopenta[*l*]phenanthrene-1-carboxylate (8.02 g, 25.1 mmol). The brown mixture was stirred and heated under reflux in an oil bath at 110-120°C for 1.3 hr. Water (30 mL) was added and the resulting black solid was removed by filtration. The black solid was boiled with a 10% sodium bisulfite solution for 5 min, the solid particles being broken up with a spatula. The mixture was filtered and the precipitate washed with water. Air drying gave a green powder (5.80 g, 25.0 mmol, 99%), m.p. 205-207 °C. The numbering scheme is shown below.

Mass spectrum (DEI$^+$), *m/z* (%): 232 (90) ([M]$^+$), 204 (100) ([M-CO]$^+$).

^{1}H NMR ($CDCl_3$): δ 8.70 (d, 8.5 Hz, 1H) H-7, 7.67-7.62 (m, 3H) H-4, H-5, H-6, 3.78 (s, 2H) H-1.

^{13}C NMR ($CDCl_3$): δ 213.9 C-2, 132.7 C-3a, 130.1 C-3b, 128.8 C-7a, 127.1 C-6, 126.6 C-5, 124.9 C-4, 123.3 C-7, 43.4 C-1.

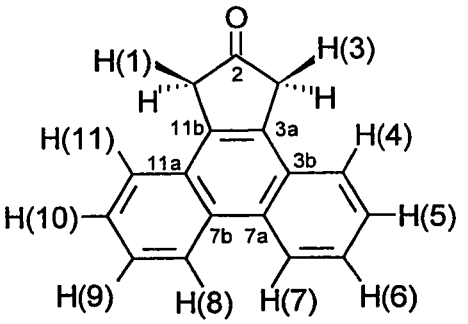

Preparation of the Tosylhydrazone of 2,3-Dihydro-2-oxo-1H-cyclopenta[*l*]phenanthrene, 108.

Following the procedure of Eliasson *et al.*,[76] to a gently boiling stirred solution of 2,3-dihydro-2-oxo-1H-cyclopenta[*l*]phenanthrene (2.11 g, 9.17 mmol) in 140 mL absolute ethanol and 60 mL dioxane was added a warm solution of *p*-tolylsulfonylhydrazide (1.80 g, 9.66 mmol) in 50 mL absolute ethanol, followed by 2 mL of glacial acetic acid. The product precipitated from the boiling solution. The mixture was cooled, the precipitate filtered, washed with absolute ethanol, and air-dried. The off-white solid (1.61 g, 4.00 mmol, 44%, based on 2,3-dihydro-2-oxo-1H-cyclopenta[*l*]phenanthrene) decomposed at 207 °C. The numbering scheme is shown below.

^{1}H NMR (DMSO-d_6) δ 10.36 (s, 1H) H-12, 8.79-8.76 (m, 2H) H-7, H-8, 7.75 (d, 8.1 Hz, 2H) H-14, 7.73 (d, 8.2 Hz, 2H) H-4, H-11, 7.66-7.58 (m, 4H) H-5, H-6, H-9, H-10, 7.35 (d, 8.1 Hz, 2H) H-15, 4.08 (s, 2H) H-3, 4.04 (3, 2H) H-1, (H-1 and H-3 may be interchanged), 2.31 (s, 3H) tosyl CH_3.

^{13}C NMR (DMSO-d_6) δ 162.5 C=N, 143.2 C-16, 136.4 C-13, 133.7, 132.7 C-3a, C-11b, 129.6, 128.4 C-3b, C-11a, 129.5, 128.5 C-7a, C-7b, 129.4 C-14, 127.5 C-15, 127.2, 127.1 C-6, C-9, 126.5, 126.4 C-5, C-10, 125.0, 124.5 C-4, C-11, 123.5, 123.3 C-7, C-8, 38.1, 35.1 C-3, C-1, 20.9 CH_3.

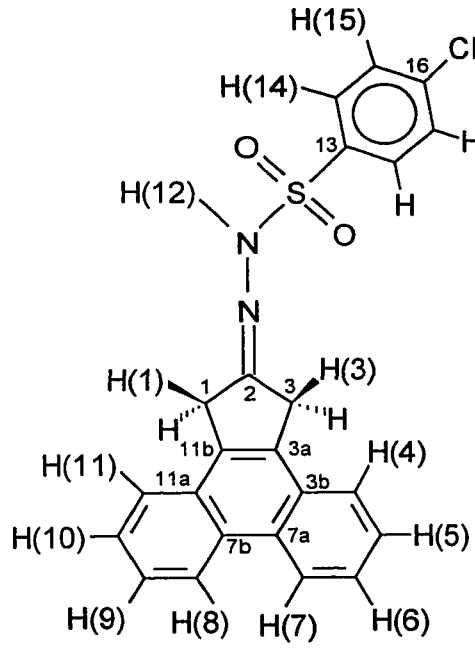

Preparation of 1H-Cyclopenta[*l*]phenanthrene, 55.

In a slight modification of the procedure of Eliasson *et al.*,[76] 10 mL of *n*-BuLi (1.4 M in hexane) was added to a stirred suspension of the tosylhydrazone of 2,3-dihydro-2-oxo-1H-cyclopenta[*l*]phenanthrene (2.01 g, 5.02 mmol) in 100 mL dry diethyl ether over 0.5 hr at room temperature . The mixture was stirred overnight, quenched with 50 mL water and stirred for 8 hr. The organic phase was separated, washed with water and dried over $MgSO_4$. A red-brown solid was obtained on evaporation of the ether. Flash chromatography on silica using carbon tetrachloride as the eluent yielded an off-white solid (0.49 g, 2.27 mmol, 45%) on evaporation of the solvent, m.p. 152-153 °C.

Mass spectrum (DEI$^+$), *m/z* (%): 216 (100) ([M]$^+$), 215 (25) ([M-H]$^+$). Mass spectrum (high resolution, DEI): calculated for mass $^{12}C_{17}H_{12}$ ([M]$^+$), 216.0939 amu; observed 216.0935 amu.

^{1}H NMR ($CDCl_3$) δ 8.74-8.72 (m, 1H) H-7, 8.71-8.69 (M, 1H) H-8, 8.19-8.17 (m, 1H) H-4, 8.03-8.01 (m, 1H) H-11, 7.66-7.62 (m, 2H) H-5, H-6, 7.61-7.55 (m, 2H) H-9, H-10, 7.49 (d, 5.5 Hz of tr, 1.7 Hz, 1H) H-3, 6.77 (d, 5.5 Hz of tr, 1.7 Hz, 1H) H-2, 3.85 (tr, 1.7 Hz, 2H) H-1.

^{13}C NMR ($CDCl_3$) δ 139.4 C-3a, 138.5 C-11b, 133.8 C-2, 130.3 C-7a, 130.0 C-3, 129.7 C-7b, 128.9 C-11a, 127.8 C-3b, 126.8 C-9, 126.4 C-6, 125.7 C-5, 125.2 C-10, 124.4 C-4, 124.0 C-11, 123.5 C-8, 123.3 C-7, 39.5 C-1.

IR (CCl_4): 3076 (w), 2957 (w), 2858 (w) cm^{-1}.

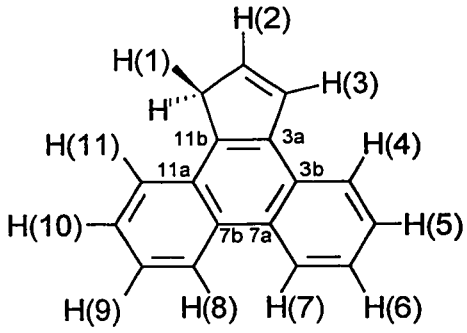

Preparation of Trimethylsilylcyclopenta[*l*]phenanthrene, 53.

To a stirred solution of 1H-cyclopenta[*l*]phenanthrene (0.45 g, 2.08 mmol) in 50 mL dry THF, was added dropwise 1.5 mL *n*-BuLi (1.4 M in hexane, 2.10 mmol) at -78 °C. After stirring for 1 hr, the reaction flask was recooled to -78°C and chlorotrimethylsilane (0.4 mL, 3.15 mmol) was added dropwise. The solution was stirred overnight and the solvent was removed *in vacuo*. After addition of dry diethyl ether (50 mL), the resulting white precipitate was filtered off using Schlenk techniques to leave a yellow solution. Removal of the ether *in vacuo* yielded a moisture-sensitive clear yellow oil (0.55 g, 1.91 mmol, 91%).

Mass spectrum (DEI$^+$), *m/z* (%): 288 (32) ([M]$^+$), 273 (5) ([M-CH_3]$^+$), 215 (15) ([M-trimethylsilyl]$^+$), 73 (100) ([trimethylsilyl]$^+$). Mass spectrum (high resolution, DEI): calculated for mass $^{12}C_{20}H_{20}Si$ ([M$^+$]), 288.1334 amu; observed 288.1370 amu.

^{1}H NMR (CD_2Cl_2): δ 8.76 (d, 8.3 Hz of d, 1.5 Hz of d, 0.5 Hz, 1H) H-7, 8.73 (d, 8.3 Hz of d, 1.8 Hz of d, 0.6 Hz, 1H) H-8, 8.26 (d, 8.3 Hz of d, 1.5 Hz of d, 0.5 Hz, 1H) H-4, 8.03 (d, 8.3 Hz of d, 1.8 Hz of d, 0.6 Hz, 1H) H-11, 7.66 (d, 8.3 Hz of d, 6.8 Hz of d, 1.5 Hz, 1H) H-5, 7.63 (d, 8.3 Hz of d, 6.8 Hz of d, 1.5 Hz, 1H) H-6, 7.60 (d, 8.3 Hz of d, 6.7 Hz of d, 1.8 Hz, 1H) H-10, 7.57 (d, 8.3 Hz of d, 6.7 Hz of d, 1.8 Hz, 1H) H-9, 7.56 (d, 5.2 Hz of d, 1.0 Hz, 1H) H-3, 6.92 (d, 5.2 Hz of d, 1.7 Hz, 1H) H-2, 4.40 (tr, 1.3 Hz, 1H) H-1, -0.05 (s, 9H) CH_3.

^{13}C NMR (CD_2Cl_2): δ 140.7 C-11b, 138.4 C-3a, 136.3 C-2, 129.8 C-3b, 129.6 C-7b, 129.0 C-11a, 128.6 C-7a, 126.8 C-6, 126.6 C-3, 126.3 C-9, 126.0 C-11, 125.8 C-5, 125.2 C-10, 124.7 C-4, 123.8 C-8, 123.6 C-7, 49.2 C-1, -1.6 CH_3.

^{29}Si NMR (CD_2Cl_2): δ 5.1.

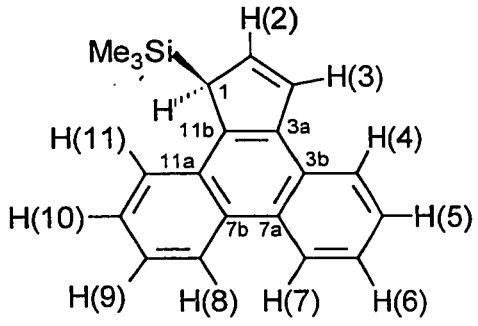

Preparation of the Diels-Alder Adduct of Trimethylsilylcyclopenta[*l*]phenanthrene with TCNE, 64.

To a partially dissolved mixture of tetracyanoethylene (0.155 g, 1.20 mmol) in 10 mL dry diethyl ether was added a solution of 0.050 g trimethylsilylcyclopenta[*l*]phenanthrene (0.174

mmol) in 5 mL dry ether. After several minutes, the mixture turned purple and a white solid precipitated from solution. Stirring was continued for two days and the white solid was filtered off and washed with ether. It was chromatographed on a silica gel column by using methylene chloride as eluent. After evaporation of the solvent, 0.060 g of the Diels-Alder adduct (0.144 mmol; 83%) was obtained. Recrystallization from methylene chloride/hexane yielded clear colorless crystals.

Mass spectrum $(CEI)^+$, *m/z* (%): 434 (10) ($[M + NH_4]^+$), 290 (60) ($[M - C_2(CN)_4 - CH_3]^+$), 289 (85) ($[M - C_2(CN)_4 - CH_3 - H]^+$), 90 (100) ($[SiMe_3]^+$).

^1H NMR (CD_3CN): δ 8.87 (m, 2H) H-7, 8.29 (m,2H) H-4, 7.81 (m, 4H) H-5, H-6, 5.39 (d, 1.1 Hz, 2H) H-1, 2.32 (tr, 1.1 Hz, 1H) H-2, -0.31 (s, 9H) CH_3.

^{13}C NMR (CD_3CN): δ 138.1 C-3a, 131.8 C-3b, 129.3, 129.0 C-5, C-6 (may be interchanged), 128.0 C-7a, 125.8 C-4, 124.9 C-7, 114.2 equatorial CN, 112.5 axial CN, 60.5 C-1, 52.3 C-2, 51.3 C-12, -1.7 CH_3.

^{29}Si NMR (CD_3CN): δ 2.1.

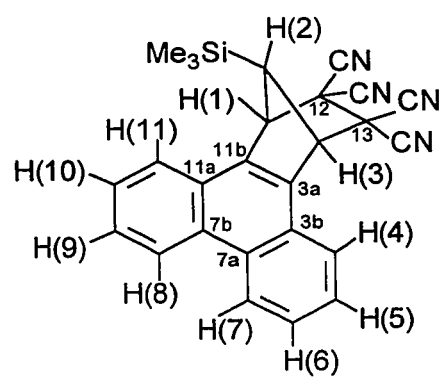

Preparation of 2,3-Dihydro-2-hydroxy-2-trimethylsilylethynyl-*1H*-cyclopenta[*l*]phenanthrene, 99.

To a solution of trimethylsilylacetylene (1.27 mL, 8.793 mmol) in 20 mL dry THF was added dropwise *n*-BuLi (5.77 mL 1.6 M in hexane, 9.2 mmol) at -78°C. The solution was stirred for one hr, while maintaining the temperature of the reaction vessel below 0°C. The flask was then recooled to -78°C. A solution of 2,3-dihydro-2-oxo-1H-cyclopenta[*l*]phenanthrene (2.040 g, 8.793 mmol) in 80 mL dry THF was added dropwise. The reaction flask was gradually warmed to room temperature, and stirring was continued overnight. The solvent was removed under reduced pressure to give a 2:1 mixture of starting ketone:product alcohol. Extraction with diethyl ether followed by column chromatography using 1:9 diethyl ether:hexane yielded mainly the product alcohol, (0.456 g, 1.38 mmol; 16%), which was not further purified before reaction with $Co_2(CO)_8$. M.p. 148-149°C.

Mass spectrum $(DEI)^+$, *m/z* (%): 330 (30) ($[M]^+$), 239 (10) ($[M - Me_3Si - H_2O]^+$), 205 (100) ($[M - C_3OSiMe_3]^+$), 73 (10) ($[Me_3Si]^+$).

^1H NMR (CD_2Cl_2): δ 8.73 (m, 2H) H-7, 7.81 (m, 2H) H-4, 7.67 (m, 4H) H-5, H-6, 1.27 (s, 1H) O<u>H</u>, 3.78 (dd, 4H) H-1, 0.21 (s, 9H) CH_3.

^{13}C NMR (CD_2Cl_2): δ 134.3 C-3a, 130.7 C-3b, 129.9 C-7a, 127.2 C-6, 126.4 C-5, 125.1 C-4, 123.6 C-7, 109.4 C-2, 88.4 C-12, 73.6 C-13, 50.1 C-1, -0.5 CH_3.

^{29}Si NMR (CD_2Cl_2): δ -13.1.

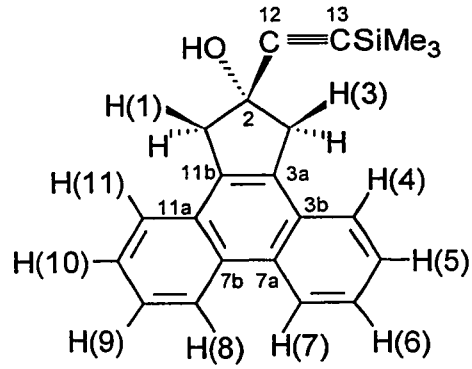

Preparation of [2,3-Dihydro-2-hydroxy-2-trimethylsilylethynyl-*1H*-cyclopenta[*l*]phenanthrene][$Co_2(CO)_6$], 100.

To a solution of $Co_2(CO)_8$ (0.311 g, 0.909 mmol) in 20 mL dry THF was added a solution of 2,3-dihydro-2-hydroxy-2-trimethylsilylethynyl-*1H*-cyclopenta[*l*]phenanthrene (0.300 g, 0.909 mmol) in 20 mL dry THF. The solution was stirred overnight and the solvent removed under reduced pressure. The dark red solid was chromatographed on silica gel by using 3:1 hexane:methylene chloride as eluent. After evaporation of the solvent, 0.301 g (0.512 mmol, 56%) of product were obtained. Decomposes at 163-164°C.

Mass spectrum $(DEI)^+$, *m/z* (%): 532 (5) ($[M - 3CO]^+$), 476 (10) ($[M - 5CO]^+$), 330 ($[ligand]^+$), 232 (50) ($[M - Co_2(CO)_6 - Me_3SiC_2H]^+$), 204 (100) ($[ligand - Me_3SiC_3OH]^+$), 73 (20) ($[Me_3Si]^+$).

^1H NMR (CD_2Cl_2): δ 8.75 (m, 2H) H-7, 7.84 (m, 2H) H-4, 7.67 (m, 4H) H-5, H-6, 3.75 (dd, 2H) H-1, 2.46 (s, 1H) O<u>H</u>, 0.25 CH_3.

^{13}C NMR (CD_2Cl_2): δ 200.9 CO, 134.7 C-3a, 130.8 C-3b, 129.9 C-7a, 127.3 C-5, 126.5 C-6 (C-5 and C-6 may be interchanged), 125.0 C-4, 123.6 C-7, 119.0 C-2, 83.4 C-12, 76.0 C-13, 51.8 C-1, 1.0 CH_3.

^{29}Si NMR (CD_2Cl_2): δ 0.49.

IR (CCl_4): 2957 (w), 2927 (w), 2856 (w), 2090 (s), 2051 (vs), 2026 (vs) cm^{-1}.

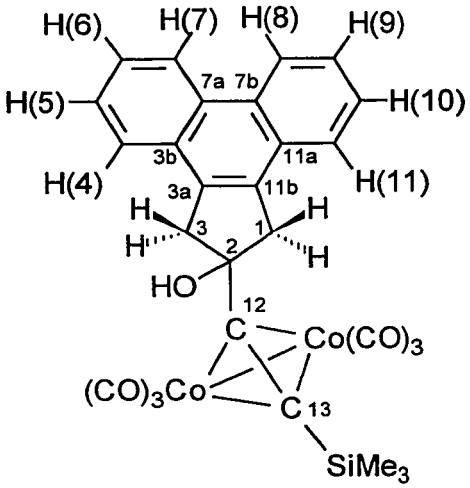

Preparation of 2,3-Dihydro-2-hydroxy-2-trimethylsilylethynyl-*1H*-cyclopenta[*l*]phenanthrene][$Co_2(CO)_6$] Cation, 101.

A solution of the $Co_2(CO)_6$ complex of 2,3-dihydro-2-hydroxy-2-trimethylsilylethynyl-*1H*-cyclopenta[*l*]phenanthrene in CD_2Cl_2 in an NMR tube was cooled in a dry ice/acetone bath, and 2 drops of HBF_4 in ether were added. The sample was placed in a spectrometer probe that had been cooled to -64°C, and ^1H and ^{13}C NMR spectra were recorded.

^1H NMR (CD_2Cl_2, 200K): δ 8.60 (br, 2H) H-7, H-8, 7.72 (br, 2H) H-4, H-11, 7.57 (br, 4H) H-5, H-6, H-9, H-10, 4.27 (d,1H) H-1, 4.24 (d,1H) H-1, 4.07 (d,1H) H-3, 3.93 (d,1H) H-3 (H-1 and H-3 may be interchanged), 0.52 (s,9H) CH_3.

^{13}C NMR (CD_2Cl_2, 210K): δ 136.2 C-3a, C-11b, 133.1 C-3b, 132.8 C-11a (C-3b and C-11a may be interchanged), 129.3 C-7a, C-7b, 127.0, 126.9, 126.6 C-5, C-6, C-9, C-10, 124.2 C-2, 124.0 C-4, 123.8 C-11 (C-4 and C-11 may be interchanged), 122.9 C-7, C-8, 49.0 C-1, 44.3 C-3 (C-1 and C-3 may be interchanged) -0.3 CH_3.

At 190K, there are 6 CO resonances: 197.3, 195.3, 193.7, 192.8, 190.4 and 185.8 ppm. At 200K, there are three CO resonances: 199.9, 197.5 and 195.2 ppm. By 210K, no carbonyl resonances are observed.

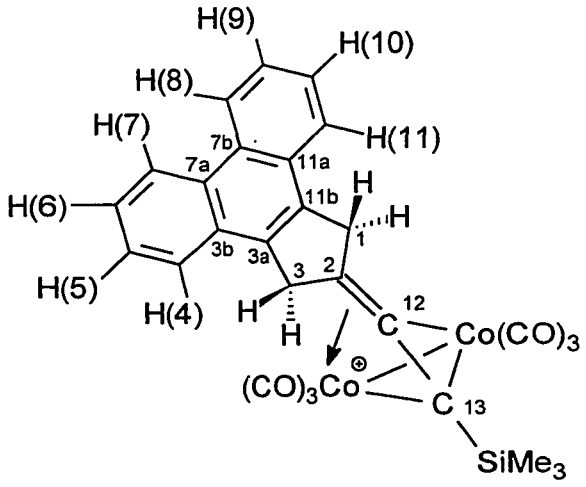

Preparation of (η^5-cyclopenta[*l*]phenanthrenyl)Mn(CO)$_3$, 78.

To a solution of cyclopenta[*l*]phenanthrene (0.200 g, 0.926 mmol) in 20 mL dry THF was added dropwise 0.7 mL *n*-BuLi at -78°C. The dark red solution was stirred for 1 hr at -78°C. A solution of $BrMn(CO)_5$ (0.254 g, 0.924 mmol) in 20 mL dry THF was added dropwise. The reaction vessel was allowed to warm to room temperature, and then was heated under reflux overnight. Removal of the solvent left a dark red oil which was purified by flash chromatography on silica using hexane/ether 9:1. 0.069 g of red solid was obtained (0.19 mmol; 21 %). m.p. 192-193°C.

Mass spectrum $(DEI)^+$, *m/z* (%): 298 (30) ($[M - 2CO]^+$), 270 (100) ($[M - 3CO]^+$), 215 ($[M - Mn(CO)_3]^+$), 55 (40) ($[Mn]^+$). Mass spectrum (high resolution, DEI): calculated for mass $^{12}C_{17}H_{11}Mn$ ($[M - 3(CO)]^+$), 270.0241 amu; observed 270.0248 amu.

^{1}H NMR (CD_2Cl_2): δ 8.49 (m, 2H) H-76, 7.97 (m, 2H) H-4, 7.62 (m, 4H) H-5, H-6, 5.60 (d, 2.8 Hz, 2H) H-1, 5.17 (tr, 2.8 Hz, 1H) H-2.

^{13}C NMR (CD_2Cl_2): δ 221.0 CO, 130.5 C-3b, C-7a, 128.4, 128.3, C-5, C-6 (C-5 and C-6 may be interchanged), 124.6 C-4, 124.5 C-7, 99.0 C-3a, 86.3 C-2, 73.3 C-1.

IR (CCl_4): 3078 (vw), 2959 (w), 2928 (w), 2857 (w), 2022 (vs), 1943 (vs) cm^{-1}.

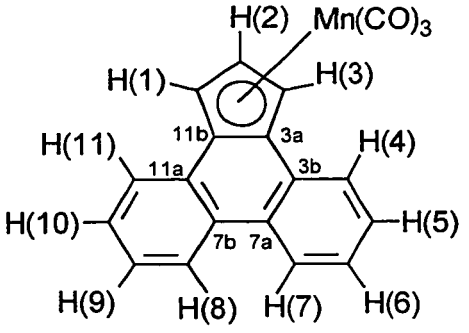

Attempt to protonate (η^5-cyclopenta[*l*]phenanthrenyl)Mn(CO)$_3$.

In an NMR tube, a solution of (η^5-cyclopenta[*l*]phenanthrenyl)Mn(CO)$_3$ in CD_2Cl_2 was treated with a drop of HBF_4 in ether at -78°C. There was no change in the ^{1}H NMR spectrum of the compound at -78°C or upon slowly warming the solution up to 35°C.

In another attempt to protonate (η^5-cyclopenta[*l*]phenanthrenyl)Mn(CO)$_3$, a solution of the compound in C_6D_6 was treated with a drop of HBF_4 in ether and heated under reflux overnight. After cooling, there was no change in the ^{1}H NMR spectrum.

In another attempt to protonate (η^5-cyclopenta[*l*]phenanthrenyl)Mn(CO)$_3$, a solution of the compound in CD_2Cl_2 was treated with a drop of CF_3COOH at room temperature. Again, there was no change in the ^{1}H NMR spectrum.

Attempt to add triethylphosphine to (η^5-cyclopenta[*l*]phenanthrenyl)Mn(CO)$_3$.

Triethylphosphine (0.26 mL, 1.7 mmol) was syringed into a stirred, orange solution of

(η^5-cyclopenta[*l*]phenanthrenyl)$Mn(CO)_3$ (0.070 g, 0.276 mmol) in 10 mL dry hexane, under nitrogen. No colour change was observed, as in the analogous indenyl and related systems. The solution was heated under reflux under nitrogen for two weeks. After cooling, the solvent was removed under vacuum to yield a brown oil. The ^1H NMR spectrum of this oil indicated decomposition products only.

Preparation of (η^1-cyclopenta[*l*]monohydrophenanthrene)$Mn(CO)_5$, 109.

When the synthesis for (η^5-cyclopenta[*l*]phenanthrenylMn$(CO)_3$) was followed, but the ligand had not been carefully dried, traces of (η^1-cyclopenta[*l*]monohydrophenanthrene)$Mn(CO)_5$ were identified by ^1H NMR.

^1H NMR (CD_2Cl_2): δ 8.7 (m, 2H) H-7, 7.8 (m, 2H) H-4, 7.5 (m, 4H) H-5, H-6, 3.50 (d, 12.3 Hz of d, 8.3 Hz, 2H) H-1/3, 2.93 (d, 15.0 Hz of d, 7.0 Hz, 2H) H-1'/3', 2.70 (quintet, 1H) H-2.

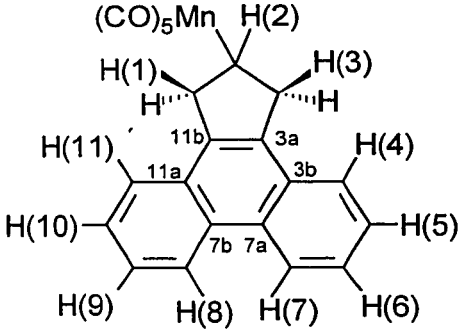

Preparation of (η^5-cyclopenta[*l*]phenanthrenyl)$TiCl_3$, 83.

Following the general procedure of Rausch *et al.*, trimethylsilylcyclopenta[*l*]phenanthrene (0.628 g, 2.18 mmol) was dissolved in dry CH_2Cl_2, and cooled to 0°C. $TiCl_4$ (0.24 mL, 2.18 mmol) was added dropwise. The solution immediately turned very dark purple. The solution was warmed to room temperature and stirred overnight. The solvent was removed under vacuum and the

residue was washed with dry pentane. Dry methylene chloride (30 mL) was added and the purple solution was filtered. The filtrate was concentrated to 10 mL and cooled to -20°C overnight. Filtration yielded 0.380 g (1.03 mmol, 47%) purple crystals. m.p. 211-212°C (with decomposition). Mass spectrum $(DEI)^+$, *m/z* (%): 430 (8) ($[C_{34}H_{22}]^+$), 370 (6) ($[M]^+$), 215 (100) ($[C_{17}H_{11}]^+$).

^1H NMR ($CDCl_3$): δ 8.56 (d, 8.5 Hz, 2H) H-7, 8.23 (d, 7.7 Hz, of d, 1.5 Hz, 2H) H-4, 7.74-7.67 (m, 4H) H-5, H-6, 7.62 (d, 3.3 Hz, 2H) H-1, 7.25 (tr, 3.3 Hz, 1H) H-2.

^{13}C NMR ($CDCl_3$): δ 131.2 C-7a, 131.1 C-3a, 130.1 C-6, 128.3 C-5, 127.6 C-3b, 125.5 C-4, 124.1 C-7, 123.1 C-2, 115.4 C-1.

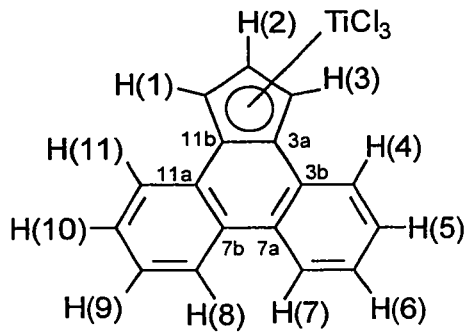

Preparation of (η^5-cyclopenta[*l*]phenanthrenyl)Rh(C_2H_4)$_2$, 79.

$Rh_2Cl_2(C_2H_4)_4$ was prepared by the standard method.[98] (η^5-cyclopenta[*l*]phenanthrenyl)$Rh(C_2H_4)_2$ was prepared using Green's procedure for the synthesis of (η^5-indenyl)-$Rh(C_2H_4)_2$.[108,109]

To a solution of cyclopenta[*l*]phenanthrene (0.533 g, 2.47 mmol) in 20 mL dry THF was added dropwise 1.55 mL (2.48 mmol) *n*-BuLi at -78°C. The dark red solution was stirred for 1 hr at -78°C. This solution was then syringed into a suspension of $Rh_2Cl_2(C_2H_4)_4$ (0.464 g, 1.19 mmol) in 20 mL dry THF. The mixture was stirred for 1 hr, and the solvent removed under vacuum. The

dark red residue was extracted repeatedly (8 x 50 mL) with hexanes. Removal of the solvent under reduced pressure yielded 0.485 g (1.29 mmol, 60%) of a yellow solid, which decomposes at 96°C.

Mass spectrum $(DEI)^+$, *m/z* (%): 533 (18) ($[C_{34}H_{22}Rh]^+$), 374 (5) ($[M]^+$), 346 (20) ($[M\text{-}C_2H_4]^+$), 318 (100) ($[M - 2(C_2H_4)]^+$), 216 (30) ($[C_{17}H_{11}]^+$). Mass spectrum (high resolution, DEI): calculated for mass $^{12}C_{17}H_{11}Rh$ ($[M - 2(C_2H_4)]^+$), 317.9916 amu; observed 317.9913 amu.

^1H NMR (CD_2Cl_2): δ 8.61-8.59 (m, 2H) H-7, 7.83-7.81 (m, 2H) H-4, 7.58-7.56 (m, 4H) H-5, H-6, 6.16 (d, 1.5 Hz of tr, 2.8 Hz, 1H) H-2, 5.68 (d, 2.8 Hz, 2H) H-1, 1.84 (s, broad, 8H) ethylene H's.

^{13}C NMR (CD_2Cl_2): δ 129.0 C-3b, 127.7 C-5, 127.6 C-7a, 126.0 C-6, 124.2 C-7, 123.7 C-3, 102.8 C-3a, 89.2 (d, 4.5 Hz) C-2, 80.2 (d, 3.0 Hz) C-1, 44.5, 44.2, ethylene C's.

IR (CCl_4): 3083 (vw), 3060 (w), 3019 (vw), 2991 (vw), 2958 (w), 2927 (w), 2856 (w) cm^{-1}.

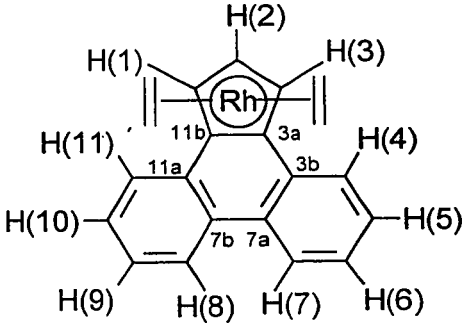

Protonation of (η^5-cyclopenta[*l*]phenanthrenyl)Rh(ethylene)$_2$.

In an attempt to protonate (η^5-cyclopenta[*l*]phenanthrenyl)Rh(ethylene)$_2$, a solution of the compound in CD_2Cl_2 (in an NMR tube) was treated with a drop of CF_3COOH at -90°C. The solution immediately changed colour from yellow to red. The sample was placed into the pre-

cooled NMR magnet, and spectra were recorded. The sample was gradually heated to 10°C in the NMR magnet. ^{1}H NMR spectra and 2-D EXSY and COSY spectra were recorded at 10° intervals.

Attempt to add diphos to (η^5-cyclopenta[*l*]phenanthrenyl)Rh(ethylene)$_2$.

(η^5-cyclopenta[*l*]phenanthrenyl)Rh(ethylene)$_2$ (0.100 g, 0.267 mmol) and diphos (0.106 g, 0.267 mmol) were stirred under N_2, in dry CH_2Cl_2 overnight. Upon removal of the solvent *in vacuo*, no change was observed in the ^{1}H NMR spectrum. Benzene (10 mL) was added, and the solution heated under reflux overnight. The solvent was removed *in vacuo*, and only decomposition products were present.

Attempt to add PMe_3 to (cyclopenta[*l*]phenanthrenyl)Rh(ethylene)$_2$.

(η^5-cyclopenta[*l*]phenanthrenyl)Rh(ethylene)$_2$ (0.055 g, 0.255 mmol) and PMe_3 (0.40 mL, 3.86 mmol) were stirred under N_2, in dry decalin overnight. Upon removal of the solvent *in vacuo*, no change was observed in the ^{1}H NMR spectrum.

Preparation of (η^5-cyclopenta[*l*]phenanthrenyl)$_2$Fe, 80.

Following the procedure for the analogous (indenyl)$_2$Fe,[109], to a solution of cyclopenta[*l*]phenanthrene (0.400 g, 1.852 mmol) in 20 mL dry THF was added dropwise 1.16 mL (1.856 mmol) *n*-BuLi at -78°C. The dark red solution was stirred for 1 hr at -78°C. In a separate flask, 0.100 g (0.617 mmol) $FeCl_3$ and 0.017 g Fe (0.308 mmol) were stirred in 10 mL dry THF for 1 hr at room temperature. This mixture was syringed drop by drop into the cold (-78°C) flask containing the anion. The mixture was stirred overnight and the solvent was removed *in vacuo*. The orange residue was extracted with ether to remove any unreacted ligand and LiCl. The orange residue was extracted with hot benzene and the solvent removed under reduced pressure

to yield 0.150 g (0.309 mmol, 33%) of an orange solid. Orange crystals were obtained upon recrystallization from benzene. M.p. 246-247°C.

Mass spectrum (DEI)$^+$, *m/z* (%): 486 (100) ([M]$^+$), 271 (5) ([M -215]$^+$), 243 (15) ([M]$^{2+}$), 215 (40) ([$C_{17}H_{11}$]$^+$). Mass spectrum (high resolution, DEI): calculated for mass $^{12}C_{34}H_{22}Fe$ ([M]$^+$), 486.1071 amu; observed 486.1079 amu.

^{1}H NMR (C_6D_6): δ 7.68 (d, 8.1 Hz, 4H) H-7, 7.17 (d, 1.1 Hz of tr, 7.6 Hz, 4H) H-6, 7.12 (d, 1.2 Hz of d, 7.8 Hz, 4H) H-43, 6.96 (d, 1.0 Hz of tr, 7.4 Hz, 4H) H-5, 4.66 (d, 2.5 Hz, 2H) H-1, 4.14 (tr, 2.5 Hz, 1H) H-2.

^{13}C NMR (C_6D_6): δ 130.8 C-3b, 129.9 C-7a, 126.9 C-5, 124.9 C-6 (C-5 and C-6 may be interchanged), 123.7 C-4, 123.5 C-7, 82.9 C-3a, 69.9 C-2, 63.5 C-1.

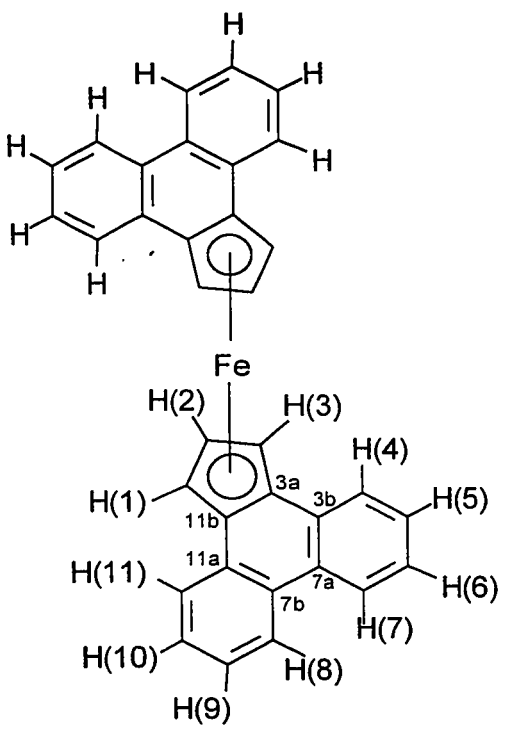

Attempt to protonate (η^5-cyclopenta[*l*]phenanthrenyl)$_2$Fe.

In an attempt to protonate (η^5-cyclopenta[*l*]phenanthrenyl)$_2$Fe, a solution of the compound in DMSO-d_6 (in an NMR tube) was treated with a drop of CF_3COOH at room temperature. There was no change in the ^{1}H NMR spectrum. The sample was gradually heated to 90°C. No changes in the ^{1}H NMR spectrum were observed.

Reaction of (η^5-C_5H_5)Fe(CO)$_2$I with cyclopenta[*l*]phenanthrenyl anion.

To a solution of cyclopenta[*l*]phenanthrene (0.300 g, 1.39 mmol) in 40 mL dry THF was added dropwise *n*-BuLi (0.86 mL, 1.38 mmol) at -78°C. The dark red solution was stirred for 1 hr at -78°C. (η^5-C_5H_5)Fe(CO)$_2$I (0.422 g, 1.39 mmol) was added and the reaction mixture stirred overnight at room temperature. The solvent was removed under vacuum. Flash chromatography on silica using hexanes:CH_2Cl_2, followed by use of a Chromatotron using hexanes as eluent, yielded (η^5-cyclopenta[*l*]phenanthrenyl)Fe(cyclopentadienyl), **81**, as an orange solid (0.025 g, 0.074 mmol, 5%). m.p. 201-202°C. Most of the ligand (0.259 g, 1.12 mmol, 81%) was recovered.

Mass spectrum $(DEI)^+$, *m/z* (%): 336 (100) ($[M]^+$), 215 (15) ($[C_{17}H_{11}]^+$), 121 (5) ($[C_5H_5Fe]^+$).

Mass spectrum (high resolution, DEI): calculated for mass $^{12}C_{22}H_{16}Fe$ ($[M]^+$), 336.060 amu; observed 336.061 amu.

^{1}H NMR (THF-d_8): δ 8.42 (m, 2H) H-7, 7.97 (m, 2H) H-4, 7.44 (m, 4H) H-5, H-6, 5.28 (d, 6.3 Hz, 2H) H-1, 4.39 (tr, 6.3 Hz, 1H) H-2, 3.59 (s, broad, 5H) H-7.

^{13}C NMR (THF-d_8): δ 135.5 C-3b, 131.0 C-7a, 128.1 C-5, 126.4 C-6 (C-5 and C-6 may be interchanged), 124.7 C-4, 124.4 C-7, 82.2 C-3a, 70.6 C-12, 69.9 C-2, 63.3 C-1.

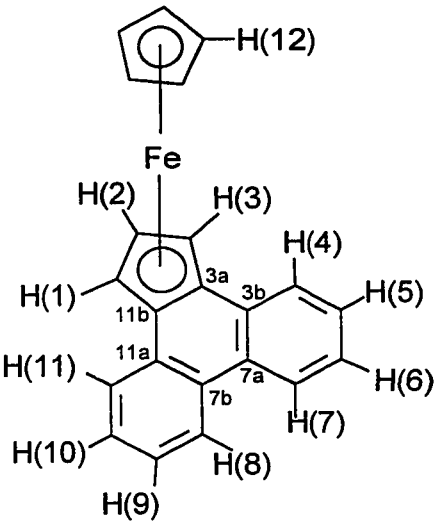

Preparation of cyclopenta[*l*]phenanthrene-TCNE adduct, 95.

To a stirred solution of cyclopenta[*l*]phenanthrene (0.033 g, 0.153 mmol) in 25 mL dry THF was added TCNE (0.078 g, 0.609 mmol). The solution immediately turned very deep purple. Stirring was continued for 1 week. Removal of the solvent under vacuum, followed by flash chromatography, using methylene chloride as eluent, yielded 0.045 g (0.131 mmol, 86%) of a light pink solid. Decomposes at 197-198°C.

Mass spectrum $(DEI)^+$, *m/z* (%): 344 (30) ($[M]^+$), 216 (100) ($[C_{17}H_{12}]^+$). Mass spectrum (high resolution, DEI): calculated for mass $^{12}C_{21}H_{12}N_4$ ($[M]^+$), 334.1062 amu; observed 344.1059 amu.

^1H NMR (THF-d_8): δ 8.87-8.84 (m, 2H) H-8, H-7, 8.01 (d, 1.0 Hz of d, 7.9 Hz, 1H) H-4, 7.83-7.80 (m, 1H) H-11, 7.78-7.75 (m, 1H) H-6, 7.74-7.69 (m, 3H) H-5, H-9, H-10, 5.42 (d, 1.6 Hz of d, 8.2 Hz, 1H) H-3, 4.46 (d, 2.3 Hz of tr, 8.5 Hz, 1H) H-2, 4.02 (d, -18.2 Hz of d, 2.3 Hz of d, 1.6 Hz, 1H) H-1, 3.92 (d, -18.2 Hz of d, 8.8 Hz, 1H) H-1'.

^{13}C NMR (THF-d_8): δ 140.9 C-3a, C-11b, 133.0 C-7a, 132.2 C-7b, 131.5 C-11a, 129.5 C-3b (C-11a and C-3b may be interchanged), 128.9 C-6, 128.3 C-5, 128.2 C-10 (C-5 and C-10 may be

interchanged), 128.0 C-9, 126.7 C-4, 125.7 C-11, 124.6 C-7, 124.5 C-8 (C-7 and C-8 may be interchanged), 113.0, 113.1, 110.6, 110.3, CN's, 54.7 C-3, 45.4 C-2, 41.3 C-12, C-13, 37.5 C-1.

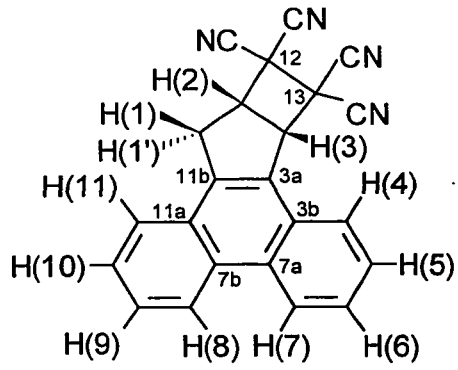

Attempts to π-complex a metal to a six-membered ring of cyclopenta[*l*]phenanthrene

Preparation of (η^6-cyclopenta[*l*]dihydrophenanthrene)$Cr(CO)_3$, 88.

This compound was isolated in an attempt to synthesize (η^6-cyclopenta[*l*]phenanthrene)$Cr(CO)_3$ from ligand that had not been carefully dried. A solution of cyclopenta[*l*]phenanthrene (0.600 g, 2.778 mmol) and $Cr(CO)_6$ (0.611 g, 2.778 mmol) in 60 mL *n*-Bu_2O was heated under reflux for 3 days. The green solid was filtered off using Schlenk procedures. The solvent was removed *in vacuo*, leaving a greenish residue. Flash chromatography on silica using hexane/ether 1:1 gave 0.238 g of the alkane, **89** (1.1 mmol; 39%) and 0.050g of (η^6-cyclopenta[*l*]dihydrophenanthrene)$Cr(CO)_3$, **88** (0.14 mmol; 5%). Yellow crystals of the chromium complex were grown from methylene chloride/hexane. m.p. 186-187°C. Mass spectrum $(DEI)^+$, *m/z* (%): 354 (15) ($[M]^+$), 298 (10) ($[M - 2CO]^+$), 270 (80) ($[M - 3CO]^+$), 215 (15) ($[M - Cr(CO)_3 - 3H]^+$), 52 (100) ($[Cr]^+$). Mass spectrum (high resolution, DEI): calculated for mass $^{12}C_{17}H_{11}Cr$ ($[M - 3CO]^+$), 270.0501 amu; observed 270.0506 amu.

^{1}H NMR (CD_2Cl_2): δ 8.42 - 8.40 (m,1H) H-8, 7.85 - 7.83 (m,1H) H-11, 7.71 - 7.69 (m,2H) H-9, H-10, 6.80 (d, 6.9 Hz) H-7, 6.08 (d, 6.7 Hz) H-4, 5.67 (tr, 6.7 Hz) H-5, 5.60 (tr, 6.7 Hz) H-6, 3.39 - 3.18 (m, 4H) H-1, H-3, 2.42 - 2.30 (m, 2H) H-2.

IR (CCl_4): 3063 (vw), 2926 (w), 2862 (vw), 2022 (s), 1943 (s) cm^{-1}.

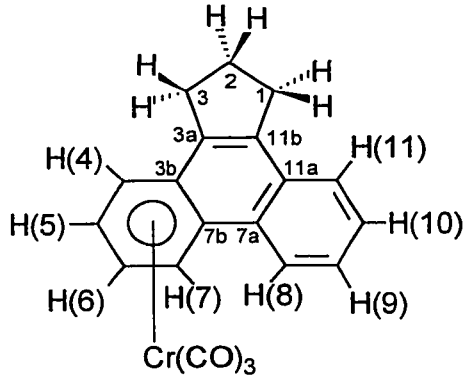

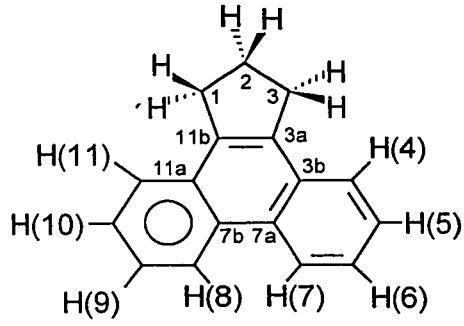

m.p. 152-153°C.

Mass spectrum $(DEI)^+$, *m/z* (%): 218 (100) ($[M]^+$). Mass spectrum (high resolution, DEI): calculated for mass $^{12}C_{17}H_{14}$ ($[M]^+$), 218.1096 amu; observed 218.1091 amu.

^{1}H NMR (CD_2Cl_2): δ 8.72 (m, 2H) H-7, 7.89 (m,2H) H-4, 7.63 (m, 4H) H-5, H-6, 3.37 (tr, 7.5 Hz, 4H) H-1, 2.37 (quintet, 7.5 Hz, 2H) H-2.

^{13}C NMR (CD_2Cl_2): δ 138.0 C-3a, 130.5, 130.4, C-3b, C-7a (C-3b and C-7a may be interchanged), 126.9 C-6, 125.9 C-5, 125.3 C-4, 123.4 C-7, 32.6 C-1, 23.8 C-2.

Preparation of the dimer of cyclopenta[*l*]phenanthrene, 94.

This compound was first isolated in an attempt to synthesize (η^6-cyclopenta[*l*]phenanthrene)$Cr(CO)_3$. A solution of carefully dried cyclopenta[*l*]phenanthrene (0.231 g, 1.069 mmol) and $Cr(CO)_6$ (0.235 g, 1.069 mmol) in 18 mL *n*-Bu_2O and 2 mL THF was heated under reflux for 3 days. The green solid was filtered off using Schlenk procedures. The solvent was removed *in vacuo*, leaving a greenish residue. Flash chromatography on silica using hexane/methylene chloride 2:1 gave starting ligand and 0.020 g dimer (0.046 mmol; 9%). M.p. 239-240°C.

Mass spectrum $(DEI)^+$, *m/z* (%): 432 (10) ($[M]^+$), 216 (100) ($[M - 216]^+$). Anal. Calcd. for $C_{34}H_{24}$: C, 94.40; H, 5.60. Found: C, 94.31; H, 5.76.

^1H NMR (CD_2Cl_2): δ 8.43 (d, 8.0 Hz, 1H) H-4, 8.40 (d, 8.3 Hz, 1H) H-19, 8.39 (d, 8.2 Hz, 1H) H-7, 8.31 (d, 8.3 Hz, 1H) H-8, 8.25 (d, 8.3 Hz, 1H) H-18, 8.14 (d, 8.0 Hz, 1H) H-22, 7.78 (tr, 7.6 Hz, 1H) H-5, 7.64 (tr, 7.3 Hz, 1H) H-21, 7.57 (tr, 7.3 Hz, 1H) H-6, 7.48 (tr, 7.2 Hz, 1H) H-20, 7.38 (d, 8.0 Hz, 1H) H-15, 7.31 (tr, 7.1 Hz, 1H) H-9, 7.22 (tr, 7.4 Hz, 1H) H-10, 7.13 (tr, 7.1 Hz, 1H) H-17, 7.12 (d, 7.4 Hz, 1H) H-11, 6.92 (tr, 7.5 Hz, 1H) H-16, 4.76 (d, 8.7 Hz, 1H) H-3, 4.72 (s, 1H) H-14, 4.33 (d, 3.5 Hz, 1H) H-12, 3.77 (m, 1H) H-2, 3.10 (d, 16.9 Hz of d, 10.1 Hz, 1H) H-1a, 2.55 (d, 16.6 Hz, 1H) H-1b, 2.28 (d, 8.3 Hz of d, 26.9 Hz, 2H) H-13.

^{13}C NMR (CD_2Cl_2): δ 140.8 C-14a, 139.1 C-22b, 138.6 C-11b, 137.4 C-3a, 130.4 C-3b, 130.0 C-22a, 129.9 C-7b, 129.6 C-11a, 129.2 C-18b, 128.9 C-18a, 128.6 C-14b, 126.8 C-21, C-5, 126.4 C-10, 125.7 C-6, 125.6 C-9, 125.5 C-4, 125.4 C-16, 125.3 C-20, 124.8 C-17, 124.6 C-15, C-22, C-11, 123.5 C-19, 123.2 C-7, 122.9 C-8, 122.7 C-18a, 55.0 C-3, 53.0 C-13, 47.9 C-14, 47.1 C-12, 43.5 C-2, 35.0 C-1.

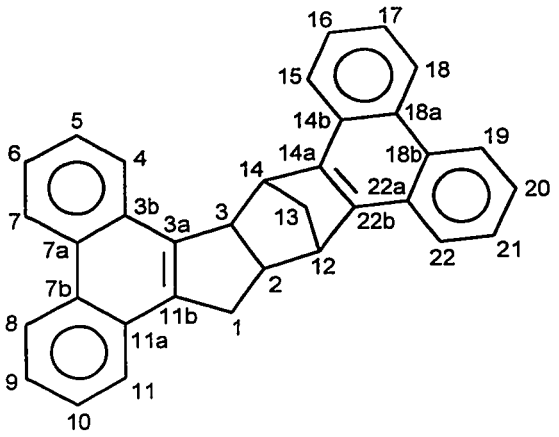

The compound was also prepared by refluxing a solution of cyclopenta[*l*]phenanthrene (0.100 g, 0.463 mmol) in 30 mL *n*-Bu_2O for 3 days. After removal of the solvent, ^1H NMR of the crude product revealed it to be about 1:1 ligand to dimer. The dimer was separated from the ligand using a chromatotron, with hexane as eluent, yielding 0.051 g ligand (0.236 mmol) and 0.042 g of the white solid dimer (0.097 mmol, 42%). The product was recrystallized from acetone/heptane to give clear colourless plates.

Reaction between Cyclopenta[*l*]phenanthrene and $Cr(NH_3)_3(CO)_3$

Cyclopenta[*l*]phenanthrene (0.200 g, 0.926 mmol) and $Cr(NH_3)_3(CO)_3$ (0.350 g, 1.871 mmol) were heated under reflux in *n*-hexane overnight. Solvent was removed *in vacuo*. The ^1H NMR revealed only ligand.

Reaction between Cyclopenta[*l*]phenanthrene, ferrocene, Al and $AlCl_3$

By analogy to the procedure of Lee *et al.*,[111] cyclopenta[*l*]phenanthrene (0.500 g, 2.32 mmol), ferrocene (2.176 g, 11.574 mmol), aluminum powder (0.0625 g, 2.315 mmol) and $AlCl_3$

(0.618 g, 4.63 mmol) were heated in decalin (15 mL) at 185°C for 4 hr. The mixture was cooled to 0°C, H_2O (25 mL) added and the inorganic salts removed on a sintered funnel. The aqueous layer was isolated and extracted with ether (2 X 25 mL), then treated with NH_4PF_6 (2.00 g, 12.5 mmol) in H_2O (5 mL). No precipitate was formed. ^1H NMR of the organic layer revealed only ligand.

Reaction between Cyclopenta[*l*]phenanthrene, $BrMn(CO)_5$ and $AlCl_3$

Cyclopenta[*l*]phenanthrene (0.216 g, 1.00 mmol), $BrMn(CO)_5$ (0.280 g, 1.00 mmol) and $AlCl_3$ (0.250 g, 1.9 mmol) were heated under reflux in *n*-hexane (50 mL) overnight. Upon cooling, water (7.5 mL) and toluene (7.5 mL) were added and the precipitate removed on a sintered funnel. The aqueous layer was added dropwise to NH_4PF_6 (1.6 g, 9.8 mmol) in H_2O (5 mL). The organic layer was extracted with water (2 X 5 mL) and the combined aqueous layers added to the NH_4PF_6 solution. No precipitate was formed. ^1H NMR of the organic layer revealed only ligand.

REFERENCES

1. Chen, Y.-X.; Rausch, M. D.; Chien, J. C. W. *Organometallics* **1993**, *12*, 4607.
2. Soares, J. B. P.; Hamielec, A. E. *Polym. React. Eng.* **1995**, *3*, 131.
3. McMaster, A. D.; Stobart, S. R. *J. Chem. Soc., Dalton Trans.* **1982**, 2275.
4. McMaster, A. D.; Stobart, S. R. *J. Am. Chem. Soc.* **1982**, *104*, 2109.
5. Ashe, A. J. *J. Am. Chem. Soc.* **1970**, *92*, 1233.
6. McLean, S.; Reed, G. W. B. *Can. J. Chem.* **1970**, *48*, 3110.
7. Davison, A.; Rakita, P. E. *Inorg. Chem.* **1970**, *9*, 289.
8. Sergeyev, N. M.; Avramenko, G. I.; Kisin, A. V.; Korenevsky, V. A.; Ustynyuk, Y. A. *J. Organomet. Chem.* **1971**, *32*, 55.
9. Kisin, A. V.; Korenevsky, V. A.; Sergeyev, N. M.; Ustynyuk, Y. A. *J. Organomet. Chem.* **1972**, *34*, 93.
10. Grishin, Y. K.; Sergeyev, N. M.; Ustynyuk, Y. A. *Organic Magnetic Resonance* **1972**, *4*, 377.
11. Spangler, C. W. *Chem. Rev.* **1976**, *76*, 187.
12. Davison, A.; Rakita, P. E. *J. Organomet. Chem.* **1970**, *23*, 407.
13. Sergeyev, N. M.; Grishin, Y. K.; Luzikov, Y. N.; Ustynyuk, Y. A. *J. Organomet. Chem.* **1972**, *38*, c1.
14. Luzikov, Y. N.; Sergeyev, N. M.; Ustynyuk, Y. A. *J. Organomet. Chem.* **1974**, *65*, 303.
15. Ashe, A. J. *Tetrahedron Letters* **1970**, *24*, 2105.
16. Larrabee, R. B.; Dowden, B. F. *Tetrahedron Letters* **1970**, *12*, 915.
17. Stradiotto, M.; Rigby, S. S.; Hughes, D. W.; Brook, M. A.; Bain, A. D.; McGlinchey, M. J. *Organometallics* **1996**, *15*, 5645.
18. Rigby, S. S.; Girard, L.; Bain, A. D.; McGlinchey, M. J. *Organometallics* **1995**, *14*, 3798.
19. Forsen, S.; Hoffman, R. *Journal of Chemical Physics* **1963**, *39*, 2892.
20. Forsen, S.; Hoffman, R. *Journal of Chemical Physics* **1964**, *40*, 1189.
21. Hoffman, R.; Forsen, S. *Journal of Chemical Physics* **1966**, *45*, 2049.
22. Grassi, M.; Mann, B. E.; Pickup, B. T.; Spencer, C. M. *J. Magn. Reson.* **1986**, *69*, 92.

23. Led, J. J.; Gesmar, H. *J. Magn. Reson.* **1982**, *49*, 444.

24. Muhandiram, D. R.; McClung, R. E. D. *J. Magn. Reson.* **1987**, *71*, 187.

25. Bain, A. D.; Cramer, J. A. *J. Magn. Reson.* **1993**, *Series A 103*, 217.

26. Kwart, H.; King, K.*D Orbitals in the Chemistry of Silicon, Phosphorus and Sulfur*; Springer: New York, **1977**.

27. Shambayati, S.; Blake, J. F.; Wierschke, S. G.; Jorgensen, W. L.; Schreiber, S. L. *J. Am. Chem. Soc.* **1990**, *112*, 697.

28. Tossell, J. A.; Moore, J. H.; McMillan, K.; Coplan, M. A. *J. Am. Chem. Soc.* **1991**, *113*, 1031.

29. Xiao, S.; Trogler, W. C.; Ellis, D. E.; Berkovitch-Yellin, Z. *J. Am. Chem. Soc.* **1983**, *105*, 7033.

30. Marynick, D. S. *J. Am. Chem. Soc.* **1984**, *106*, 4064.

31. Field, D. J.; Jones, D. W.; Kneen, G. *J. Chem. Soc., Faraday Trans.* **1978**, 1050.

32. Epiotis, N. D.; Shaik, S. *J. Am. Chem. Soc.* **1977**, *99*, 4936.

33. Ashe, A. J. *J. Org. Chem.* **1972**, *37*, 2053.

34. Larrabee, R. B. *J. Am. Chem. Soc.* **1971**, *93*, 1510.

35. Miller, S. A.; Tebboth, J. A.; Tremaine, J. F. *J. Chem. Soc.* **1952**, 632.

36. Pauson, P. L.; Kealy, T. J. *Nature* **1951**, *168*, 1039.

37. Fischer, E. O.; Hafner, W. *Z. Naturforsch.* **1955**, *B10*, 665.

38. Timms, P. L. *J. Chem. Soc. , Chem. Commun.* **1969**, 1033.

39. Fischer, E. O.; Oefele, K. *Chem. Ber.* **1957**, *90*, 2532.

40. Coffield, T. H.; Sandel, V.; Closson, R. D. *J. Am. Chem. Soc.* **1957**, *79*, 5826.

41. Eischenbroich, C.; Salzer, A.*Organometallics - A Concise Introduction*; VCH Publishers: Weinheim,Germany, **1989**; pp 345.

42. Fischer, E. O.; Kriebitzsch, N.; Fischer, R. D. *Chem. Ber.* **1959**, *92*, 3214.

43. Albright, T. A.; Hofmann, P.; Hoffmann, R.; Lillya, C. P.; Dobosh, P. A. *J. Am. Chem. Soc.* **1983**, *105*, 3396.

44. Kundig, E. P.; Timms, P. L. *J. Chem. Soc. Dalton Trans.* **1980**, 991.

45. Rerek, M. E.; Ji, L.-N.; Basolo, F. *J. Chem. Soc., Chem. Commun.* **1983**, 1208.

46. Schonberg, P. R.; Paine, R. T.; Campana, C. F.; Duesler, E. N. *Organometallics* **1982**, *1*, 799.

47. Huttner, G.; Brintzinger, H. H.; Bell, L. G.; Friedrich, P.; Bejenke, V.; Neugebauer, D. *J. Organomet. Chem.* **1978**, *145*, 329.

48. Müller, J.; Goser, P.; Elian, M. *Angew. Chem., Int. Ed. Engl.* **1969**, *8*, 374.

49. Stanger, A.; Vollhardt, K. P. C. *Organometallics* **1992**, *11*, 317.

50. Scott, F.; Kruger, C.; Betz, P. *J. Organomet. Chem.* **1990**, *387*, 113.

51. Klein, H. F.; Ellrich, K.; Lamac, S.; Lull, G.; Zsolnai, L.; Huttner, G. *Z. Naturforsch.* **1985**, *40b*, 1377.

52. Kiriss, R. U.; Treichel, P.M. *J. Am. Chem. Soc.* **1986**, *108*, 853.

53. Oprunenko, Y. F.; Malugina, S. G.; Ustynyuk, Y. A.; Ustynyuk, N. A.; Kravtsov, D. N. *J. Organomet. Chem.* **1988**, *338*, 357.

54. Kundig, E. P.; Desobry, V.; Grivet, C.; Rudolph, B.; Spichiger, S. *Organometallics* **1987**, *6*, 1173.

55. White, C.; Thompson, S. J.; Maitlis, P. M. *J. Chem. Soc. Dalton Trans.* **1977**, 1654.

56. Crabtree, R. H.; Parnell, C. P. *Organometallics* **1984**, *3*, 1727.

57. Stanger, A.; Boese, R. *J. Organomet. Chem.* **1992**, *430*, 235.

58. Treichel, P. M.; Johnson, J. W. *J. Organomet. Chem.* **1975**, *88*, 207.

59. Bang, H.; Lynch, T. J.; Basolo, F. *Organometallics* **1992**, *11*, 40.

60. Nesmeyanov, A. N.; Ustynyuk, N. A.; Makarova, L. G.; Andre, S.; Ustynyuk, Y. A.; Novikova, L. N.; Luzikov, Y. N. *J. Organomet. Chem.* **1978**, *154*, 45.

61. Novikova, L. N.; Ustynyuk, N. A.; Zvorykin, V. E.; Dneprovskaya, L. S.; Ustynyuk, Y. A. *J. Organomet. Chem.* **1985**, *292*, 237.

62. Salzer, A.; Taschler, C. *J. Organomet. Chem.* **1985**, 261.

63. Mlekuz, M.; Bougeard, P.; Sayer, B. G.; McGlinchey, M. J.; Rodger, C. A.; Churchill, M. R.; Ziller, J. W.; Kang, S. K.; Albright, T. A. *Organometallics* **1986**, *5*, 1656.

64. Evans, J.; Johnson, B. F. G.; Lewis, J.; Yarrow, D. J. *J. Chem. Soc., Dalton Trans.* **1974**, 2375.

65. Ceccon, A.; Gambarotto, A. *J. Organomet. Chem.* **1981**, *217*, 79.

66. Nicholas, K. M.; Kerber, R. C.; Stiefel, E. I. *Inorg. Chem.* **1971**, *10*, 1519.

67. Johnson, J. W.; Triechel, P. M. *J. Chem. Soc., Chem. Commun.* **1976**, 688.

68. Johnson, J. W.; Treichel, P. M. *J. Am. Chem. Soc.* **1977**, *99*, 1427.

69. Treichel, P. M.; Johnson, J. W. *Inorg. Chem.* **1977**, *16*, 749.

70. Treichel, P. M.; Fivizzani, K. P.; Haller, K. J. *Organometallics* **1982**, *1*, 931.

71. Yezernitskaya, M. G.; Lokshin, B. V.; Zdanovich, V. I.; Lobanova, I. A.; Kolobova, N. E. *J. Organomet. Chem.* **1982**, *234*, 329.

72. Heuer, L.; Bode, U. K.; Jones, P. G.; Schmutzler, R. *Z. Naturforsch.* **1989**, *44b*, 1082.

73. Decken, A.; Britten, J. F.; McGlinchey, M. J. *J. Am. Chem. Soc.* **1993**, *115*, 7275.

74. Foster, P.; Chien, J. C. W.; Rausch, M. D. *Organometallics* **1996**, *15*, 2404.

75. Cope, A. C.; Field, L.; MacDowell, D. W. H.; Wright, M. E. *J. Am. Chem. Soc.* **1956**, *78*, 2547.

76. Eliasson, B.; Nouri-Sorkhabi, M. H.; Trogen, L.; Setson, I.; Edlund, U.; Sygula, A.; Rabinowitz, M. *J. Org. Chem.* **1989**, *54*, 171.

77. Dewar, M. J. S.; Stewart, J. J. P., *Austen Method 1,* Package 1.0 QCPE 506, *QCPE Bulletin* **1986**, *6*, 2.

78. Stewart, J. J. P., MOPAC, A Semi-Empirical Molecular Orbital Program. QCPE **1993**.

79. Gutowsky, H. S.; Holm, C. H. *J. Chem. Phys.* **1956**, *25*, 1228.

80. Top, S.; Jaouen, G.; Sayer, B. G.; McGlinchey, M. J. *J. Am. Chem. Soc.* **1983**, *105*, . 6426.

81. Sanders, J. K. M.; Hunter, B. K.*Modern NMR Spectroscopy, A Guide for Chemists*; Oxford University Press: Oxford, **1987**; p 224.

82. Cramer, R. *J. Am. Chem. Soc.* **1964**, *86*, 217.

83. Rogers, R. D.; Atwood, J. L.; Albright, T. A.; Lee, W. A.; Rausch, M. D. *Organometallics* **1984**, *3*, 263.

84. Guss, J. M.; Mason, R. *J. Chem. Soc., Dalton Trans.* **1973**, 1834.

85. Muetterties, E. L.; Bleeke, J. R.; Wucherer, E. J.; Albright, T. A. *Chem. Rev.* **1982**, *82*, 499.

86. Rigby, S. S.; Gupta, H. K.; Werstiuk, N. H.; Bain, A. D.; McGlinchey, M. J. *Polyhedron* **1995**, *14*, 2787.

87. McGlinchey, M. J.; Girard, L.; Ruffolo, R. *Coordination Chemistry Reviews* **1995**, *143*, 331.

88. Dunn, J. D.; Ruffolo, R.; Rigby, S. S.; Brook, M. A.; McGlinchey, M. J., manuscript in preparation.

89. Schilling, B. E. R.; Hoffmann, R. *J. Am. Chem. Soc.* **1979**, *101*, 3456.

90. D'Agostino, M. F.; Mlekuz, M.; Kolis, J.; Sayer, B. G.; Rodger, C. A.; Halet, J.-F.; Saillard, J.-Y.; McGlinchey, M. J. *Organometallics* **1986**, *5*, 2345.

91. Padmanabhan, S.; Nicholas, K. M. *J. Organomet. Chem.* **1984**, *212*, C23.

92. Schreiber, S. L.; Klimas, M. T.; Sammakia, S. *J. Am. Chem. Soc.* **1987**, *109*, 5749.

93. Collins, S. **1996**, personal communication.

94. Spaleck, W.; Kuber, F.; Winter, A.; Rohrmann, J.; Bachmann, B.; Antberg, M.; Dolle, V.; Paulus, E. F. *Organometallics* **1994**, *13*, 954.

95. Stehling, U.; Diebold, J.; Kirsten, R.; Roll, W.; Brintzinger, H.-H. *Organometallics* **1994**, *13*, 964.

96. Perrin, D. D.; Perrin, D. R. In *Purification of Laboratory Chemicals*; Pergamon Press: New York, **1980**.

97. Eisch, J. J.; King, R. B. *Organometallic Synth.* **1965**, *1*, 174.

98. Cramer, R. *Inorganic Chemistry* **1962**, *1*, 722.

99. Marechal, E.; Chaintron, G. *Bull. Soc. Chim. Fr.* **1967**, *3*, 987.

100. Oddy, H. *J. Am. Chem. Soc.* **1923**, *45*, 2163.

101. Baddeley, G.; Holt, G.; Makar, S. M.; Iwinson, M. G. *J. Chem. Soc.* **1965**, 3605.

102. Sheldrick, G. M. SHELXTL PC **1990**, Release 4.1 Siemens Crystallographic Research Systems. Madison, WI 53719, U.S.A.

103. SMART (1996), Release 4.05; Siemens Energy and Automation Inc., Madison, WI 53719.

104. SAINT (1996), Release 4.05; Siemens Energy and Automation Inc., Madison, WI 53719.

105. Sheldrick, G.M. SADABS (Siemens Area Detector Absorption Corrections) (1996).

106. Sheldrick, G.M. Siemens SHELXTL (1994), Version 5.03; Siemens Crystallographic Research Systems, Madison, WI 53719.

107. PCMODEL, Version 4.0. A molecular mechanics package including MM2 (N.L. Allinger-QCPE 395), MMP1 Pi (N.L. Allinger-QCPE 318), and MODEL parameters (W.C. Still)

plus more atoms and constants by K.E. Gilbert and J.J. Gajewski, Indiana University. Available from Dr. K.E. Gilbert, Serena Software, P.O. Box 3096, Bloomington, IN. 47402-3076.

108. Caddy, P.; Green, M.; O'Brien, E.; Smart, L. E.; Woodward, P. *Angew. Chem. Int. Ed. Engl.* **1977**, *16*, 648.

109. Caddy, P.; Green, M.; O'Brien, E.; Smart, L. E.; Woodward, P. *J. Chem. Soc. Dalton Trans.* **1980**, 962.

110. Pauson, P. L.; Wilkinson, G. *J. Am. Chem. Soc.* **1954**, 2024.

111. Lee, C. C.; Demchuk, K. J.; Pannekoek, W. J.; Sutherland, R. G. *J. Organomet. Chem.* **1978**, *162*, 253.

Table 1. Crystal data and structure refinement for $(\eta^6\text{-}C_{17}H_{14})Cr(CO)_3$, 88.

Empirical formula	C20 H14 Cr O3	
Formula weight	354.31	
Crystal size	0.13 x 0.13 x 0.62 mm	
Color and habit	Orange, needle	
Diffractometer used	Enraf Nonius CAD4	
Temperature	293(2) K	
Wavelength	0.71073 Å	
Monochromator used	Graphite	
Crystal system	Monoclinic	
Space group	$P2_1/n$	
Unit cell dimensions	a = 10.264(6) Å	α = 90°
	b = 9.326(3) Å	β = 93.03(4)°
	c = 16.077(6) Å	γ = 90°
Volume	1536.8(12) $Å^3$	
Z	4	
Density (calculated)	1.531 g/cm^3	
Absorption coefficient	7.59 cm^{-1}	
F(000)	728	
Theta range for data collection	2.30 to 24.99°	
Scan type	θ - 2θ	
Scan speed	Variable; Max. speed 5.49°/min.	
	Max. time 40 sec.	
Scan range	0.7° plus K_α separation	
Standard reflections	3 every 30 min. of X-ray exposure time	
Crystal decomposition	0.9769 < decay < 1.0370	
Index ranges	-1 £ h £ 12, -1 £ k £ 11, -19 £ l £ 19	
Reflections collected	3469	
Independent reflections	2626 [R(int) = 0.0586]	

System used	Siemens SHELXTL 4.21
Solution	Patterson methods
Hydrogen atoms	Calculated positions, isotropic U
Refinement method	Full-matrix least-squares on F^2
Data / restraints / parameters	2626 / 0 / 219
Goodness-of-fit on F^2	1.094
Final R indices [I>2s(I)]	R1 = 0.0630, wR2 = 0.1698
R indices (all data)	R1 = 0.1334, wR2 = 0.2023
Absorption correction	N/A
Min./Max. transmission	N/A
Largest/mean Δ/σ	0.000/0.000
Largest diff. peak and hole	0.652 and -0.584 $eÅ^{-3}$

$wR2 = (\sum[w(F_o^2-F_c^2)^2/\sum[wF_o^4])^{1/2}$

$R1 = \sum ||F_o| - |F_c|| / \sum|F_o|$

$Weight = 1/[\sigma^2(F_o^2) + (0.100 * P)^2 + (0.400 * P)]$

where $P = (\max(F_o^2, 0) + 2 * F_c^2)/3$

Table 2. Atomic coordinates (x 104) and equivalent isotropic displacement parameters (A^2 x 10^3) for (η^6-$C_{17}H_{14}$)Cr(CO)$_3$, 88. U(eq) is defined as one third of the trace of the orthogonalized Uij tensor.

	x	y	z	U(eq)
Cr	8301(1)	8163(1)	5862(1)	43(1)
C(1)	5751(7)	3050(7)	5133(4)	53(2)
C(2)	5788(7)	2812(9)	6074(4)	68(2)
C(3)	6698(7)	3928(8)	6485(4)	58(2)
C(3A)	7309(6)	4642(7)	5759(4)	44(2)
C(3B)	8322(6)	5703(6)	5807(4)	41(1)
C(4)	8889(7)	6220(7)	6575(4)	51(2)
C(5)	9922(7)	7152(8)	6600(4)	58(2)
C(6)	10398(7)	7686(8)	5863(4)	53(2)
C(7)	9834(6)	7248(7)	5102(4)	49(2)
C(7A)	8805(6)	6248(7)	5042(4)	42(2)
C(7B)	8195(6)	5762(6)	4246(4)	42(2)
C(8)	8607(7)	6269(7)	3479(4)	50(2)
C(9)	8034(7)	5771(8)	2741(4)	56(2)
C(10)	7057(7)	4772(8)	2749(4)	53(2)
C(11)	6631(7)	4246(7)	3477(4)	53(2)
C(11A)	7205(6)	4736(7)	4244(4)	41(1)
C(11B)	6783(6)	4167(6)	5024(4)	42(2)
C(21)	7511(7)	9056(8)	4946(5)	54(2)
C(22)	6765(7)	8265(8)	6393(4)	51(2)
C(23)	8671(7)	9920(8)	6312(4)	55(2)
O(1)	7013(6)	9591(7)	4367(3)	82(2)
O(2)	5820(5)	8379(6)	6732(3)	76(2)
O(3)	879(5)	11014(6)	6610(3)	71(2)

Table 3. Selected Bond lengths [Å] and angles [°] for $(\eta^6\text{-}C_{17}H_{14})Cr(CO)_3$, 88.

Cr-C(23)	1.824(8)
Cr-C(22)	1.835(7)
Cr-C(21)	1.843(8)
Cr-C(6)	2.198(7)
Cr-C(5)	2.203(7)
Cr-C(4)	2.212(7)
Cr-C(7)	2.213(6)
Cr-C(7A)	2.295(6)
Cr-C(3B)	2.296(6)
C(1)-C(11B)	1.503(9)
C(1)-C(2)	1.529(9)
C(2)-C(3)	1.525(10)
C(3)-C(3A)	1.509(9)
C(3A)-C(11B)	1.346(8)
C(3A)-C(3B)	1.435(9)
C(3B)-C(4)	1.422(9)
C(3B)-C(7A)	1.443(8)
C(4)-C(5)	1.370(10)
C(5)-C(6)	1.397(9)
C(6)-C(7)	1.387(9)
C(7)-C(7A)	1.409(9)
C(7A)-C(7B)	1.466(8)
C(7B)-C(11A)	1.396(8)
C(7B)-C(8)	1.407(8)
C(8)-C(9)	1.377(9)
C(9)-C(10)	1.369(9)
C(10)-C(11)	1.362(9)
C(11)-C(11A)	1.415(9)
C(11A)-C(11B)	1.449(8)
C(21)-O(1)	1.151(8)
C(22)-O(2)	1.143(7)
C(23)-O(3)	1.142(8)
C(23)-Cr-C(22)	86.3(3)
C(23)-Cr-C(21)	89.1(3)
C(22)-Cr-C(21)	89.8(3)
C(23)-Cr-C(6)	89.9(3)
C(22)-Cr-C(6)	151.1(3)
C(21)-Cr-C(6)	118.8(3)
C(23)-Cr-C(5)	92.0(3)
C(22)-Cr-C(5)	114.5(3)
C(21)-Cr-C(5)	155.7(3)
C(6)-Cr-C(5)	37.0(3)
C(23)-Cr-C(4)	119.0(3)
C(22)-Cr-C(4)	91.1(3)

C(21)-Cr-C(4)	151.8(3)
C(6)-Cr-C(4)	66.0(3)
C(5)-Cr-C(4)	36.2(2)
C(23)-Cr-C(7)	115.2(3)
C(22)-Cr-C(7)	158.5(3)
C(21)-Cr-C(7)	91.6(3)
C(6)-Cr-C(7)	36.7(2)
C(5)-Cr-C(7)	66.0(3)
C(4)-Cr-C(7)	77.8(3)
C(23)-Cr-C(7A)	151.5(3)
C(22)-Cr-C(7A)	122.2(3)
C(21)-Cr-C(7A)	89.7(3)
C(6)-Cr-C(7A)	66.0(2)
C(5)-Cr-C(7A)	77.9(2)
C(4)-Cr-C(7A)	66.2(2)
C(7)-Cr-C(7A)	36.4(2)
C(23)-Cr-C(3B)	155.7(3)
C(22)-Cr-C(3B)	94.6(3)
C(21)-Cr-C(3B)	115.2(3)
C(6)-Cr-C(3B)	77.7(2)
C(5)-Cr-C(3B)	65.5(2)
C(4)-Cr-C(3B)	36.7(2)
C(7)-Cr-C(3B)	65.5(2)
C(7A)-Cr-C(3B)	36.6(2)
C(11B)-C(1)-C(2)	103.5(5)
C(3)-C(2)-C(1)	108.2(6)
C(3A)-C(3)-C(2)	103.6(5)
C(11B)-C(3A)-C(3B)	122.0(6)
C(11B)-C(3A)-C(3)	111.7(6)
C(3B)-C(3A)-C(3)	126.3(6)
C(4)-C(3B)-C(3A)	122.9(6)
C(4)-C(3B)-C(7A)	118.6(6)
C(3A)-C(3B)-C(7A)	118.5(5)
C(4)-C(3B)-Cr	68.4(4)
C(3A)-C(3B)-Cr	133.1(4)
C(7A)-C(3B)-Cr	71.7(3)
C(5)-C(4)-C(3B)	121.4(6)
C(5)-C(4)-Cr	71.6(4)
C(3B)-C(4)-Cr	74.9(4)
C(4)-C(5)-C(6)	120.4(6)
C(4)-C(5)-Cr	72.2(4)
C(6)-C(5)-Cr	71.3(4)
C(7)-C(6)-C(5)	119.7(6)
C(7)-C(6)-Cr	72.3(4)
C(5)-C(6)-Cr	71.7(4)
C(6)-C(7)-C(7A)	122.1(6)
C(6)-C(7)-Cr	71.1(4)
C(7A)-C(7)-Cr	75.0(3)
C(7)-C(7A)-C(3B)	117.7(6)
C(7)-C(7A)-C(7B)	123.3(6)
C(3B)-C(7A)-C(7B)	119.0(6)

C(7)-C(7A)-Cr	68.7(3)
C(3B)-C(7A)-Cr	71.7(3)
C(7B)-C(7A)-Cr	130.0(4)
C(11A)-C(7B)-C(8)	118.8(6)
C(11A)-C(7B)-C(7A)	119.4(5)
C(8)-C(7B)-C(7A)	121.8(6)
C(9)-C(8)-C(7B)	120.5(7)
C(10)-C(9)-C(8)	120.1(6)
C(11)-C(10)-C(9)	121.4(6)
C(10)-C(11)-C(11A)	119.6(6)
C(7B)-C(11A)-C(11)	119.6(6)
C(7B)-C(11A)-C(11B)	120.0(5)
C(11)-C(11A)-C(11B)	120.5(6)
C(3A)-C(11B)-C(11A)	121.0(6)
C(3A)-C(11B)-C(1)	112.3(5)
C(11A)-C(11B)-C(1)	126.8(6)
O(1)-C(21)-Cr	178.8(7)
O(2)-C(22)-Cr	177.5(6)
O(3)-C(23)-Cr	178.2(6)

Table 4. Anisotropic displacement parameters ($Å^2$ x 10^3) for (η^6-$C_{17}H_{14}$)$Cr(CO)_3$, 88.
The anisotropic displacement factor exponent takes the form:
$-2\pi^2$ [h^2 a^{*2} U11 + ... + 2 h k a* b* U12]

	U11	U22	U33	U23	U13	U12
Cr	43(1)	42(1)	43(1)	-5(1)	4(1)	1(1)
C(1)	53(4)	47(4)	60(4)	-1(3)	8(3)	-2(4)
C(2)	62(5)	77(6)	65(5)	24(4)	14(4)	-2(4)
C(3)	67(5)	57(4)	51(4)	3(3)	9(4)	-1(4)
C(3A)	44(4)	42(4)	45(3)	-1(3)	7(3)	6(3)
C(3B)	42(3)	40(3)	39(3)	-1(3)	0(3)	11(3)
C(4)	57(4)	53(4)	43(4)	-3(3)	0(3)	6(4)
C(5)	51(4)	60(5)	61(4)	-11(4)	-8(3)	8(4)
C(6)	46(4)	58(4)	56(4)	-21(3)	2(3)	-9(3)
C(7)	42(4)	45(4)	61(4)	-12(3)	12(3)	5(3)
C(7A)	40(3)	39(3)	47(3)	-14(3)	6(3)	1(3)
C(7B)	43(3)	40(3)	44(3)	-1(3)	9(3)	7(3)
C(8)	59(4)	46(4)	47(4)	-3(3)	7(3)	-4(4)
C(9)	73(5)	57(4)	39(4)	3(3)	11(3)	2(4)
C(10)	62(4)	56(4)	41(4)	-2(3)	2(3)	-1(4)
C(11)	49(4)	48(4)	60(4)	-12(3)	2(3)	-5(3)
C(11A)	40(3)	42(3)	42(3)	0(3)	2(3)	5(3)
C(11B)	39(3)	35(3)	52(4)	4(3)	8(3)	4(3)
C(21)	58(4)	50(4)	53(4)	-6(4)	6(4)	4(4)
C(22)	50(4)	49(4)	54(4)	-6(3)	9(3)	-2(4)
C(23)	58(4)	46(4)	63(4)	-2(4)	20(4)	-1(4)
O(1)	103(5)	85(4)	57(3)	10(3)	-9(3)	19(4)
O(2)	57(3)	97(5)	77(3)	-12(3)	20(3)	-7(3)
O(3)	86(4)	50(3)	78(4)	-18(3)	11(3)	-11(3)

Table 5. Hydrogen coordinates (x 10^4) and isotropic displacement parameters (Å ^{2} x 10^3) for (η^6-$C_{17}H_{14}$)Cr(CO)$_3$, 88.

	x	y	z	U(eq)
H(1A)	4913(7)	3396(7)	4929(4)	70(9)
H(1B)	5950(7)	2183(7)	4843(4)	70(9)
H(2A)	6104(7)	1865(9)	6205(4)	70(9)
H(2B)	4927(7)	2904(9)	6274(4)	70(9)
H(3A)	7348(7)	3486(8)	6852(4)	70(9)
H(3B)	6218(7)	4613(8)	6793(4)	70(9)
H(4A)	8464(7)	6009(7)	7079(4)	64(7)
H(5A)	10210(7)	7582(8)	7120(4)	64(7)
H(6A)	11011(7)	8464(8)	5880(4)	64(7)
H(7A)	10050(6)	7749(7)	4606(4)	64(7)
H(8A)	9293(7)	6969(7)	3476(4)	64(7)
H(9A)	8320(7)	6122(8)	2220(4)	64(7)
H(10A)	6667(7)	4433(8)	2230(4)	64(7)
H(11A)	5942(7)	3549(7)	3473(4)	64(7)

Table 6. Crystal data and structure refinement for the dimer of cyclopenta[*l*]phenanthrene, 94.

Empirical formula	C34H24
Molecular Weight	432.53
Description	colourless prism
Crystal Size	0.1 mm X 0.2 mm X 0.2 mm
Temperature, K	302(2)
Wavelength, Å	(Mo-Kα) 0.71073
Crystal system	triclinic
Space group	*P(-1)*
a, Å	10.958(5)
b, Å	13.537(5)
c, Å	16.064(4)
α, deg.	79.11(2)
β, deg.	74.10(2)
γ, deg.	81.35(1)
Volume, Å3	2422(1)
Z	4
Calcd Density, g/cm3	1.281
Abs coeff, mm-1	0.072
Scan Mode	ω-scans
F(000)	912
θ-range for collection, deg.	1.92 to 25.01 ≤
Index ranges	-13 ≤h ≤13
	-16 ≤k ≤16
	-12 ≤l ≤20
No. Reflections collected	12606
No. Independent reflections	5739
R(int)	0.0431
Refinement method	Full-matrix least-squares on F2
Weighting Scheme	w = 1/[σ2Fo2+(0.0597((Fo2+2Fc2)/3))2]

Data / restraints / parameters	5697 / 0 / 614
Goodness-of-fit on F2	0.995
Final R indices (I>2σ(I))*	R1 = 0.0494; wR2 = 0.1056
R indices (all data)*	R1 = 0.0995; wR2 = 0.1313
Mean shift/error	<0.001
Max. shift/error	<0.001
Rel. Trans. (max., min.)	1.0000, 0.7912
Largest diff. Peak, e/Å3	0.153
Largest diff. Hole, e/Å3	-0.151

*R1 = $\Sigma(\|\,|Fo|-|Fc|\,\|)/\Sigma|Fo|$; wR2 = [Σ[w(Fo2-Fc2)2]/ Σ[w(Fo2)2]] 0.5.

Table 7. Atomic coordinates (x 10^4) and equivalent isotropic displacement parameters (A^2 x 10^3) for the dimer of cyclopenta[*l*]phenanthrene, 94. U(eq) is defined as one third of the trace of the orthogonalized Uij tensor.

	x	y	z	U(eq)
C(1)	7339(3)	341(2)	2363(2)	52(1)
C(2)	8501(3)	337(2)	1568(2)	50(1)
C(3)	9300(3)	1182(2)	1606(2)	46(1)
C(3A)	8535(3)	1657(2)	2393(2)	41(1)
C(3B)	8856(3)	2489(2)	2705(2)	40(1)
C(4)	9986(3)	2951(2)	2292(2)	54(1)
C(5)	10292(4)	3712(3)	2629(3)	67(1)
C(6)	9495(4)	4046(3)	3372(3)	68(1)
C(7)	8389(3)	3630(2)	3779(2)	57(1)
C(7A)	8026(3)	2841(2)	3463(2)	44(1)
C(7B)	6854(3)	2380(2)	3882(2)	45(1)
C(8)	5964(3)	2722(3)	4619(2)	63(1)
C(9)	4890(4)	2253(3)	5025(2)	76(1)
C(10)	4641(4)	1436(3)	4711(2)	73(1)
C(11)	5463(3)	1097(3)	3992(2)	57(1)
C(11A)	6587(3)	1551(2)	3560(2)	43(1)
C(11B)	7469(3)	1201(2)	2805(2)	40(1)
C(12)	9501(3)	-610(2)	1527(2)	56(1)
C(13)	10719(3)	-136(2)	982(2)	57(1)
C(14)	10640(3)	597(2)	1626(2)	45(1)
C(14A)	10495(3)	-136(2)	2465(2)	42(1)
C(14B)	10925(3)	-126(2)	3227(2)	43(1)
C(15)	11615(3)	636(3)	3295(2)	55(1)
C(16)	12081(3)	594(3)	4010(2)	71(1)
C(17)	11892(4)	-223(3)	4667(2)	80(1)
C(18)	11200(4)	-958(3)	4631(2)	68(1)
C(18A)	10677(3)	-942(2)	3915(2)	49(1)
C(18B)	9905(3)	-1704(2)	3866(2)	50(1)
C(19)	9557(4)	-2499(3)	4548(2)	68(1)
C(20)	8834(4)	-3211(3)	4479(3)	81(1)
C(21)	8439(4)	-3178(3)	3720(3)	78(1)
C(22)	8751(3)	-2418(3)	3051(2)	65(1)
C(22A)	9473(3)	-1667(2)	3101(2)	48(1)
C(22B)	9814(3)	-868(2)	2407(2)	45(1)
C(23)	5698(3)	5176(2)	2990(2)	54(1)
C(24)	4348(3)	5463(2)	3554(2)	51(1)
C(25)	3926(3)	6572(2)	3193(2)	48(1)
C(25A)	5047(3)	6881(2)	2474(2)	43(1)
C(25B)	5174(3)	7853(2)	1952(2)	43(1)
C(26)	4207(3)	8662(2)	2094(2)	58(1)

C(27)	4345(4)	9581(3)	1593(2)	63(1)
C(28)	5445(4)	9735(2)	940(2)	61(1)
C(29)	6407(3)	8971(2)	783(2)	55(1)
C(29A)	6304(3)	8005(2)	1284(2)	42(1)
C(29B)	7324(3)	7181(2)	1151(2)	44(1)
C(30)	8480(3)	7284(3)	504(2)	58(1)
C(31)	9439(3)	6505(3)	417(2)	69(1)
C(32)	9303(3)	5597(3)	962(2)	67(1)
C(33)	8189(3)	5453(2)	1591(2)	54(1)
C(33A)	7180(3)	6242(2)	1696(2)	43(1)
C(33B)	6008(3)	6118(2)	2355(2)	42(1)
C(34)	3269(3)	4881(2)	3492(2)	54(1)
C(35)	2116(3)	5679(3)	3712(2)	60(1)
C(36)	2669(3)	6471(2)	2949(2)	49(1)
C(36A)	2988(3)	5853(2)	2209(2)	43(1)
C(36B)	2967(3)	6132(2)	1311(2)	45(1)
C(37)	2688(3)	7134(3)	945(2)	60(1)
C(38)	2669(4)	7365(3)	91(3)	70(1)
C(39)	2920(3)	6619(3)	-443(2)	69(1)
C(40)	3201(3)	5639(3)	-109(2)	60(1)
C(40A)	3241(3)	5353(2)	773(2)	45(1)
C(40B)	3552(3)	4312(2)	1142(2)	44(1)
C(41)	3738(3)	3501(3)	665(2)	61(1)
C(42)	4035(4)	2537(3)	1021(3)	75(1)
C(43)	4184(3)	2323(3)	1865(3)	69(1)
C(44)	3997(3)	3084(2)	2361(2)	58(1)
C(44A)	3663(3)	4085(2)	2016(2)	44(1)
C(44B)	3338(3)	4889(2)	2532(2)	43(1)

Table 8. Selected Bond lengths [Å] and angles [°] for the dimer of cyclopenta[*l*]phenanthrene, 94.

C(1)-C(11B)	1.509(4)
C(1)-C(2)	1.536(4)
C(2)-C(12)	1.556(4)
C(2)-C(3)	1.560(4)
C(3)-C(3A)	1.504(4)
C(3)-C(14)	1.566(4)
C(3A)-C(11B)	1.354(4)
C(3A)-C(3B)	1.435(4)
C(3B)-C(4)	1.414(4)
C(3B)-C(7A)	1.417(4)
C(4)-C(5)	1.368(4)
C(5)-C(6)	1.376(5)
C(6)-C(7)	1.361(5)
C(7)-C(7A)	1.410(4)
C(7A)-C(7B)	1.453(4)
C(7B)-C(8)	1.411(4)
C(7B)-C(11A)	1.415(4)
C(8)-C(9)	1.368(5)
C(9)-C(10)	1.384(5)
C(10)-C(11)	1.360(5)
C(11)-C(11A)	1.409(4)
C(11A)-C(11B)	1.433(4)
C(12)-C(22B)	1.515(4)
C(12)-C(13)	1.541(4)
C(13)-C(14)	1.533(4)
C(14)-C(14A)	1.510(4)
C(14A)-C(22B)	1.357(4)
C(14A)-C(14B)	1.430(4)
C(14B)-C(15)	1.403(4)
C(14B)-C(18A)	1.416(4)
C(15)-C(16)	1.368(4)
C(16)-C(17)	1.384(5)
C(17)-C(18)	1.356(5)
C(18)-C(18A)	1.414(4)
C(18A)-C(18B)	1.454(4)
C(18B)-C(19)	1.408(4)
C(18B)-C(22A)	1.423(4)
C(19)-C(20)	1.373(5)
C(20)-C(21)	1.392(5)
C(21)-C(22)	1.358(5)
C(22)-C(22A)	1.404(4)
C(22A)-C(22B)	1.420(4)
C(23)-C(33B)	1.504(4)
C(23)-C(24)	1.542(4)

C(24)-C(34)	1.549(4)
C(24)-C(25)	1.560(4)
C(25)-C(25A)	1.490(4)
C(25)-C(36)	1.564(4)
C(25A)-C(33B)	1.358(4)
C(25A)-C(25B)	1.433(4)
C(25B)-C(26)	1.408(4)
C(25B)-C(29A)	1.413(4)
C(26)-C(27)	1.360(4)
C(27)-C(28)	1.379(5)
C(28)-C(29)	1.365(4)
C(29)-C(29A)	1.410(4)
C(29A)-C(29B)	1.455(4)
C(29B)-C(30)	1.409(4)
C(29B)-C(33A)	1.413(4)
C(30)-C(31)	1.369(5)
C(31)-C(32)	1.379(5)
C(32)-C(33)	1.369(4)
C(33)-C(33A)	1.414(4)
C(33A)-C(33B)	1.433(4)
C(34)-C(44B)	1.521(4)
C(34)-C(35)	1.539(4)
C(35)-C(36)	1.530(4)
C(36)-C(36A)	1.507(4)
C(36A)-C(44B)	1.356(4)
C(36A)-C(36B)	1.430(4)
C(36B)-C(37)	1.403(4)
C(36B)-C(40A)	1.426(4)
C(37)-C(38)	1.358(4)
C(38)-C(39)	1.387(5)
C(39)-C(40)	1.363(4)
C(40)-C(40A)	1.413(4)
C(40A)-C(40B)	1.458(4)
C(40B)-C(41)	1.407(4)
C(40B)-C(44A)	1.417(4)
C(41)-C(42)	1.358(4)
C(42)-C(43)	1.384(5)
C(43)-C(44)	1.369(4)
C(44)-C(44A)	1.404(4)
C(44A)-C(44B)	1.428(4)

C(11B)-C(1)-C(2)	104.3(3)
C(1)-C(2)-C(12)	118.1(2)
C(1)-C(2)-C(3)	107.1(2)
C(12)-C(2)-C(3)	102.3(3)
C(3A)-C(3)-C(2)	104.1(2)
C(3A)-C(3)-C(14)	118.7(2)
C(2)-C(3)-C(14)	103.3(2)
C(11B)-C(3A)-C(3B)	121.9(3)
C(11B)-C(3A)-C(3)	112.0(3)
C(3B)-C(3A)-C(3)	126.1(3)

C(4)-C(3B)-C(7A)	119.2(3)
C(4)-C(3B)-C(3A)	122.1(3)
C(7A)-C(3B)-C(3A)	118.7(3)
C(5)-C(4)-C(3B)	120.6(3)
C(4)-C(5)-C(6)	120.3(3)
C(7)-C(6)-C(5)	120.7(3)
C(6)-C(7)-C(7A)	121.5(3)
C(7)-C(7A)-C(3B)	117.7(3)
C(7)-C(7A)-C(7B)	122.9(3)
C(3B)-C(7A)-C(7B)	119.4(3)
C(8)-C(7B)-C(11A)	118.0(3)
C(8)-C(7B)-C(7A)	122.1(3)
C(11A)-C(7B)-C(7A)	119.9(3)
C(9)-C(8)-C(7B)	121.2(3)
C(8)-C(9)-C(10)	120.4(3)
C(11)-C(10)-C(9)	120.1(4)
C(10)-C(11)-C(11A)	121.3(3)
C(11)-C(11A)-C(7B)	118.9(3)
C(11)-C(11A)-C(11B)	122.2(3)
C(7B)-C(11A)-C(11B)	118.9(3)
C(3A)-C(11B)-C(11A)	121.2(3)
C(3A)-C(11B)-C(1)	112.3(3)
C(11A)-C(11B)-C(1)	126.5(3)
C(22B)-C(12)-C(13)	99.6(3)
C(22B)-C(12)-C(2)	107.4(2)
C(13)-C(12)-C(2)	100.8(3)
C(14)-C(13)-C(12)	94.2(2)
C(14A)-C(14)-C(13)	99.7(2)
C(14A)-C(14)-C(3)	108.3(2)
C(13)-C(14)-C(3)	98.9(2)
C(22B)-C(14A)-C(14B)	122.0(3)
C(22B)-C(14A)-C(14)	107.6(3)
C(14B)-C(14A)-C(14)	130.4(3)
C(15)-C(14B)-C(18A)	119.9(3)
C(15)-C(14B)-C(14A)	122.3(3)
C(18A)-C(14B)-C(14A)	117.8(3)
C(16)-C(15)-C(14B)	121.0(3)
C(15)-C(16)-C(17)	119.5(4)
C(18)-C(17)-C(16)	120.8(3)
C(17)-C(18)-C(18A)	121.9(3)
C(18)-C(18A)-C(14B)	116.8(3)
C(18)-C(18A)-C(18B)	123.3(3)
C(14B)-C(18A)-C(18B)	119.9(3)
C(19)-C(18B)-C(22A)	117.2(3)
C(19)-C(18B)-C(18A)	122.9(3)
C(22A)-C(18B)-C(18A)	119.9(3)
C(20)-C(19)-C(18B)	121.4(4)
C(19)-C(20)-C(21)	120.8(3)
C(22)-C(21)-C(20)	119.3(4)
C(21)-C(22)-C(22A)	121.7(4)
C(22)-C(22A)-C(22B)	122.5(3)

C(22)-C(22A)-C(18B)	119.6(3)
C(22B)-C(22A)-C(18B)	117.9(3)
C(14A)-C(22B)-C(22A)	122.2(3)
C(14A)-C(22B)-C(12)	106.8(3)
C(22A)-C(22B)-C(12)	130.9(3)
C(33B)-C(23)-C(24)	104.0(3)
C(23)-C(24)-C(34)	116.7(3)
C(23)-C(24)-C(25)	107.0(2)
C(34)-C(24)-C(25)	102.8(3)
C(25A)-C(25)-C(24)	104.4(2)
C(25A)-C(25)-C(36)	118.3(2)
C(24)-C(25)-C(36)	102.6(2)
C(33B)-C(25A)-C(25B)	121.1(3)
C(33B)-C(25A)-C(25)	112.0(3)
C(25B)-C(25A)-C(25)	126.9(3)
C(26)-C(25B)-C(29A)	119.2(3)
C(26)-C(25B)-C(25A)	121.6(3)
C(29A)-C(25B)-C(25A)	119.2(3)
C(27)-C(26)-C(25B)	120.9(3)
C(26)-C(27)-C(28)	120.3(3)
C(29)-C(28)-C(27)	120.7(3)
C(28)-C(29)-C(29A)	121.0(3)
C(29)-C(29A)-C(25B)	118.0(3)
C(29)-C(29A)-C(29B)	122.5(3)
C(25B)-C(29A)-C(29B)	119.5(3)
C(30)-C(29B)-C(33A)	117.8(3)
C(30)-C(29B)-C(29A)	122.5(3)
C(33A)-C(29B)-C(29A)	119.7(3)
C(31)-C(30)-C(29B)	121.1(3)
C(30)-C(31)-C(32)	120.9(3)
C(33)-C(32)-C(31)	120.2(3)
C(32)-C(33)-C(33A)	120.2(3)
C(29B)-C(33A)-C(33)	119.8(3)
C(29B)-C(33A)-C(33B)	118.7(3)
C(33)-C(33A)-C(33B)	121.5(3)
C(25A)-C(33B)-C(33A)	121.8(3)
C(25A)-C(33B)-C(23)	112.5(3)
C(33A)-C(33B)-C(23)	125.7(3)
C(44B)-C(34)-C(35)	99.2(2)
C(44B)-C(34)-C(24)	108.7(2)
C(35)-C(34)-C(24)	100.1(3)
C(36)-C(35)-C(34)	94.1(2)
C(36A)-C(36)-C(35)	99.8(2)
C(36A)-C(36)-C(25)	108.9(2)
C(35)-C(36)-C(25)	99.2(2)
C(44B)-C(36A)-C(36B)	121.4(3)
C(44B)-C(36A)-C(36)	107.5(3)
C(36B)-C(36A)-C(36)	131.1(3)
C(37)-C(36B)-C(40A)	119.2(3)
C(37)-C(36B)-C(36A)	122.7(3)
C(40A)-C(36B)-C(36A)	118.1(3)

C(38)-C(37)-C(36B)	120.8(3)
C(37)-C(38)-C(39)	121.0(3)
C(40)-C(39)-C(38)	119.8(3)
C(39)-C(40)-C(40A)	121.8(3)
C(40)-C(40A)-C(36B)	117.5(3)
C(40)-C(40A)-C(40B)	122.8(3)
C(36B)-C(40A)-C(40B)	119.8(3)
C(41)-C(40B)-C(44A)	117.5(3)
C(41)-C(40B)-C(40A)	122.5(3)
C(44A)-C(40B)-C(40A)	120.0(3)
C(42)-C(41)-C(40B)	121.4(3)
C(41)-C(42)-C(43)	120.8(3)
C(44)-C(43)-C(42)	120.1(3)
C(43)-C(44)-C(44A)	120.3(3)
C(44)-C(44A)-C(40B)	119.8(3)
C(44)-C(44A)-C(44B)	122.4(3)
C(40B)-C(44A)-C(44B)	117.7(3)
C(36A)-C(44B)-C(44A)	122.8(3)
C(36A)-C(44B)-C(34)	106.7(3)
C(44A)-C(44B)-C(34)	130.5(3)

Table 9. Anisotropic displacement parameters ($A^2 \times 10^3$) for the dimer of cyclopenta[*l*]phenanthrene, 94. The anisotropic displacement factor exponent takes the form:

$-2p^2 [h^2 a^{*2} U11 + ... + 2 h k a^* b^* U12]$

	U11	U22	U33	U23	U13	U12
C(1)	54(2)	50(2)	62(2)	-11(2)	-29(2)	-3(2)
C(2)	63(2)	51(2)	42(2)	-9(2)	-24(2)	-1(2)
C(3)	56(2)	44(2)	39(2)	0(2)	-17(2)	-3(2)
C(3A)	43(2)	38(2)	41(2)	-4(1)	-16(2)	1(2)
C(3B)	42(2)	33(2)	48(2)	-2(1)	-19(2)	0(2)
C(4)	44(2)	45(2)	72(2)	-7(2)	-16(2)	-4(2)
C(5)	49(2)	49(2)	108(3)	-11(2)	-27(2)	-10(2)
C(6)	63(3)	55(2)	104(3)	-24(2)	-41(2)	-8(2)
C(7)	58(2)	55(2)	68(2)	-23(2)	-29(2)	4(2)
C(7A)	47(2)	39(2)	50(2)	-4(2)	-22(2)	2(2)
C(7B)	45(2)	49(2)	41(2)	-4(2)	-17(2)	0(2)
C(8)	58(3)	77(3)	56(2)	-22(2)	-15(2)	-1(2)
C(9)	54(3)	110(4)	59(2)	-25(2)	-2(2)	0(2)
C(10)	51(3)	105(3)	60(3)	0(2)	-12(2)	-18(2)
C(11)	50(2)	67(2)	56(2)	-4(2)	-16(2)	-14(2)
C(11A)	39(2)	47(2)	45(2)	-3(2)	-19(2)	-2(2)
C(11B)	44(2)	36(2)	44(2)	-4(1)	-21(2)	-1(2)
C(12)	77(3)	47(2)	50(2)	-17(2)	-27(2)	2(2)
C(13)	69(2)	56(2)	43(2)	-11(2)	-12(2)	6(2)
C(14)	50(2)	46(2)	38(2)	-7(2)	-10(2)	1(2)
C(14A)	47(2)	38(2)	39(2)	-7(1)	-11(2)	5(2)
C(14B)	37(2)	50(2)	40(2)	-7(2)	-11(2)	6(2)
C(15)	45(2)	67(2)	54(2)	-9(2)	-17(2)	-3(2)
C(16)	65(3)	88(3)	71(3)	-15(2)	-36(2)	-8(2)
C(17)	77(3)	110(4)	66(3)	-6(3)	-46(2)	-7(3)
C(18)	69(3)	82(3)	53(2)	5(2)	-28(2)	2(2)
C(18A)	46(2)	56(2)	41(2)	-1(2)	-14(2)	8(2)
C(18B)	48(2)	46(2)	47(2)	0(2)	-7(2)	7(2)
C(19)	65(3)	65(3)	57(2)	7(2)	-5(2)	5(2)
C(20)	72(3)	56(3)	86(3)	18(2)	7(2)	-6(2)
C(21)	71(3)	54(3)	100(3)	-4(2)	-10(2)	-10(2)
C(22)	66(3)	46(2)	81(3)	-7(2)	-19(2)	-5(2)
C(22A)	45(2)	40(2)	55(2)	-9(2)	-11(2)	6(2)
C(22B)	52(2)	40(2)	42(2)	-8(2)	-13(2)	3(2)
C(23)	51(2)	48(2)	62(2)	-5(2)	-18(2)	-3(2)
C(24)	59(2)	53(2)	43(2)	-7(2)	-12(2)	-9(2)
C(25)	48(2)	52(2)	46(2)	-16(2)	-8(2)	-2(2)
C(25A)	44(2)	41(2)	45(2)	-10(2)	-14(2)	-4(2)
C(25B)	46(2)	41(2)	49(2)	-12(2)	-17(2)	-6(2)

C(26)	58(2)	44(2)	72(2)	-15(2)	-16(2)	-1(2)
C(27)	59(3)	42(2)	89(3)	-17(2)	-23(2)	6(2)
C(28)	77(3)	38(2)	74(3)	-4(2)	-31(2)	-5(2)
C(29)	65(2)	50(2)	54(2)	-8(2)	-20(2)	-10(2)
C(29A)	47(2)	38(2)	47(2)	-9(2)	-18(2)	-6(2)
C(29B)	46(2)	47(2)	43(2)	-11(2)	-15(2)	-5(2)
C(30)	57(2)	55(2)	60(2)	-12(2)	-9(2)	-7(2)
C(31)	54(3)	72(3)	70(2)	-14(2)	2(2)	-7(2)
C(32)	55(3)	62(3)	77(3)	-18(2)	-9(2)	8(2)
C(33)	52(2)	49(2)	62(2)	-8(2)	-17(2)	0(2)
C(33A)	41(2)	46(2)	45(2)	-11(2)	-15(2)	-2(2)
C(33B)	49(2)	40(2)	42(2)	-8(1)	-17(2)	-6(2)
C(34)	55(2)	53(2)	50(2)	-3(2)	-5(2)	-12(2)
C(35)	48(2)	70(2)	59(2)	-21(2)	-1(2)	-11(2)
C(36)	43(2)	46(2)	54(2)	-19(2)	-4(2)	1(2)
C(36A)	36(2)	42(2)	52(2)	-12(2)	-9(2)	-3(2)
C(36B)	36(2)	42(2)	57(2)	-9(2)	-11(2)	0(2)
C(37)	60(2)	51(2)	72(3)	-14(2)	-28(2)	9(2)
C(38)	76(3)	59(3)	79(3)	-1(2)	-35(2)	3(2)
C(39)	72(3)	79(3)	60(2)	-4(2)	-30(2)	-1(2)
C(40)	54(2)	70(3)	58(2)	-19(2)	-15(2)	-3(2)
C(40A)	33(2)	52(2)	50(2)	-12(2)	-10(1)	-2(2)
C(40B)	32(2)	41(2)	62(2)	-15(2)	-11(2)	-1(2)
C(41)	63(2)	56(2)	73(2)	-27(2)	-23(2)	-1(2)
C(42)	86(3)	47(3)	101(3)	-32(2)	-30(2)	-2(2)
C(43)	73(3)	38(2)	97(3)	-15(2)	-24(2)	-1(2)
C(44)	61(2)	39(2)	73(2)	-8(2)	-16(2)	-3(2)
C(44A)	33(2)	42(2)	56(2)	-9(2)	-7(2)	-7(2)
C(44B)	36(2)	45(2)	48(2)	-11(2)	-7(1)	-6(2)

Table 10. Hydrogen coordinates (x 10^4) and isotropic displacement parameters ($Å^2$ x 10^3) for the dimer of cyclopenta[*l*]phenanthrene, 94.

	x	y	z	U(eq)
H(1B)	7355(3)	-294(2)	2752(2)	63
H(2A)	8212(3)	486(2)	1029(2)	60
H(3A)	9372(3)	1681(2)	1077(2)	55
H(4A)	10526(3)	2735(2)	1786(2)	65
H(5A)	11042(4)	4006(3)	2355(3)	80
H(6A)	9715(4)	4560(3)	3599(3)	82
H(7A)	7860(3)	3873(2)	4277(2)	69
H(8A)	6111(3)	3276(3)	4832(2)	75
H(9A)	4322(4)	2485(3)	5514(2)	91
H(10A)	3912(4)	1118(3)	4992(2)	87
H(11A)	5278(3)	555(3)	3780(2)	68
H(12A)	9294(3)	-1174(2)	1301(2)	67
H(13A)	11479(3)	-616(2)	924(2)	68
H(13B)	10643(3)	206(2)	412(2)	68
H(14A)	11349(3)	1013(2)	1486(2)	55
H(15A)	11757(3)	1178(3)	2848(2)	66
H(16A)	12522(3)	1111(3)	4054(2)	85
H(17A)	12243(4)	-269(3)	5140(2)	96
H(18A)	11065(4)	-1488(3)	5090(2)	82
H(19A)	9822(4)	-2544(3)	5057(2)	82
H(20A)	8605(4)	-3721(3)	4944(3)	97
H(21A)	7966(4)	-3672(3)	3672(3)	94
H(22A)	8481(3)	-2394(3)	2547(2)	78
H(23A)	6304(3)	4992(2)	3347(2)	64
H(23B)	5706(3)	4617(2)	2685(2)	64
H(24A)	4366(3)	5417(2)	4166(2)	62
H(25A)	3747(3)	7003(2)	3651(2)	58
H(26A)	3463(3)	8568(2)	2535(2)	69
H(27A)	3696(4)	10107(3)	1692(2)	75
H(28A)	5532(4)	10366(2)	602(2)	73
H(29A)	7141(3)	9089(2)	340(2)	66
H(30A)	8593(3)	7890(3)	130(2)	70
H(31A)	10194(3)	6590(3)	-16(2)	82
H(32A)	9971(3)	5080(3)	903(2)	80
H(33A)	8096(3)	4835(2)	1949(2)	65
H(34A)	3193(3)	4221(2)	3859(2)	65
H(35A)	1330(3)	5470(3)	3668(2)	72
H(35B)	1998(3)	5889(3)	4278(2)	72
H(36A)	2112(3)	7100(2)	2874(2)	58

H(37A)	2514(3)	7645(3)	1292(2)	71
H(38A)	2484(4)	8034(3)	-140(3)	85
H(39A)	2898(3)	6787(3)	-1026(2)	83
H(40A)	3370(3)	5145(3)	-473(2)	72
H(41A)	3656(3)	3627(3)	94(2)	74
H(42A)	4140(4)	2014(3)	694(3)	89
H(43A)	4410(3)	1663(3)	2096(3)	83
H(44A)	4092(3)	2937(2)	2929(2)	70

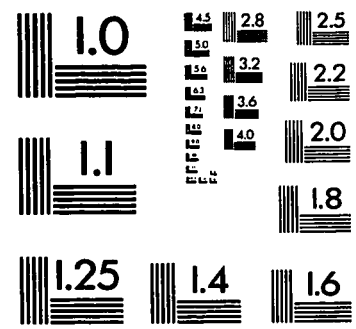

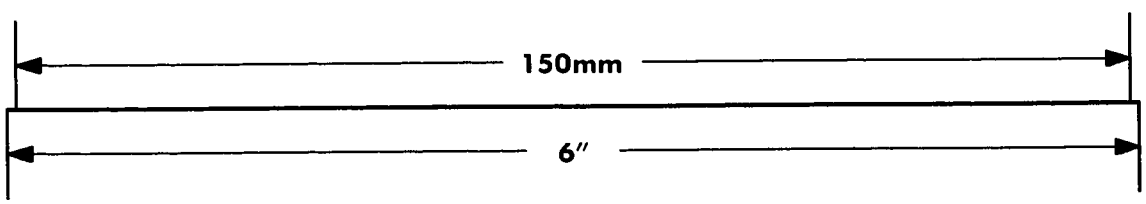

APPLIED IMAGE, Inc
1653 East Main Street
Rochester, NY 14609 USA
Phone: 716/482-0300
Fax: 716/288-5989